

การสังเคราะห์พอลิ(ไดแอลคิลเบนซัลมาโลเนต-4-ไวนิลอีเทอร์)



นางสาวรัฐนันท์ ตวงอุดมทรัพย์

สถาบันวิทยบริการ จุฬาลงกรณ์มหาวิทยาลัย

วิทยานิพนธ์นี้เป็นส่วนหนึ่งของการศึกษาตามหลักสูตรปริญญาวิทยาศาสตรมหาบัณฑิต

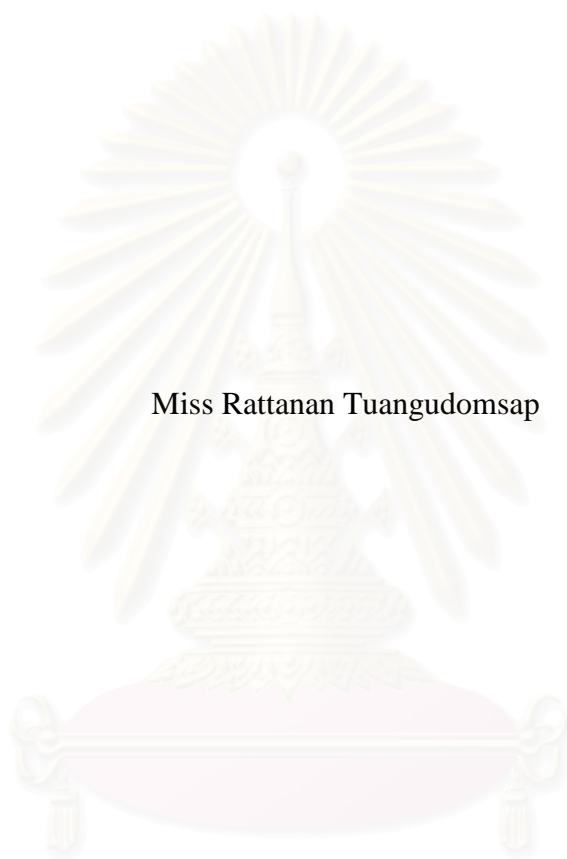
สาขาวิชาปิโตรเคมีและวิทยาศาสตร์พอลิเมอร์

คณะวิทยาศาสตร์ จุฬาลงกรณ์มหาวิทยาลัย

ปีการศึกษา 2549

ลิขสิทธิ์จุฬาลงกรณ์มหาวิทยาลัย

SYNTHESIS OF POLY(DIALKYL BENZALMALONATE-4-VINYL ETHER)



Miss Rattanan Tuangudomsap

สถาบันวิทยบริการ
จุฬาลงกรณ์มหาวิทยาลัย

A Thesis Submitted in Partial Fulfillment of the Requirements
for the Degree of Master of Science Program in Petrochemistry and Polymer Science

Faculty of Science

Chulalongkorn University

Academic Year 2006

Copyright of Chulalongkorn University

Thesis Title SYNTHESIS OF POLY(DIALKYL BENZALMALONATE-4-VINYL ETHER)
By Miss Rattanan Tuangudomsap
Field of Study Petrochemistry and Polymer Science
Thesis Advisor Associate Professor Supason Wanichwecharungruang, Ph.D.

Accepted by the Faculty of Science, Chulalongkorn University in Partial Fulfillment of the Requirements for the Master's Degree

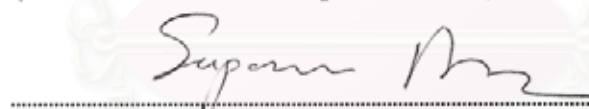


..... Dean of the Faculty of Science
(Professor Piamsak Menasveta, Ph.D.)

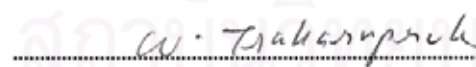
THESIS COMMITTEE



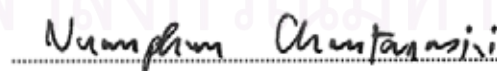
..... Chairman
(Associate Professor Supawan Tantayanon, Ph.D.)



..... Thesis Advisor
(Associate Professor Supason Wanichwecharungruang, Ph.D.)



..... Member
(Associate Professor Wimonrat Trakarnpruk, Ph.D.)



..... Member
(Associate Professor Nuanphun Chantarasiri, Ph.D.)

รศ.ดร.ศุภสร วณิชเวชารุ่งเรือง
 วิทยานิพนธ์ ศึกษาศาสตร์ : การสังเคราะห์พอลิ(ไดอัลคิลเบนซัลมาโลเนต-4-ไวนิลอีเทอร์).
 (SYNTHESIS OF POLY(DIALKYL BENZALMONATE-4-VINYL ETHER)) อ.ที่ปรึกษา : รศ. ดร. ศุภสร วณิชเวชารุ่งเรือง, 92 หน้า.

งานวิจัยนี้เป็นการสังเคราะห์โพลิโกเมอร์ที่มีสมบัติกรองรังสียูวีได้ โดยได้ทำการสังเคราะห์โพลิโกเมอร์ที่มีหมู่ไดอัลคิลเบนซัลมาโลเนตจากไวนิลมอนอเมอร์ คือ ไดเอทิลเบนซัลมาโลเนต-4-ไวนิลอีเทอร์ และ ได(2-เอทิลเฮกซิลเบนซัลมาโลเนต-4-ไวนิลอีเทอร์) พบว่าโพลิโกเมอร์ที่สังเคราะห์ได้มีน้ำหนักโมเลกุลโดยประมาณเท่ากับ 3600 และ 1900 ตามลำดับ โพลิโกเมอร์ทั้งสองสามารถดูดกลืนรังสียูวีได้ดี เมื่อศึกษาความเสถียรหลังการดูดกลืนแสงของโพลิโกเมอร์ทั้งสองพบว่าความเสถียรในการดูดกลืนแสงมากกว่า 2-เอทิลเฮกซิลพาราเมทอกซีซินนามต ซึ่งเป็นสารกรองรังสียูวีที่ใช้กันอยู่ในปัจจุบัน นอกจากนี้ พอลิ(ได(2-เอทิลเฮกซิล)เบนซัลมาโลเนต-4-ไวนิลอีเทอร์) ที่สังเคราะห์ได้เป็นของเหลวสีน้ำตาลอมแดง สามารถละลายในตัวทำละลายอินทรีย์ได้ดี อีกทั้งยังสามารถเข้ากับซิลิโคนเหลวที่ใช้ในอุตสาหกรรมเครื่องสำอางได้อีกด้วย



สถาบันวิทยบริการ จุฬาลงกรณ์มหาวิทยาลัย

สาขาวิชา ปิโตรเคมีและวิทยาศาสตร์พอลิเมอร์ ลายมือชื่อนิสิต วิทยานิพนธ์ ศึกษาศาสตร์

ปีการศึกษา 2549 ลายมือชื่ออาจารย์ที่ปรึกษา ศุภสร วณิชเวชารุ่งเรือง

4772434323 : MAJOR PETROCHEMISTRY AND POLYMER SCIENCE
 KEY WORD : DIALKYL BENZALMALONATE, UV SCREENING OLIGOMER

RATTANAN TUANGUDOMSAP : SYNTHESIS OF POLY
 (DIALKYL BENZALMALONATE-4-VINYL ETHER). THESIS
 ADVISOR : ASSOC. PROF. SUPASON WANICHWECHA
 RUNGRUANG, Ph.D., 92 pp.

UV screening oligomers were synthesized in this work. Two oligomers bearing dialkylbenzalmalonate moieties were synthesized from their vinylic monomers; diethylbenzalmalonate-4-vinyl ether and di(2-ethylhexyl)benzalmalonate-4-vinyl ether. Molecular weight of each oligomer was 3600 and 1900, respectively. Both oligomers exhibit UVB absorption in their absorption profiles. Photostability test indicated that the synthesized oligomers were more photostable than 2-ethylhexyl-*p*-methoxycinnamate (EHMC), the common UVB filter. In addition, the obtained poly(di(2-ethylhexyl)benzalmalonate-4-vinyl ether), a reddish brown oil, showed good solubility in various organic solvents and cosmetically used silicone fluid.

สถาบันวิทยบริการ
 จุฬาลงกรณ์มหาวิทยาลัย

Field of Study Petrochemistry and Polymer Science Student's signature สุรัตน์ ทองอุดมทรัพย์
 Academic Year 2006 Advisor's signature Supason Wanichwecha

ACKNOWLEDGEMENTS

First of all, I would like to express my gratitude to Associate Professor Dr. Supason Wanichwecharungruang, my advisor, for her kindly helpful suggestions, valuable assistance and encouragement throughout the entire period of this research. Sincere thanks are also extended to Associate Professor Supawan Tantayanon, Associate Professor Wimonrat Trakarnpruk and Associate Professor Nuanphun Chantarasiri, attending as the chairman and members of my thesis committee, respectively, for their valuable comments and suggestions.

I greatly appreciated the Graduate School of Chulalongkorn University for granting financial support for this research.

Finally, I thank my parents and family members for their encouragement and understanding throughout the entire study and all the members of my research group for their companionship, helpful discussion and support.



สถาบันวิทยบริการ
จุฬาลงกรณ์มหาวิทยาลัย

CONTENTS

	Page
ABSTRACT IN THAI.....	iv
ABSTRACT IN ENGLISH.....	v
ACKNOWLEDGEMENTS.....	vi
CONTENTS.....	vii
LIST OF FIGURES.....	ix
LIST OF SCHEMES.....	x
LIST OF TABLES.....	x
LIST OF ABBREVIATIONS.....	xi
CHAPTER I: INTRODUCTION.....	1
1.1 Classification of UV filters.....	3
1.2 Mechanism of chemical absorber.....	5
1.3 Literature reviews.....	5
1.3.1 Absorption of sunscreen.....	6
1.3.2 Photostability of sunscreen.....	7
1.4 Development of sunscreen: EHMC.....	8
1.5 Polymeric UV filters.....	10
1.6 Chain polymerization.....	15
1.7 Polymer with cinnamate.....	16
1.8 Research goal.....	18
CHAPTER II: EXPERIMENTAL.....	19
2.1 Instruments and equipments.....	19
2.2 Chemicals.....	20
2.3 Synthesis of poly(diethylbenzalmalonate-4-vinyl ether).....	20
2.3.1 Preparation of diethylbenzalmalonate-4-vinyl ether monomer.....	20
2.3.2 Synthesis of poly(diethylbenzalmalonate-4-vinyl ether).....	24
2.4 Synthesis of poly(di(2-ethylhexyl)benzalmalonate-4-vinyl ether).....	25
2.4.1 Preparation of di(2-ethylhexyl)benzalmalonate-4-vinyl ether monomer.....	25
2.4.2 Synthesis of poly(di(2-ethylhexyl)benzalmalonate-4-vinyl ether).....	27

	Page
2.5 Synthesis of 2-ethylhexyl cinnamate-4-allyl ether.....	28
2.6 General procedure for molar absorptivity measurements.....	31
2.7 General procedure for photostability test.....	31
CHAPTER III: RESULTS AND DISCUSSION.....	32
3.1 Syntheses of monomers.....	32
3.2 Syntheses of polymers.....	37
3.3 Solubility test.....	42
3.4 Photostability test.....	44
3.5 Physical properties test.....	45
3.6 Spectroscopic data of all synthesized compounds.....	47
3.6.1 Infrared spectroscopy.....	47
3.6.2 NMR spectroscopy.....	48
3.6.3 Mass spectroscopy.....	49
3.6.4 Gel permeation chromatography.....	49
CHAPTER IV: CONCLUSION.....	50
REFERENCES.....	52
APPENDICES.....	59
APPENDIX A.....	60
APPENDIX B.....	62
VITA.....	92

สถาบันวิทยบริการ
จุฬาลงกรณ์มหาวิทยาลัย

LIST OF FIGURES

	Page
Figure 1.1 The total spectrum of radiant energy.....	1
Figure 1.2 Skin penetration of UV radiation.....	2
Figure 1.3 Schematic representation of process in which a sunscreen chemical absorbs the harmful high-energy rays and renders them relatively harmless low energy rays.....	5
Figure 1.4 Conversion of <i>trans</i> -EHMC to <i>cis</i> -EHMC after exposure to UV radiation.....	8
Figure 1.5 Chemical structure of (I) [3-(<i>p</i> -methoxycinnamido) propyl](methyl) dimethylsiloxane copolymer, G-AS and (II) poly[(methyl)(octyl) (methyl)(propyl-4-methoxycinnamate siloxane)], G-MHS respectively.....	11
Figure 1.6 Variation of molecular weight with conversion of chain polymerization.....	16
Figure 1.7 Photochemical reactions of the polymers with cinnamate pendant group.....	16
Figure 1.8 Synthesis of poly(vinyl alcohol- <i>co</i> -vinyl- <i>trans</i> -cinnamate) by esterification of poly(vinyl alcohol).....	17
Figure 3.1 Expected oligomeric structures.....	32
Figure 3.2 UV spectra of (a) M-6 and (b) M-7 in chloroform.....	37
Figure 3.3 The conversion of polymerizations: (a) P-6 and (b) P-7.....	38
Figure 3.4 ¹ H-NMR spectra of (a) M-6 (b) P-6 (c) M-7 and (d) P-7.....	40
Figure 3.5 IR spectra of (a) M-6, P-6 and (b) M-7, P-7.....	41
Figure 3.6 UV spectra of (a) P-6 and (b) P-7 in chloroform.....	42
Figure 3.7 Photostability of P-6, P-7 and 2-ethylhexyl- <i>p</i> -methoxycinnamate (EHMC) in chloroform.....	44
Figure 3.8 UV spectra of (a) P-6, (b) P-7 and (c) 2-ethylhexyl- <i>p</i> -methoxy cinnamate (EHMC) in chloroform; the irradiation was done for 3 hours at 8.30 mW/cm ² UVA and 0.66 mW/cm ² UVB.....	45
Figure 4.1 Structures of poly(diethylbenzalmalonate-4-vinyl ether) (I) P-6 and poly(di(2-ethylhexyl)benzalmalonate-4-vinyl ether) (II) P-7.....	51

LIST OF SCHEMES

	Page
Scheme 3.1 Syntheses of dialkylbenzalmalonate-4-vinyl ether.....	33
Scheme 4.1 The overall syntheses of monomers and polymers.....	50

LIST OF TABLES

	Page
Table 1.1 Approved sunscreen ingredients.....	4
Table 3.1 Comparison of %yield in various temperatures.....	34
Table 3.2 Comparison of yielding from each pathway.....	36
Table 3.3 UV spectral data of monomers in chloroform.....	37
Table 3.4 UV absorption properties of polymers (in chloroform).....	42
Table 3.5 Solubility of synthesized polymers and monomers.....	43
Table 3.6 Refractive index of polymers.....	46
Table 3.7 Glass temperature of polymers bearing <i>n</i> -alkylic side chains.....	47
Table 3.8 Molecular weight of polymers from GPC technique.....	49

สถาบันวิทยบริการ
จุฬาลงกรณ์มหาวิทยาลัย

LIST OF ABBREVIATIONS

UV	ultraviolet
δ	chemical shift
d	doublet
dd	doublet of doublet
t	triplet
m	multiplet
br	broad
J	coupling constant
Hz	hertz
ppm	parts per million
m/z	mass per charge
$^{\circ}\text{C}$	Degree Celsius
g	gram
mg	milligram
mL	milliliter
mmol	millimol
cm^{-1}	per centimeter
ACN	acetonitrile
CDCl_3	deuterated chloroform
CH_2Cl_2	dichloromethane
EtOAc	ethyl acetate
Hex	hexane
THF	tetrahydrofuran
AIBN	2,2'-azo- <i>bis</i> -isobutyronitrile
BPO	dibenzoyl peroxide
EDCI	1-(3-dimethylaminopropyl)-3-ethylcarbodiimide hydrochloride
KBr	potassium bromide
R_f	retardation factor
n_D	refractive index
T_g	glass-transition temperature
\overline{M}_w	weight-average molecular weight

LIST OF ABBREVIATIONS

\bar{M}_n	number-average molecular weight
IR	infrared
NMR	nuclear magnetic resonance
MS	mass spectrometry
GPC	gel permeation chromatography
DSC	differential scanning calorimetry
h	hour
ϵ	molar absorptivity
λ	wavelength
J	unit of energy (Joule)
mW	milliwatt



สถาบันวิทยบริการ
จุฬาลงกรณ์มหาวิทยาลัย

CHAPTER I

INTRODUCTION

The sun radiates energy in a wide range of wavelengths, part of which are visible to human eyes. Ultraviolet (UV) radiation is a component of sunlight characterized by invisible light waves that are shorter and more energetic than the wavelengths of visible light. UV radiation is subdivided into three categories based on wavelength: the short wavelength UVC (100-290 nm), intermediate wavelength UVB (290-320 nm), and the long wavelength UVA (320-400 nm). UV-A can be further subdivided into UVA-I (340-400 nm) and UVA-II (320-340 nm) (Figure 1.1). Shorter wavelengths of light are more energetic and potentially more destructive than longer wavelengths. Fortunately, UVC, the shortest wavelengths in the UV spectrum, is completely absorbed by the gases in the atmosphere and does not reach the skin [1]. UVB and UVA are of much greater concern.

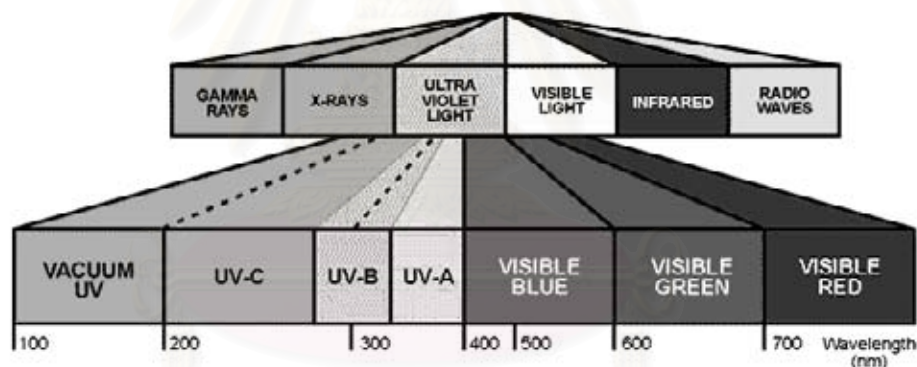


Figure 1.1 The total spectrum of radiant energy [2]

The UVB radiation plays essential role in formation of vitamin D and increases skin pigmentation or tanning [3]. In addition, UVB inhibits or interferes DNA, RNA and protein synthesis, induces early and prolonged erythema responses that would lead to photoaging, keratinocyte hyperplasia, immunosuppression and skin cancer [4,5]. UVB causes skin cancers by directly damaging cellular DNA, and also by suppressing the skin's immune system. UVB damages DNA by causing base changes in the DNA sequence and inducing the formation of pyrimidine (primarily thymine) dimers [6,7].

UVA also causes sunburn, but to a much lesser degree than UVB, and many of the potential damaging effects of UVA were overlooked until early in the last decade. UVA is now known to also play a part in melanin pigmentation, photoaging and cancer [8]. The potential damaging effects of UVA warrant concern because UVA, when compared to UVB, is approximately twenty times more abundant, is not filtered by window glass, is relatively unaffected by altitude and atmospheric conditions, is relatively constant throughout the seasons, and is 100 times more likely to penetrate into the dermis [9]. Cellular components affected by UV radiation include nucleic acids, proteins and lipids [10]. UVA has been shown to have indirect effects on biological systems and its damaging effects are often synergistically enhanced in the presence of sensitizers, the mechanism usually involves the induction of reactive oxygen species [11,12].

The penetration of UV radiation into skin varies with wavelength. UVA is less energetic than UVB but has higher penetration properties into the dermis (Figure 1.2).

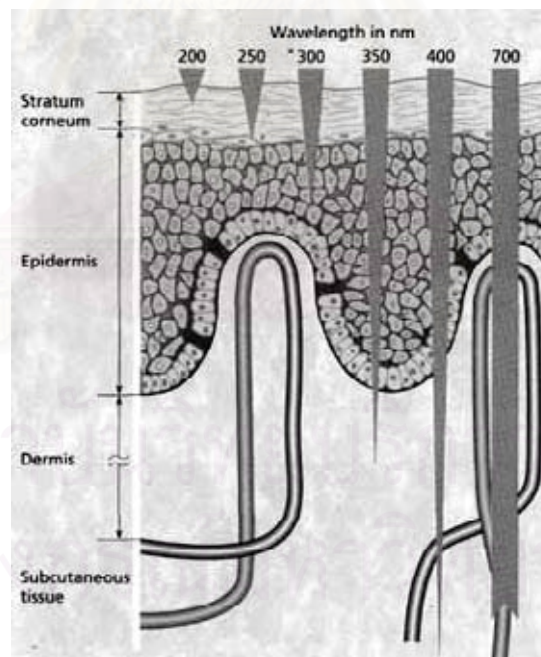


Figure 1.2 Skin penetration of UV radiation [13]

1.1 Classification of UV filters

UV filters could not only alleviate the carcinogenic potential of solar radiation but also can minimize other damaging effects of UV exposure. As a result there is a widely use of numerous compounds to protect human skin from various harmful effects of ultraviolet radiation.

UV filters may be classified according to the type of protection they offer as either physical blockers (inorganic or mineral filters) or chemical absorbers (organic or chemical filters).

A. Physical blockers

These are chemicals that reflect or scatter the ultraviolet radiation. Most of them are inorganic compounds. Its physical appearance is non-soluble and therefore, can reflect part of the UV radiation. Recent research indicates that the new microsized forms of physical blockers may also function in part by absorption. Sometimes referred to as nonchemical sunscreens, they may be more appropriately designated as inorganic particulate sunscreen ingredients. Examples of physical blockers include zinc oxide, titanium dioxide and red petrolatum. Most physical blockers are currently being use in conjugation with organic UV filters to achieve high sun protection factors (SPF).

These metallic oxides (TiO_2 and ZnO) have been found to be highly protective against harmful UV rays because they mobilize electron within their atomic structure while absorbing UV [14,15]. However, because of the semiconductor properties of them, they have been increasingly used as photocatalysts for the degradation of organic pollutants in wastewaters [16]. Since, by their nature, sunscreen preparations are exposed to sunlight, the photocatalytic behavior of these blockers needs to be considered. There are many reports which affirm that photoexcited titanium dioxide can cause cell death both *in vitro* and *in vivo* [17].

B. Chemical absorbers

These chemicals absorb the harmful ultraviolet radiation. They are classified into either UVA or UVB blockers, depending upon the type of radiation they can absorb. Chemical sunscreens are generally single or multiple aromatic structures, sometimes conjugated with carbon-carbon double bonds and/or carbonyl moieties.

In 1999 the US Food and Drug Administration published a monograph for sunscreens, which enables manufacturers to market sunscreens as over-the-counter products. This monograph covers aspects of sunscreen production and marketing such as acceptable ingredients, doses, formulation, and labeling. The sixteen approved active sunscreen ingredients, their respective maximum allowable concentrations, and their ranges of UV protection are listed in Table 1.1 [18,19].

Table 1.1 Approved sunscreen ingredients

Medicinal ingredient	Allowable concentration, %	Range of protection
Chemical absorbers		
<i>p</i> -Aminobenzoic acid	up to 15	UVB
Cinoxate	up to 3	UVB
Homosalate	up to 15	UVB
Octocrylene	up to 10	UVB
Octyl methoxycinnamate	up to 7.5	UVB
Octyl salicylate	up to 5	UVB
Padimate O	up to 8	UVB
Phenylbenzimidazole sulfonic acid	up to 4	UVB
Trolamine salicylate	up to 12	UVB
Dioxybenzone	up to 3	UVB, UVA-II
Oxybenzone	up to 6	UVB, UVA-II
Sulisobenzone	up to 10	UVB, UVA-II
Menthyl anthranilate	up to 5	UVA-II
Avobenzone	up to 3	UVA-I
Physical blockers		
Titanium dioxide	up to 25	UVB, UVA-II
Zinc oxide	up to 25	UVB, UVA-II, UVA-I

1.2 Mechanism of chemical absorber

In general chemical absorbers usually contain an aromatic ring conjugated with a carbonyl group. Often an electron-releasing group such as amine or methoxy group, is substituted in the ortho- or para- position of the aromatic ring. In other words, these molecules contain conjugated systems those allow electron delocalization upon absorption of photons. They absorb the harmful (high-energy) UV rays and the energy lost results in conversion of the remaining energy into longer lower energy wavelengths with return to ground state. Figure 1.3 shows the mechanism of UV-absorbers.

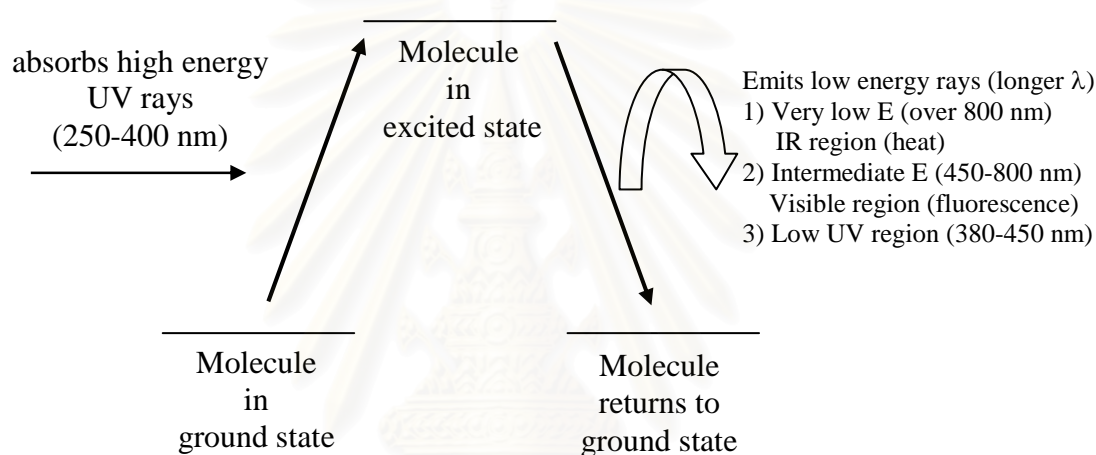


Figure 1.3 Schematic representation of process in which a sunscreen chemical absorbs the harmful high-energy rays and renders them relatively harmless low energy rays

1.3 Literature reviews

The International Agency for Research on Cancer (IARC) of the World Health Organization (WHO) concluded that sunscreens should be only one part of a comprehensive sun avoidance strategy [20]. Sunscreen chemicals are incorporated into a wide range of everyday hair and skin products and may therefore be used without the wearer making a conscious decision to apply a sunscreen. Safety of sunscreens has remained a major topic of discussion, so several reports have appeared in the literature regarding allergy and photoallergy to sunscreens.

1.3.1 Absorption of sunscreen

The ideal sunscreen should situate on skin (in epidermal layer) to help shielding the UV light, however, many reports have demonstrated transdermal absorption of organic UV filters including cinnamate derivatives.

In 1995, Leweke and Lippold [21] detected the absorption of isoamyl-4-methoxycinnamate into the human skin. Similarly, in 1995 Hanny and Nagel [22] reported the detection of sunscreen agents including 2-ethylhexyl-*p*-methoxycinnamate (EHMC) in human breast milk. In 1997, Hayden and coworkers [23] could not detect EHMC in urine of volunteers after applied a commercially sunscreen product about 48 hours. These studies agreed with the hydrophobic nature of EHMC.

In 1999, Gupta and coworkers [24] studied percutaneous absorption of sunscreens through Micro-Yucatan pig skin *in vitro* and evaluate the influence of formulation differences by diffusion cell technique. They observed that EHMC reached the stratum corneum layer (SC) within an hour and the amount penetrated into viable skin and receptor fluid increased slowly over time. Hydro-alcoholic formulation showed higher penetration rates than the oil base, diisopropyl adipate, vehicle formulation.

In 2000, Potard and coworkers [25] studied absorption and penetration of five UV filters including EHMC on excised fresh human skin *in vitro* by using the stripping technique. EHMC could slightly penetrate into the skin.

In 2003, Chatelain and coworkers [26] compared the skin penetration of UV filters from two vehicles; oil-in-water (o/w) emulsion gel and petrolatum jelly using Franz-cells and a tape-stripping method. They found that the amount of UV filters retained in the SC was significantly higher with the o/w emulsion gel than with the petrolatum jelly.

In 2004, Sarveiya and coworkers [27] studied the skin penetration and systemic absorption of sunscreen filters after topical application to human volunteers by using liquid chromatographic assay and diffusion cell. EHMC was highly recovered in phosphate buffer, plasma and epidermis layer.

In 2006, Hanson and coworkers [28] studied sunscreen enhancement of UV-induced reactive oxygen species (ROS) in the skin by using the fluorescent ROS indicator dihydrorhodamine (DHR) to find ROS levels in the nucleated epidermis after the application of the UV filters (octocrylene, EHMC and benzophenone-3).

Their result show that the UV filters applied to the skin surface not only lose their screening capability after a period of incubation, but also may lead to enhanced ROS generation in nucleated epidermis through photogeneration.

1.3.2 Photostability of sunscreen

Photostability refers to the ability of a molecule to remain intact with irradiation. As mentioned earlier, the photoactivated sunscreen molecule that absorbs UV radiation must dissipate or convert the absorbed energy. Three pathways are available, namely radiative decay (emission), non-radiative decay (heat) and photochemistry i.e., an excited molecule undergoes photochemical changes that may lead to its breakdown and generate photoproducts that may no longer provide protection and that may cause allergies or photoallergies [29].

The lack of photostability of chemical organic UV filters is now recognized as a common problem for organic absorbers [20,30,31]. This change has also been observed with 2-ethylhexyl-*p*-methoxycinnamate (EHMC).

In 1999, Tarras-Wahlberg and coworkers [32] reported that butylmethoxy dibenzoylmethane, octyl dimethyl PABA and EHMC were not stable against UV irradiation. Their UV absorbance decreased rapidly upon exposure to UV light.

In 2001, Pattanaargson and Limpong [33] affirmed that a *trans* to *cis* configurational change of EHMC does occur upon light exposure and its photoisomerized product, *cis*-EHMC, was isolated (Figure 1.4) and its molar absorption coefficient (ϵ) was determined. The ϵ value of *cis*-EHMC is about only half of that of *trans*-EHMC. This explains the decrease in absorption property of EHMC upon UV exposure. Similar findings were reported by group of Sayre in 2005 [34].

In 2002, Serpone and coworkers [35] examined the photostability of commercially available sunscreen lotions and their active ingredients. The loss of filtering efficacy can occur because of the possible photochemical modifications of the sunscreen active agents. Photodegradation of EHMC was rather significant in the most polar solvent and the presence of oxygen was rapidly photodegraded.

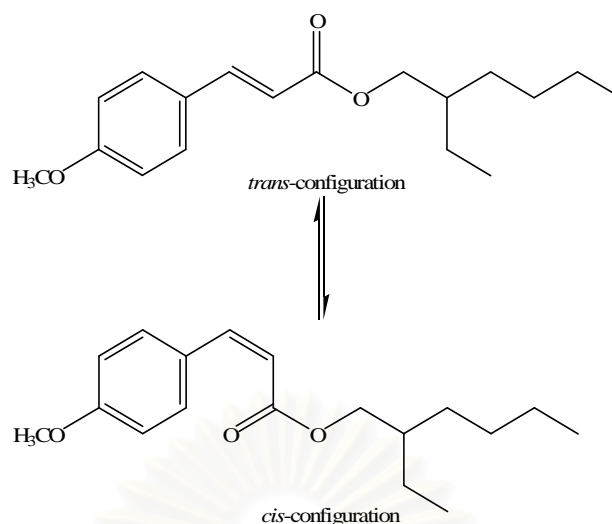


Figure 1.4 Conversion of *trans*-EHMC to *cis*-EHMC after exposure to UV radiation

In 2007, Huong and coworkers [36] studied the photoisomerization of EHMC under various conditions; by irradiating diluted solution using various solvents. The results show that isomerization is rapid and that the relationship of the two isomers depends more on their chemical environment than on the actual irradiation power. Rapid isomerization very probably occurs at the skin surface under the normal use of sunscreens.

1.4 Development of sunscreen: EHMC

Sunscreen preparations are usually applied to large skin areas to prevent sunlight-induced erythema. Therefore, effectiveness implies that sunscreens adhere to skin like a protective film. They should have a high affinity for the stratum corneum (SC). The UV filters are designed to remain on the uppermost layers of the skin; penetration through the skin should be low to achieve the highest protective effect and reduce the toxicological risk resulting from their percutaneous penetration. The ideal medium must provide not only the necessary solubility, but also maintain contact between the filters and the skin.

The vehicles of formulation have a dramatic influence on the evolution of sunscreen chemicals. Most of them offer several advantages, however there are numerous factors to consider with like water solubility, instability and so on. Therefore, there is a need for the development of new sunscreen systems which achieve an important remanence, and a reduced penetration into the skin.

Encapsulation is the one choice; in 2001, Roman and coworkers [37] studied photoprotection of prepared biodegradable polymer nanocapsules, poly(ϵ -caprolactone) containing EHMC. The EHMC-nanocapsules provided partial protection against UV-induced erythema, in a manner significantly better than a conventional gel. In 2002, Perugini and coworkers [38] investigated the influence of nanoparticle-based systems, ethylcellulose (EC) and poly-D,L-lactide-co-glycolide (PLGA) on the light-induced decomposition of EHMC. PLGA nanoparticles loaded with *trans*-EHMC improve the photostability of this sunscreen agent.

The encapsulated EHMC to poly(ϵ -caprolactone) and cellulose acetate phthalate (CAP) were performed to investigate the transdermal permeation and skin accumulation by groups of Jimenez [39] and Martinez [40]. Similar results show the low penetration of EHMC-nanocapsules *in vitro* and *in vivo*, respectively.

In 2002, Godwin and coworkers [41] determined the influence of Trancutol[®]CG (diethyleneglycol monoethyl ether) which was added in sunscreen formulation on the transdermal permeation and skin accumulation of sunscreen EHMC. Then, Group of Scalia [42] investigated the effect of β -cyclodextrin (β -CD) and hydroxypropyl- β -cyclodextrin (HP- β -CD) on the base-catalyzed degradation light-induced decomposition of EHMC. The complex of β -CD with *trans*-EHMC enhances the chemical- and photo-stability of EHMC.

Solid lipid microspheres (SLM) which is another controlled release system was applied to EHMC by Yener and coworkers [43]. In this work, they prepared solid lipid microspheres of EHMC and studied the release, penetration and photostability of EHMC in SLM. The rate of penetration was significantly dependent upon the formulation and could be decreased in SLM formulation. Additionally, photostability was shown to be improved in this form.

In 2006, Gaspar and Campos [44] evaluated the photostability of four different UV filter combinations in a sunscreen by using HPLC analysis and spectrophotometry. The four UV filter combinations showed different photostability profiles and the best one was formulation containing octocrylene (OC) which as a good UV stabilizer.

Another methodology in reducing sunscreen transdermal absorption is to use less UV filter in the formulation. This can be done by using SPF enhancer. It can increase the skin's protection ability with less amount of UV absorber used. This

method was demonstrated by group of Hossel [45] in which the N-vinylimidazole polymer was prepared and used as SPF enhancer in the formulation.

1.5 Polymeric UV filter

At present, research as far as sunscreens concerned moves towards the conception of new cosmetic formulas, which have a total innocuity, a small capacity to overcome the skin barrier, a good substantiality and an important remanence.

Hence, sunscreen polymers are introduced as the new generation for cosmetics, especially for UV blockers for the use on human skin and/or hair. Various types of polymers have been tested because of their previously demonstrated safety with other applications. These large molecular weight compounds achieve almost no penetration beyond the stratum corneum, thereby limiting unfavourable side effects such as inflammation. Traditional polymeric enhancers have included benzalkonium chloride and hexadecylpyridinium bromide type polymers (PEG/PDMS) [46]. Recently, the group of Nagase and coworkers [47] have demonstrated the enhancing properties of polyethylene glycol or polydimethylsiloxane block copolymer with a cationic end-group. Furthermore, this polymer has been shown to have enhancement activity for both hydrophilic and hydrophobic drugs. They suggested that the mechanism of action was limited to an increase in the partition coefficient at the skin surface rather than a change in the diffusion coefficient of the skin.

Although polymers described above do not absorb UV themselves, they help retain small UV filter molecules on the upper skin layers. Another approach is to make polymers with UV absorption property themselves. In 2004, Pattanaargson and coworkers [48] studied the grafting of EHMC absorption chromophore, 4-methoxycinnamoyl moieties, onto silicone polymer to produce suncreening polymer that can be effectively retained on skin surface.

Photostability test indicated that both [3-(*p*-methoxycinnamido)propyl] (methyl)-dimethylsiloxane copolymer, (I) and poly[(methyl)(octyl)(methyl)(propyl-4-methoxycinnamate siloxane)], (II) (Figure 1.5) were more photostable than free EHMC. The large size of sunscreen molecule making them possess much lower skin permeation than free EHMC.

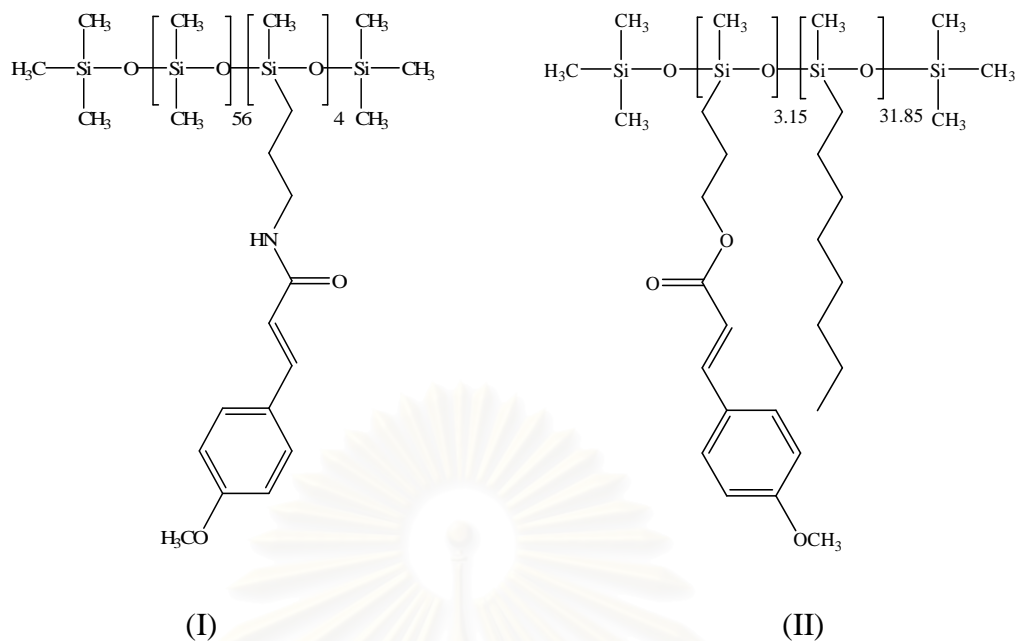
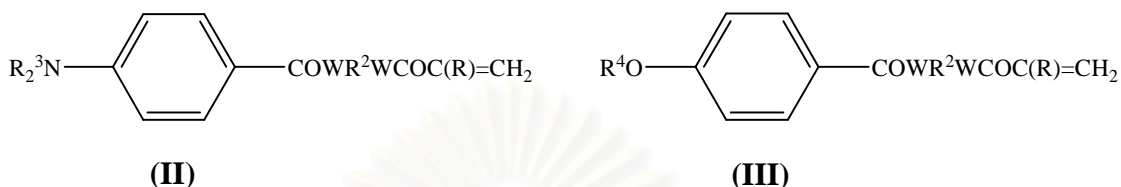
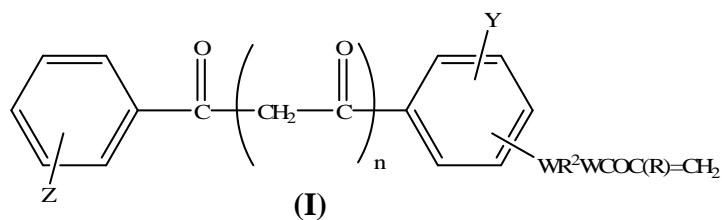


Figure 1.5 Chemical structure of (I) [3-(*p*-methoxycinnamido)propyl](methyl)-dimethylsiloxane copolymer, G-AS and (II) poly[(methyl)(octyl)(methyl)(propyl-4-methoxycinnamate siloxane)], G-MHS respectively

In US Patent No. 5,487,885 (1996), Sovak and coworkers [49] prepared a novel sun blocking polymeric compositions which have UVA, UVB and UVC absorbing moieties on the acrylic backbone by combining the individual monomers under addition polymerizing conditions. UVA absorbers monomer is benzophenones or bis-benzoylmethane compounds (I), UVB absorbers monomer is benzoyloxy derivatives, substituted benzoyloxy derivatives or *p*-amino substituted benzoyloxy derivatives (II) and UVC absorbers monomer is oxybenzoyl derivatives bonded to an acryl group through a divalent bridging moiety (III). The polymer is insoluble in water and swellable in a polyethylene glycol-water composition comprising about 50-95% polyethylene glycol. The structure is shown below:



wherein: n is 0 or 1

R is H, alkyl of from 1 to 3, usually 1 to 2, which may be substituted with a functional group having from 1 to 2 heteroatoms, which are N or O

R² is H, alkyl of up to 6 carbon atoms

R³ is a divalent hydrocarbylene group

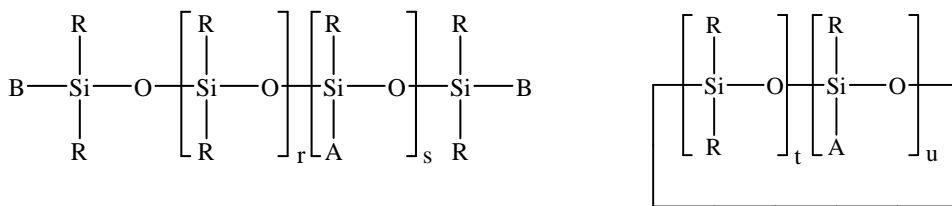
R⁴ is H, alkyl of from 1 to 6 carbon atoms

W is oxy or amino

Y is non-oxo carbonyl of not more than about 12 carbon atoms

Z is oxy or amino of not more than about than about 12 carbon atoms

In US Patent No. 6,080,880 (2000), Richard and coworkers [50] provisioned a novel compound by grafting cinnamamide, benzalmalonamide or benzalmalonate group onto a short-chain silicone molecule. These compounds have a very high-performance screening property and very good solubility in the usual organic solvents and in particular fatty substances such as oils, as well as excellent cosmetic properties, which render them particularly suitable for use as sunscreens. In addition, these compounds have an excellent intrinsic screening power with regard to UVA and UVB radiation.



wherein: R,B is methyl

r is 0 or 1

s is 1

t+u ranges from 3 to 5

n is 0 or 1

Z is H, alkyl or $-(C=O)XR_2$ or $-(C=O)YW$

X,Y is O or $-NR_3$

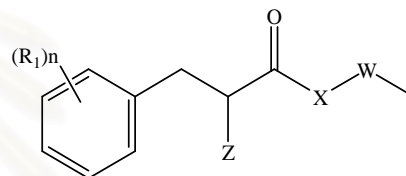
W is alkyl substituted with -OH

R₁ is methoxy

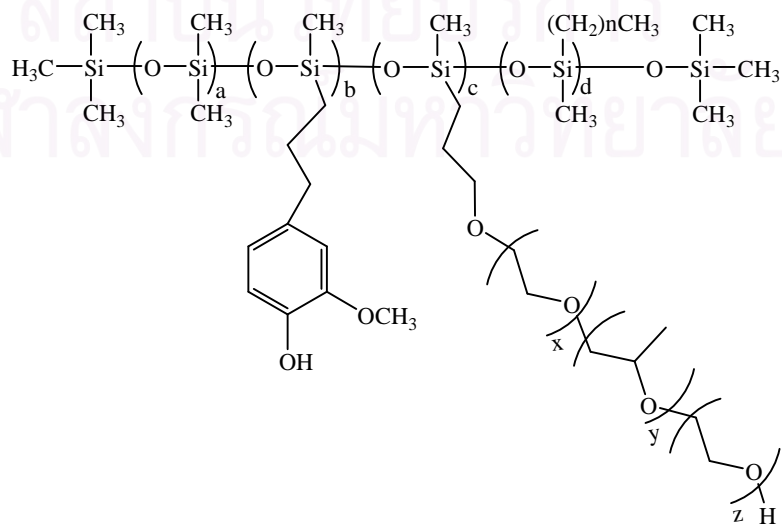
R₂ is methyl or ethyl

R₃ is H

A is



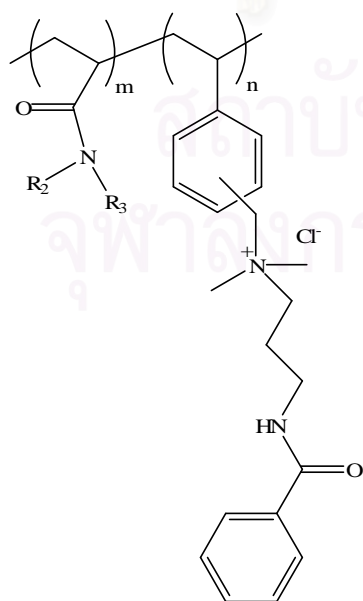
In US Patent No. 6,346,595 (2002), O'Lenick and Dacula [51] provided a series of novel silicone compounds that contain a UV absorber, derived from eugenol, (2-methoxy-4-(2-propenyl)phenol), and a dimethicone copolyol group. The dimethicone copolyol group functions not only to alter the UV absorption properties of the compounds making them acceptable UVB screens, but also modifies the solubility of the silicone compounds making them acceptable for formulation into water, silicone and oil phases. The higher molecular weight of the compounds make it stay on the skin surface, rather than penetrate through the skin.



wherein: a is an integer ranging from 0 to 2000;
 b is an integer ranging from 1 to 20;
 c is an integer ranging from 1 to 20;
 d is an integer ranging from 0 to 20;
 n is an integer ranging from 10 to 20;
 w is an integer ranging 0 to 20;
 x is an integer ranging 0 to 20;
 y is an integer ranging 0 to 20;
 z is an integer ranging 0 to 20.

In US Patent No. 7,087,692 B2 (2006), Koshti and coworkers [52] synthesized water soluble macromolecules with cinnamido and benzamido moieties to provide UV absorption and improve levels of substantivity especially during an activity like swimming. These macromolecules have cationic centres which help enhance substantivity.

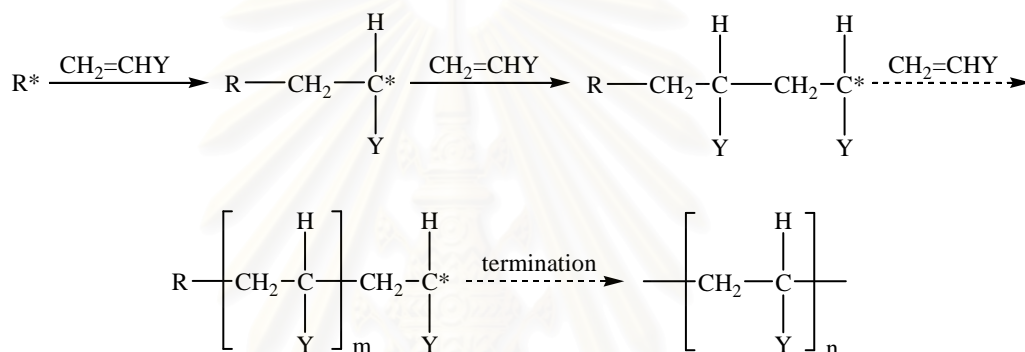
The synthesized water-soluble polymers have a lower critical solution temperature (LCST) of 30°C. When these water-soluble polymers are applied to skin, the temperature of body as well as the temperature of surrounding and the salt content of water (in case of swimming in the sea) make them insoluble and hence do not get easily washed off either by sweat or sea water. However, they can be easily removed by plain water at ambient temperature (25°C).



wherein: R_2 and R_3 are selected from H, alkyl and cycloalkyl group containing from 1 to 6 carbon atoms;
 m is an integer from 5 to 9;
 n is an integer between 1 to 5;
 $m+n$ is an equal to 10.

1.6 Chain polymerization

Chain polymerization is a type of polymerization where an initiator is used to produce an initiator species R^* with a reactive center. The reactive center may be either a free radical, cation, or anion. Polymerization occurs by the propagation of the reactive center by the successive additions of large numbers of monomer molecules in a chain reaction. The distinguishing characteristic of chain polymerization is that polymer growth takes place by monomer reacting only with the reactive center. Monomer does not react with monomer and the different-sized species such as dimer, trimer, tetramer and n -mer do not react with each other. By far the most common example of chain polymerization is that of vinyl monomers.



Each monomer molecule that adds to a reactive center regenerates the reactive center. Polymer growth proceeds by the successive additions of hundreds or thousands or more monomer molecules. The growth of the polymer chain ceases when the reactive center is destroyed by one or more of a number of possible termination reactions.

In the typical chain polymerizations, the relationship between polymer molecular weight and the percent conversion of monomer will show the presence of high-molecular-weight polymer molecules at all percents of conversion. There are no intermediate-sized molecules in the reaction mixture but only monomer, high-polymer and initiator species. The only change that occurs with conversion (i.e., reaction time) is the continuous increase in the number of polymer molecules [53] (Figure 1.6).

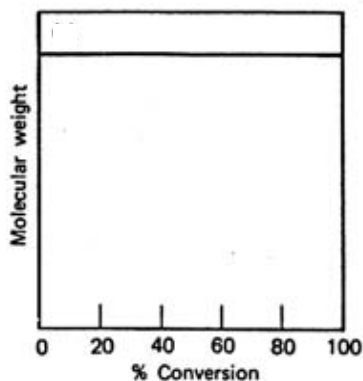


Figure 1.6 Variation of molecular weight with conversion of chain polymerization

1.7 Polymer with cinnamate

The photochemistry of cinnamates involves two photoreactions upon irradiation in the UVB region: the *trans-cis* isomerization that is favored in the early stages of UV irradiation and the photodimerization leading to the formation of a cyclobutane ring. Therefore, The polymers with cinnamate pendant group have attained much attention because of their photochemistry suit for using as photosensitive materials, for example liquid crystalline devices (LCD), microelectronics, integrated circuits, negative photoresists etc. The capability of these polymers is photoactivated due to carbon-carbon double bonds of the α,β -unsaturated carbonyl groups which undergo $[2\pi+2\pi]$ cycloaddition reactions under irradiation [54-56] (Figure 1.7).

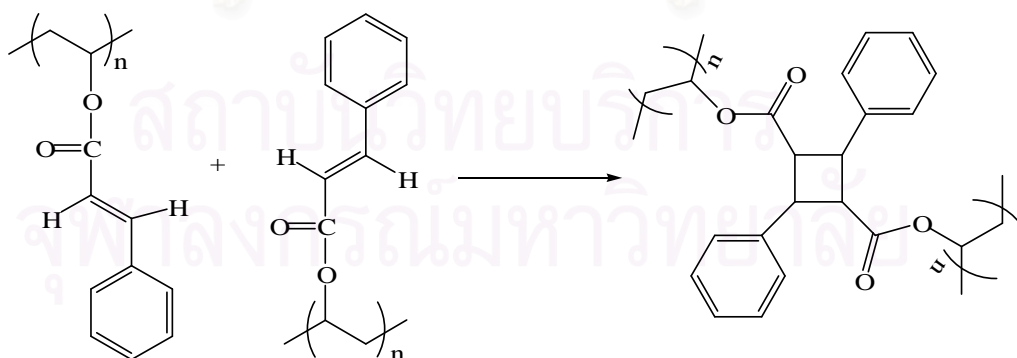


Figure 1.7 Photochemical reactions of the polymers with cinnamate pendant group

The esterification of poly(vinyl alcohol), poly(vinyl alcohol-*co*-vinyl-*trans*-cinnamate), has been prepared by the polymer reaction of poly(vinyl alcohol) and cinnamoyl chloride by Tsutsumi and coworkers in 2003 [57]. (Figure 1.8) This research was performed to producing the polymer-hydroxyapatite (HAP) composite for applying in hard tissue engineering scaffold materials for bone and teeth.

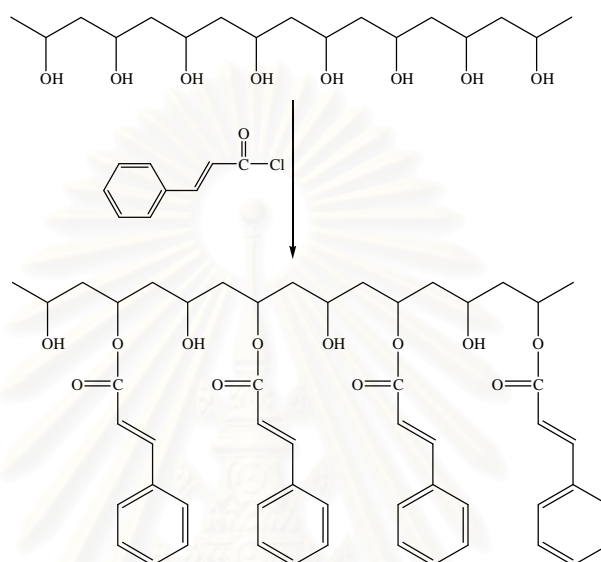


Figure 1.8 Synthesis of poly(vinyl alcohol-*co*-vinyl-*trans*-cinnamate) by esterification of poly(vinyl alcohol)

In 2002, Chae and coworkers [58] synthesized the poly(methyl-4-methacryloyloxy)cinnamate) (PMMCi) by free radical polymerization with 2,2'-azobis-isobutyronitrile (AIBN). They have examined the photochemistry of PMMCi in films and determined the reorientation sequence of the chromophore and its photoproducts during photoreaction in the film by using 2D correlation analyzes of the FTIR and UV-Vis spectroscopy. The similar method to synthesize polymer with cinnamate pendant group was done by Balaji and coworkers in 2004 [59]. They investigated thermal stability, photoreactivity and influence of various factors on the rate of photocrosslinking of poly(4-acryloyloxyphenyl-3-chlorostyryl ketone), poly(APCSK) and poly(4-acryloyloxyphenyl-3-chlorostyryl ketone-*co*-glycidyl methacrylate), poly(APCSK-*co*-GMA). As well as in 2006, Mahy and coworkers [60] prepared the new photosensitive polymers, poly(α -cynao-4-(methacryloxy) cinnamate) and poly((α -cynao-4-(methacryloxy)cinnamate-*co*-methyl methacrylate),

to study reactivity of the synthesized monomer compared with methyl methacrylate and photoreactivity by free radical polymerization.

1.8 Research goal

Although *p*-methoxycinnamate is the widely used organic UV filter in cosmetic industry, as mentioned earlier, the compound still possesses few problems including absorption through human skin and the photoinstability. Few methods have been proposed to reduce skin penetration of this sunscreen [39-41,48]. However, transdermal permeation of the sunscreens cannot be totally blocked. To solve both transdermal absorption and photostability problems, oligomeric materials containing UV absorbing property were prepared in this work. With a higher molecular weight, transdermal absorption should be considerably decreased. In addition, the absence of *cis-trans* isomerizable chromophore, the polymers should be more stable under UV radiation.



CHAPTER II

EXPERIMENTAL

2.1 Instruments and equipments

Thin layer chromatography (TLC) was performed on aluminium sheets precoated with silica gel (Merck Kieselgel 60 F254) (Merck KgaA, Darmstadt, Germany). Column chromatography was performed in silica gel (Merck Kieselgel 60 G) (Merck KgaA, Darmstadt, Germany) and sephadex (SephadexTM LH-20) (Amersham Biosciences AB, Uppsala, Sweden). Broad band UVA (320-400 nm) was generated by F24T12/BL/HO (PUVA) lamp (National Biological Corporation, Twinsburg, Ohio, USA) and broad band UVB (280-320 nm) was generated by FSX24T12/UVB/HO lamp (National Biological Corporation, Twinsburg, Ohio, USA). UV irradiance was measured using UVA-400C and UVB-500C power meter (National Biological Corporation, Twinsburg, Ohio, USA).

The FT-IR spectra were recorded on a Nicolet Fourier Transform Infrared spectrophotometer: Impact 410 (Nicolet Instruments Technologies, Inc. WI, USA). Solid samples were incorporated into a pellet of potassium bromide. Liquid samples were dropped on sodium chloride cell. The ¹H- and ¹³C-NMR spectra were obtained in deuterated chloroform (CDCl₃) with tetramethylsilane (TMS) as an internal reference using Varian Mercury NMR spectrometer which operated at 400.00 MHz for ¹H and 100.00 MHz for ¹³C nuclei (Varian Company, CA, USA). Molecular weights were determined by gel permeation chromatography: Waters styragel HR columns, Waters 600E Multisolvent Delivery System (Waters, MA, USA). Glass transition temperature and melting temperature were determined by differential scanning calorimetry: Netzsch DSC 204 (Netzsch, Germany). UV spectra were obtained with the aid of UV 2550 UV/VIS spectrophotometer (Shimudzu Corporation, Kyoto, Japan), using a quartz cell with 1 cm pathlength. ESI-MS analyses were performed with Waters Micromass Quattomicro API ESCi (Waters, MA, USA). Samples were dissolved in CH₃CN and directly injected into the mass spectrometer. Refractive index was determined by refractometer: Abbe Refractometer 1T (Atago, Tokyo, Japan) using a sodium light source.

2.2 Chemicals

Solvents used in syntheses and spectroscopic techniques were reagent or analytical grades purchased from Labscan (Bangkok, Thailand). Solvents used in column chromatography were purified from commercial grade solvents prior to use by distillation. Ethylhexyl-*p*-methoxycinnamate was kindly obtained from Merck Co., Ltd. (Bangkok, Thailand). Chemicals used in the experiment were purchased from various sources, detailed as follows:

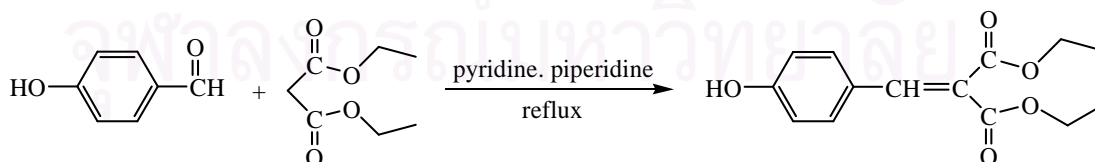
- Acros Organics (New Jersey, USA): chloroform-D1, copper(II)acetate, dibenzoyl peroxide 75% remainder water, 1,2-dibromoethane, 1-(3-dimethylaminopropyl)-3-ethylcarbodiimide hydrochloride (EDCI), 4-hydroxy benzaldehyde, N-hydroxysuccinimide and potassium *tert*-butoxide
- Aldrich Chemical Company (Steinheim, Germany): tetrabutylammonium sulfate 50 wt.% solution in water and tetravinyltin
- Carlo Erba Reagent (Milan, Italy): ammonium acetate and pyridine
- Fluka Chemical Company (Buchs, Switzerland): allyl bromide, 2,2'-azo-bis-isobutyronitrile (AIBN), 2-ethyl-1-hexanol, malonic acid, potassium carbonate and *p*-toluene sulfonic acid
- Merck Co. Ltd. (Darmstadt, Germany): diethylmalonate and sodium sulfate (anhydrous)
- Sigma Chemical Company (Missouri, USA): piperidine.

2.3 Synthesis of poly(diethylbenzmalonate-4-vinyl ether)

2.3.1 Preparation of diethylbenzmalonate-4-vinyl ether monomer

Pathway I

Step I: Preparation of diethyl-4-hydroxy benzmalonate [61]

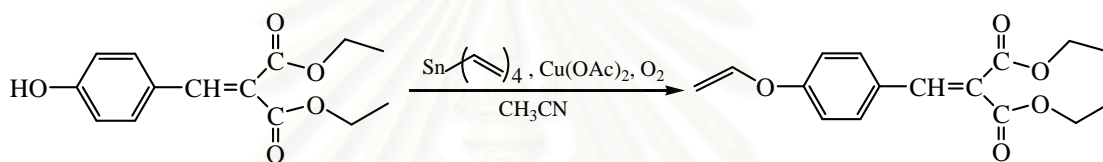


Diethyl malonate (2.42 g, 15 mmol) was dissolved in pyridine (50 mL) and 4-hydroxy benzaldehyde (1.84 g, 15 mmol) and piperidine (6.39 g, 75 mmol) were added. The mixture was refluxed for 4 hours at 80°C. After the mixture had been cooled, the solution was washed with water (3×50 mL), 15% aqueous hydrochloric

acid (2×40 mL), and saturated sodium bicarbonate (40 mL). The organic solution was dried with anhydrous sodium sulfate and the solvent was removed under reduced pressure.

Diethyl-4-hydroxy benzalmalonate: brown solid (55%), R_f 0.24 (40% EtOAc/Hex), IR (KBr, cm^{-1}): 3580-2795, 2937, 1715, 1684, 1598, 1509, 1446, 1365, 1256 and 1166 (Figure B.2); $^1\text{H-NMR}$ (CDCl_3) δ (ppm): 7.65 (s, 1H, ArCH=), 7.35 (d, 2H, ArH, $J = 8.6$ Hz), 6.82 (d, 2H, ArH, $J = 8.6$ Hz), 5.94 (br, 1H, OH), 4.38-4.26 (m, 4H, 2×OCH₂) and 1.32 (t, 6H, 2×CH₃, $J = 7.0$ Hz) (Figure B.1)

Step II: Preparation of diethylbenzalmalonate-4-vinyl ether [62]



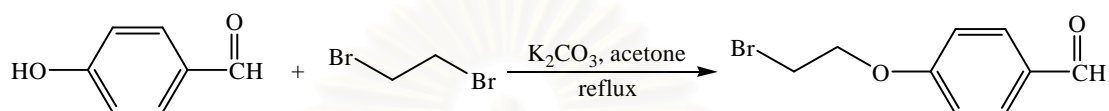
Into a septum-capped flask, anhydrous $\text{Cu}(\text{OAc})_2$ (0.51 g, 2.81 mmol) was added to a solution of diethyl-4-hydroxy benzalmalonate (0.53 g, 2.01 mmol) in acetonitrile (28 mL). Negative pressure was applied to the mixture to remove most of the air. After that, dry oxygen was introduced via a balloon fitted with a needle. Tetravinyltin (0.52 mL, 2.86 mmol) was then added to the blueish mixture that subsequently faded to a greenish color. After 92 hours at 60°C, the resulting dark green mixture was poured into aqueous 25% ammonium acetate solution (50 mL). After 15 minutes of stirring, the aqueous layer was extracted with ethyl acetate (3 times). The combined organic layers were washed with brine, dried with anhydrous sodium sulfate and concentrated. The product was further purified by a silica gel column using 20:80 (v/v) hexane:dichloromethane as an eluent.

Diethylbenzalmalonate-4-vinyl ether: pale yellowish oil (67%), R_f 0.53 (40% EtOAc/Hex), IR (neat, cm^{-1}): 2980, 1723, 1637, 1594, 1501, 1380, 1248, 1205, 1170 and 1061 (Figure B.14); $^1\text{H-NMR}$ (CDCl_3) δ (ppm): 7.67 (s, 1H, ArCH=), 7.44 (d, 2H, ArH, $J = 8.6$ Hz), 6.99 (d, 2H, ArH, $J = 8.6$ Hz), 6.67-6.62 (m, 1H, CHOAr), 4.87 (dd, 1H, CH₂CHO, $J = 14.4, 1.6$ Hz), 4.54 (dd, 1H, CH₂CHO, $J = 6.4, 1.6$ Hz), 4.37-4.27 (m, 4H, 2×OCH₂) and 1.32 (t, 6H, 2×CH₃, $J = 7.0$ Hz) (Figure B.12);

^{13}C -NMR (CDCl_3) δ (ppm): 166.8, 164.2 (2 \times -COOR), 158.5 (C-4 aro), 146.8 (=CHOAr), 141.2 (Ar-CH=), 131.4 (C-2 and C-6 aro), 127.4 (C-1 aro), 124.8 (=C(COOR) $_2$), 116.8 (C-3 and C-5), 97.0 (CH_2 =), 61.7, 61.5, 14.1 and 13.9 (alkyl carbons) (Figure B.13)

Pathway II

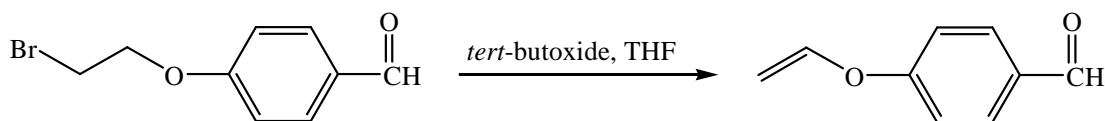
Step I: Preparation of 4-((2-bromo)ethoxy)benzaldehyde [63]



The mixture of 4-hydroxy benzaldehyde (3.66 g, 0.03 mol), dibromoethane (67.67 g, 0.36 mol), anhydrous potassium carbonate (20.74 g, 0.15 mol), and acetone (60 mL) in a round-bottomed flask is refluxed at 57°C on a sand bath for 4 hours. The mixture was then cooled and solvent was evaporated under reduced pressure. The resulting residue was added with water (200 mL) and extracted with dichloromethane (3 \times 100 mL). The combined extracts were washed with sodium bicarbonate (100 mL) and dried with anhydrous sodium sulfate. The product was further purified by a silica gel column using 35:65 (v/v) hexane:dichloromethane as an eluent.

4-((2-Bromo)ethoxy)benzaldehyde: White needle (68%), R_f 0.38 (65% $\text{CH}_2\text{Cl}_2/\text{Hex}$), IR (KBr, cm^{-1}): 2797, 2727, 1684, 1602, 1575, 1501, 1423, 1248, 1162, 1065, 1007 and 645 (Figure B.5); ^1H -NMR (CDCl_3) δ (ppm): 9.90 (s, 1H, ArCHO), 7.85 (d, 2H, ArH, $J = 8.4$ Hz), 7.02 (d, 2H, ArH, $J = 8.4$ Hz), 4.38 (t, 2H, CH_2OAr , $J = 6.4$ Hz) and 3.67 (t, 2H, CH_2Br , $J = 6.4$ Hz) (Figure B.3); ^{13}C -NMR (CDCl_3) δ (ppm): 190.7 (ArCOH), 163.0 (C-4 aro), 132.0 (C-2 and C-6 aro), 130.4 (C-1 aro), 114.8 (C-3 and C-5 aro), 67.9 (CH_2OAr) and 28.4 (CH_2Br) (Figure B.4)

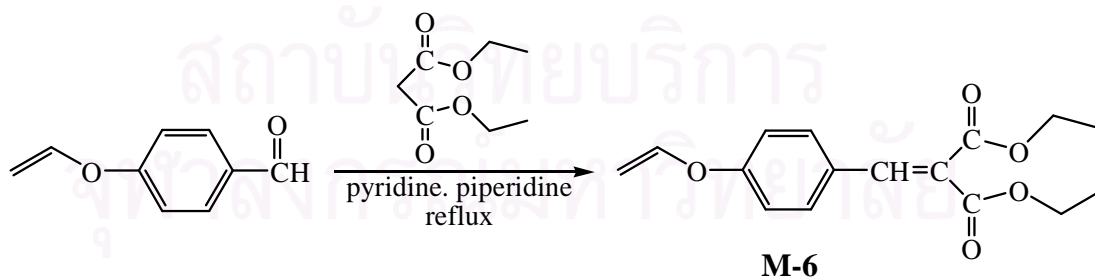
Step II: Preparation of 4-vinyloxybenzaldehyde [64]



The mixture of 4-((2-bromo)ethoxy)benzaldehyde (4.70 g, 0.02 mol) and potassium *tert*-butoxide were dissolved in freshly distilled tetrahydrofuran (80 mL) and stirred for 2 hours and 30 minutes under the nitrogen atmosphere. Four sets of reaction were carried out; at 4°C, 10°C, 15°C and room temperature. The reaction was quenched by adding water (60 mL) and diethyl ether (40 mL). The organic layer (40 mL) was washed again with water (60 mL) and then dried with anhydrous sodium sulfate and concentrated under reduced pressure. The product was further purified by a silica gel column using 45:55 (v/v) hexane:dichloromethane as an eluent.

4-Vinyloxybenzaldehyde: pale yellowish oil (50%), R_f 0.35 (55% $\text{CH}_2\text{Cl}_2/\text{Hex}$), IR (neat, cm^{-1}): 2921, 1684, 1637, 1598, 1509, 1240 and 1162 (Figure B.8); $^1\text{H-NMR}$ (CDCl_3) δ (ppm): 9.93 (s, 1H, ArCHO), 7.87 (d, 2H, ArH, $J = 8.8$ Hz), 7.10 (d, 2H, ArH, $J = 8.8$ Hz), 6.72–6.68 (m, 1H, CHOAr), 4.95 (dd, 1H, CH_2CHO , $J = 14.4, 1.6$ Hz) and 4.63 (dd, 1H, CH_2CHO , $J = 5.6, 1.6$ Hz) (Figure B.6); $^{13}\text{C-NMR}$ (CDCl_3) δ (ppm): 190.9 (ArCOH), 161.6 (C-4 aro), 146.2 (CHOAr), 132.0 (C-2 and C-6 aro), 131.5 (C-1 aro), 116.6 (C-3 and C-5 aro) and 98.2 (CH_2CHO) (Figure B.7)

Step III: Preparation of diethylbenzalmalonate-4-vinyl ether; M-6 [61]



Diethyl malonate (0.69 g, 4.34 mmol) was dissolved in pyridine (25 mL) and 4-vinyloxybenzaldehyde (0.66 g, 4.43 mmol) and piperidine (1.90 g, 22.31 mmol) were added. The mixture was refluxed for 18 hours at 75°C. After the mixture had been cooled, the solution was washed with water (2×40 mL), 15% aqueous hydrochloric acid (2×30 mL), and saturated sodium bicarbonate (30 mL). The organic

solution was dried with anhydrous sodium sulfate and the solvent was removed under reduced pressure. The product was further purified by a silica gel column using 45:55 (v/v) hexane:dichloromethane as an eluent.

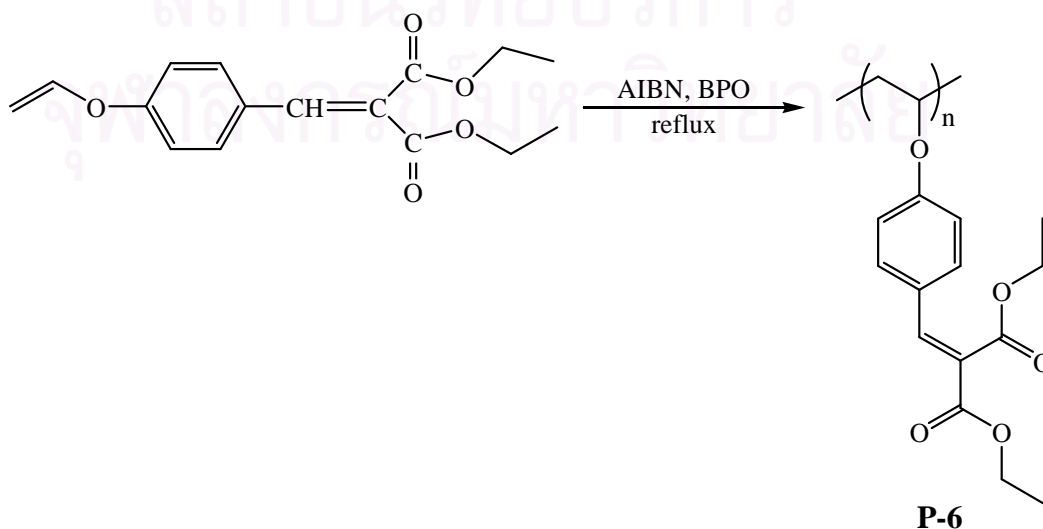
Diethylbenzalmalonate-4-vinyl ether: pale yellowish oil (61%), R_f 0.31 (55% $\text{CH}_2\text{Cl}_2/\text{Hex}$), $m/z = 290$ (Figure B.15), IR (neat, cm^{-1}): 2980, 1723, 1637, 1594, 1505, 1376, 1252, 1205, 1170 and 1069 (Figure B.14); $^1\text{H-NMR}$ (CDCl_3) δ (ppm): 7.67 (s, 1H, ArCH=), 7.44 (d, 2H, ArH, $J = 8.6$ Hz), 6.99 (d, 2H, ArH, $J = 8.6$ Hz), 6.67-6.62 (m, 1H, CHOAr), 4.87 (dd, 1H, CH_2CHO , $J = 14.4, 1.6$ Hz), 4.54 (dd, 1H, CH_2CHO , $J = 6.4, 1.6$ Hz), 4.37-4.27 (m, 4H, $2 \times \text{OCH}_2$) and 1.32 (t, 6H, $2 \times \text{CH}_3$, $J = 7.0$ Hz) (Figure B.12); $^{13}\text{C-NMR}$ (CDCl_3) δ (ppm): 166.8, 164.2 ($2 \times \text{-COOR}$), 158.5 (C-4 aro), 146.8 ($=\text{CHOAr}$), 141.2 (Ar-CH=), 131.4 (C-2 and C-6 aro), 127.4 (C-1 aro), 124.8 ($=\text{C}(\text{COOR})_2$), 116.8 (C-3 and C-5 aro), 97.0 ($\text{CH}_2=$), 61.7, 61.5, 14.1 and 13.9 (alkyl carbons) (Figure B.13)

2.3.2 Synthesis of poly(diethylbenzalmalonate-4-vinyl ether)

Step I: Recrystallization of the initiators; AIBN and BPO

2,2'-Azo-bis-isobutyronitrile (AIBN) and dibenzoyl peroxide (BPO) were dissolved in methanol or ethanol (the temperature of solvent was maintained at approximately 40°C). The clear solution was filtered and placed on an ice bath for crystallization process to take place. The white crystal was separated by suction filtration.

Step II: Polymerization of diethylbenzalmalonate-4-vinyl ether monomer; P-6 [58,59]



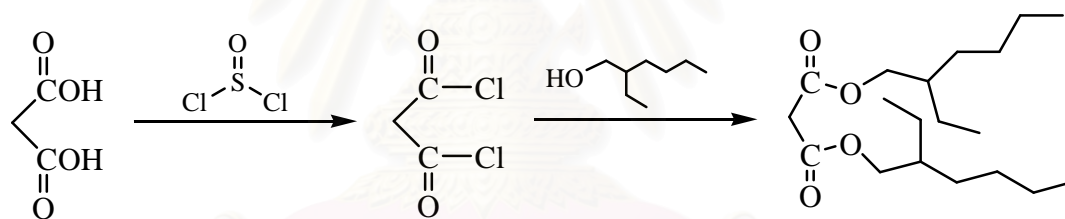
Diethylbenzmalonate-4-vinyl ether (262.70 mg, 0.91 mmol) and 2,2'-azobis-isobutyronitrile (AIBN) (45 mg, 0.27 mmol) or dibenzoyl peroxide (BPO) (40.90 mg, 0.17 mmol) were dissolved in toluene (9 mL). The solution was stirred at 85°C and 110°C, respectively for 15 minutes under a stream of dry nitrogen and then refluxed for 96 hours and 744 hours, respectively. The resulting mixture was cooled and the solvent was removed under reduced pressure. The product was further purified by a sephadex column using acetonitrile as an eluent.

Poly(diethylbenzmalonate-4-vinyl ether): pale yellowish solid, n_D 1.563, T_g 44.4°C (Figure B.23), IR (KBr, cm^{-1}) 2976, 1723, 1598, 1505, 1446, 1372, 1252, 1209, 1178 and 1061 (Figure B.22)

2.4 Synthesis of poly(di(2-ethylhexyl)benzmalonate-4-vinyl ether)

2.4.1 Preparation of di(2-ethylhexyl)benzmalonate-4-vinyl ether monomer

Step I: Preparation of di(2-ethylhexyl)malonate [65]

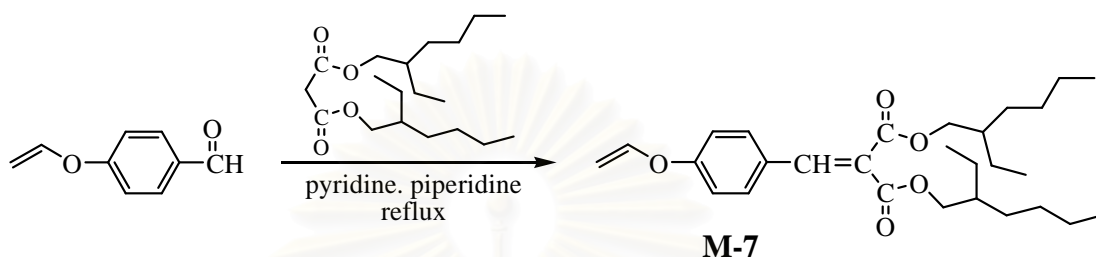


A mixture of malonic acid (1.60 g, 0.015 mol) and thionyl chloride was refluxed at 56°C. To the top of the condenser was attached an exit tube leading to a gas-absorption trap (K_2CO_3). A mixture was heated until no further evolution of hydrogen chloride (~17 hours). Then the remaining thionyl chloride was evaporated under reduced pressure before 2-ethyl-1-hexanol (4.70 mL, 0.03 mol) was added. The mixture was again refluxed at 70°C overnight. The reaction mixture was cooled and washed with water (3×40 mL) and saturated sodium bicarbonate (2×40 mL). The organic part was concentrated under reduced pressure. The product was further purified by a silica gel column using hexane:dichloromethane (gradient) as an eluent.

Di(2-ethylhexyl)malonate: pale yellowish oil (70%), IR (neat, cm^{-1}): 2941, 2863, 1742, 1462, 1380, 1322, 1267, 1147 and 1011 (Figure B.11); $^1\text{H-NMR}$ (CDCl_3) δ (ppm): 4.06-3.98 (m, 4H, $2\times\text{OCH}_2$), 3.34 (s, 2H, CH_2COO) and 1.57-0.83 (m, 30H,

$2\times\text{C}_7\text{H}_{15}$) (Figure B.9); ^{13}C -NMR (CDCl_3) δ (ppm): 166.7 ($2\times\text{-COOR}$), 67.8 (OCH_2), 41.7 (CH_2COO), 38.6, 30.2, 28.8, 23.6, 22.9, 14.0 and 10.9 (alkyl carbons) (Figure B.10)

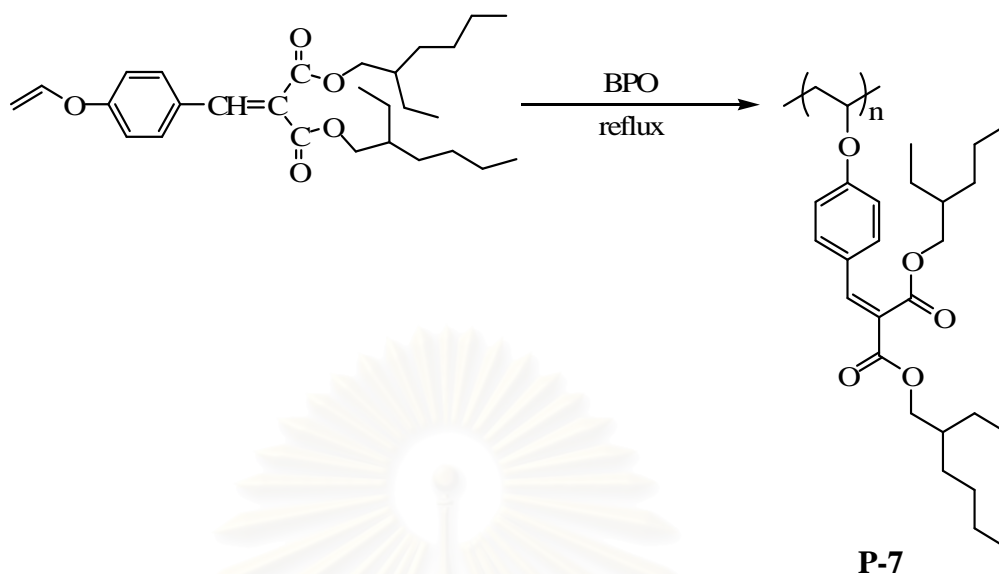
Step II: Preparation of di(2-ethylhexyl)benzalmalonate-4-vinyl ether; M-7



Di(2-ethylhexyl)malonate (0.59 g, 1.81 mmol) was dissolved in pyridine (10 mL) and 4-vinylphenoxybenzaldehyde (0.28 g, 1.91 mmol) and piperidine were added. The mixture was refluxed for 21 hours at 75°C . After the mixture had been cooled, the solution was washed with water (2×40 mL), 15% aqueous hydrochloric acid (2×30 mL) and saturated sodium bicarbonate solution (30 mL). The organic solution was dried with anhydrous sodium sulfate and the solvent was removed under reduced pressure. The product was further purified by a silica gel column using 94:6 (v/v) hexane:ethyl acetate as an eluent.

Di(2-ethylhexyl)benzalmalonate-4-vinyl ether: pale yellowish oil (66%), R_f 0.32 (6% EtOAc/Hex), $m/z = 458$ (Figure B.19), IR (neat, cm^{-1}): 2956, 2925, 2859, 1727, 1633, 1598, 1505, 1462, 1380, 1248, 1201, 1174 and 1061 (Figure B.18); ^1H -NMR (CDCl_3) δ (ppm): 7.67 (s, 1H, ArCH=), 7.42 (d, 2H, ArH, $J = 8.8$ Hz), 6.97 (d, 2H, ArH, $J = 8.8$ Hz), 6.66-6.61 (m, 1H, CHOAr), 4.86 (dd, 1H, CH_2CHO , $J = 12.8, 1.6$ Hz), 4.54 (dd, 1H, CH_2CHO , $J = 7.6, 1.6$ Hz), 4.19-4.11 (m, 4H, $2\times\text{OCH}_2$) and 1.58-0.83 (m, 30H, $2\times\text{C}_7\text{H}_{15}$) (Figure B.16); ^{13}C -NMR (CDCl_3) δ (ppm): 167.2, 164.4 ($2\times\text{-COOR}$), 158.4 (C-4 aro), 146.8 ($=\text{CHOAr}$), 141.2 (Ar-CH=), 131.3 (C-2 and C-6 aro), 127.6 (C-1 aro), 125.0 ($=\text{C}(\text{COOR})_2$), 116.8 (C-3 and C-5 aro), 97.0 ($\text{CH}_2=$), 68.1, 67.7, 38.7, 38.5, 30.3, 30.2, 28.9, 28.8, 23.7, 23.6, 23.5, 23.0, 22.9, 14.0 and 11.0 (alkyl carbons) (Figure B.17)

2.4.2 Synthesis of poly(di(2-ethylhexyl)benzalmalonate-4-vinyl ether); P-7

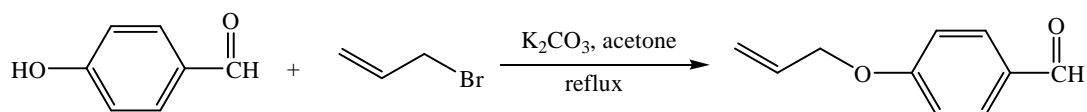


Di(2-ethylhexyl)benzalmalonate-4-vinyl ether monomer (426.4 mg, 0.93 mmol) and recrystallized dibenzoyl peroxide (BPO) (21.20 mg, 0.09 mmol) were dissolved in toluene (4 mL). The solution was stirred at 110°C for 15 minutes under a stream of dry nitrogen and then refluxed at 110°C for 102 hours. The resulting mixture was cooled and the solvent was removed under reduced pressure. The product was further purified by a sephadex column using acetonitrile as an eluent.

Poly(di(2-ethylhexyl)benzalmalonate-4-vinyl ether): reddish brown oil, n_D 1.519, T_g -45.9°C (Figure B.28), IR (neat, cm^{-1}): 2960, 2925, 2859, 1726, 1603, 1506, 1454, 1384, 1255, 1203, 1178 and 1070 (Figure B.27); $^1\text{H-NMR}$ (CDCl_3) δ (ppm): 7.64 (s, 1H, ArCH=), 7.39 (d, 2H, ArH, $J = 8.6$ Hz), 6.95 (d, 2H, ArH, $J = 8.6$ Hz), 6.04-5.99 (m, 1H, CHOAr), 4.19-4.11 (m, 4H, $2 \times \text{OCH}_2$), 1.65 (d, 2H, CH_2CHO , $J = 4.8$ Hz), 1.64-0.82 (m, 30H, $2 \times \text{C}_7\text{H}_{15}$) (Figure B.25); $^{13}\text{C-NMR}$ (CDCl_3) δ (ppm): 167.2, 164.4 ($2 \times \text{-COOR}$), 157.4 (C-4 aro), 141.2 (Ar-CH=), 131.3 (C-2 and C-6 aro), 127.2 (C-1 aro), 124.8 ($=\text{C}(\text{COOR})_2$), 117.3 (C-3 and C-5 aro), 97.4 (CH_2O , backbone), 68.0, 67.7, 38.7, 38.5, 30.3, 30.2, 28.8, 28.8, 23.7, 23.5, 22.9, 22.9, 19.9 ($\text{CH}_2\text{CH}_2\text{O}$, backbone), 14.0, 10.9 and 10.8 (alkyl carbons) (Figure B.26)

2.5 Synthesis of 2-ethylhexyl cinnamate-4-allyl ether

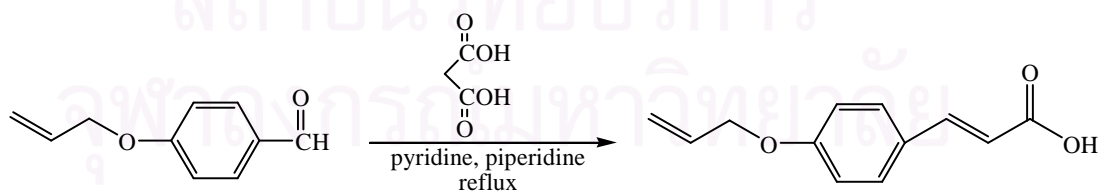
Step I: Preparation of 4-allyloxybenzaldehyde



In a round-bottomed flask, allyl bromide (1.85 g, 15 mmol) and tetrabutylammonium sulfate were added to a solution of 4-hydroxy benzaldehyde (0.62 g, 5 mmol) and anhydrous potassium carbonate (2.09 g, 15 mmol) in acetone (30 mL). The mixture was refluxed at 57°C on a sand bath for 3.30 hours and then cooled to room temperature. The solvent was evaporated under reduced pressure and the resulting residue was diluted with water (30 mL) and extracted with dichloromethane (3×30 mL). The combined extracts were washed with sodium bicarbonate (30 mL), dried with anhydrous sodium sulfate and the solvent was removed under reduced pressure.

4-Allyloxybenzaldehyde: yellowish oil (85%), R_f 0.52 (40% EtOAc/Hex), IR (neat, cm^{-1}): 2921, 2735, 1688, 1594, 1509, 1423, 1306, 1252 and 1162; 1H -NMR ($CDCl_3$) δ (ppm): 9.92 (s, 1H, ArCHO), 7.87 (d, 2H, ArH, $J = 8.4$ Hz), 7.05 (d, 2H, ArH, $J = 8.4$ Hz), 6.14-6.04 (m, 1H, CHCH₂OAr), 5.46 (dd, 1H, CH₂=CH, $J = 17.2$, 1.4 Hz), 5.37 (dd, 1H, CH₂=CH, $J = 9.2$, 1.4 Hz) and 4.66 (d, 2H, CH₂OAr, $J = 5.2$ Hz)

Step II: Preparation of 4-allyloxycinnamic acid



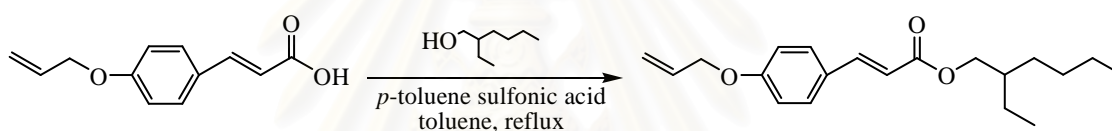
Malonic acid (0.42 g, 4.03 mmol) was dissolved in pyridine (10 mL) and then 4-allyloxybenzaldehyde (0.65 g, 4.03 mmol) and piperidine (1.72 g, 20.15 mmol) were added. The mixture was refluxed for 20 hours at 75°C. After the mixture had been cooled, the solution was washed with water (3×30 mL), with 15% aqueous

hydrochloric acid (2×20 mL) and then with saturated sodium bicarbonate (30 mL). The organic solution was dried with anhydrous sodium sulfate and the solvent was removed under reduced pressure.

4-Allyloxycinnamic acid: pale yellowish solid (73%), R_f 0.19 (40% EtOAc/Hex), IR (KBr, cm^{-1}): 3300-2780, 1684, 1622, 1598, 1509, 1424, 1245, 1214 and 1167; $^1\text{H-NMR}$ (CDCl_3) δ (ppm): 7.77 (d, 1H, ArCH=, $J = 16.4$ Hz), 7.52 (d, 2H, ArH, $J = 8.4$ Hz), 6.96 (d, 2H, ArH, $J = 8.4$ Hz), 6.35 (d, 1H, =CHCOOH, $J = 15.6$ Hz), 6.14-6.04 (m, 1H, CHCH₂OAr), 5.46 (dd, 1H, CH₂=CH, $J = 16.4, 1.6$ Hz), 5.34 (dd, 1H, CH₂=CH, $J = 11.6, 1.6$ Hz) and 4.62 (d, 2H, CH₂OAr, $J = 5.4$ Hz)

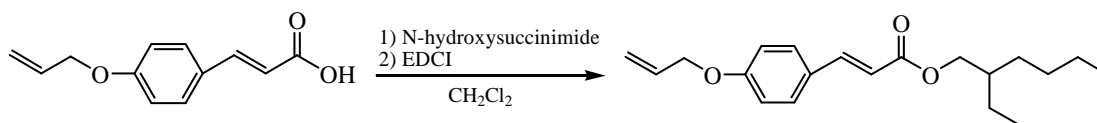
Step III: Preparation of 2-ethylhexylcinnamate-4-allyl ether

- Esterification [66]



The excess of 2-ethyl-1-hexanol and *p*-toluene sulfonic acid (0.07 g, 0.37 mmol) were added to a solution of 4-allyloxycinnamic acid (0.72 g, 3.52 mmol) in toluene (25 mL). The mixture was refluxed for 23 hours at 110°C. After the mixture had been cooled, solvent was evaporated and then dissolved with 40 mL of diethyl ether. This solution was then neutralized with saturated sodium bicarbonate solution (30 mL). The solvent was evaporated under reduced pressure, dried with anhydrous sodium sulfate and the product was further purified by a silica gel column using 90:10 (v/v) hexane:ethyl acetate as an eluent.

- Coupling reaction



4-Allyloxycinnamic acid (0.11 g, 0.52 mmol), 2-ethyl-1-hexanol (0.07, 0.55 mmol) and N-hydroxysuccinimide (0.18 g, 1.59 mmol) were dissolved in dichloromethane (14 mL). The mixture was stirred at room temperature until all solids were dissolved. The reaction mixture was cooled in ice bath and 1-(3-dimethyl aminopropyl)-3-ethylcarbodiimide hydrochloride, EDCI (0.31 g, 1.60 mmol) was added and stirred for 1 hour. Then the reaction mixture was further stirred at room temperature for 24 hours. The reaction was quenched by adding water (40 mL) and the organic part was washed with water (3×40 mL), sodium bicarbonate solution (2×30 mL). The solvent was evaporated under reduced pressure, dried with anhydrous sodium sulfate and the product was further purified by a silica gel column using 97:3 (v/v) dichloromethane:ethyl acetate as an eluent.

2-Ethylhexylcinnamate-4-allyl ether: yellowish oil (27%), R_f 0.33 (3% EtOAc/CH₂Cl₂), IR (neat, cm⁻¹): 2956, 2925, 2859, 1710, 1631, 1601, 1513, 1457, 1249, 1169 and 1022; ¹H-NMR (CDCl₃) δ (ppm): 7.62 (d, 1H, ArCH=, J = 15.6 Hz), 7.46 (d, 2H, ArH, J = 8.6 Hz), 6.90 (d, 2H, ArH, J = 8.6 Hz), 6.31 (d, 1H, =CHCOOR, J = 15.6 Hz), 6.09-6.00 (m, 1H, CHCH₂OAr), 5.42 (dd, 1H, CH₂=CH, J = 17.6, 1.4 Hz), 5.31 (dd, 1H, CH₂=CH, J = 10.4, 1.4 Hz) and 4.56 (d, 2H, CH₂OAr, J = 5.6 Hz), 4.11 (d, 2H, COOCH₂, J = 5.6 Hz), 1.66-0.87 (m, 15H, C₇H₁₅)

2.6 General procedure for molar absorptivity measurements [67,68]

A stock solution of each compound was prepared in a 100 mL volumetric flask using chloroform as a solvent. The resulting stock solution was then diluted to five final concentrations. The UV absorbance of each final dilution was recorded by scanning wavelengths between 200 and 800 nm. The molar absorptivity (ϵ) at the wavelength of maximum absorbance (λ_{\max}) was calculated using Beer's law:

$$A = \epsilon bc$$

where A is absorbance

b is the cell path length (1 cm)

c is the concentration of the absorbing species in mole per litre

2.7 General procedure for photostability test [67]

The photostability tests for the UV filters were performed in chloroform. Stock solution of each compound was prepared in a 100 mL volumetric flask. The resulting solutions were divided into two parts. One part was kept away from light (covered with foil) at room temperature (dark sample) while the other part was irradiated by artificial UVA and UVB lamps (8.3 mW/cm² UVA and 0.66 mW/cm² UVB) at room temperature (irradiated sample). Then UV absorption profile of each sample was acquired using UV/VIS spectrometer. The absorbance of irradiated sample at various irradiant times were compared to those of dark samples.

The calculation of percent relative absorbance of each irradiated sample was done using the following equation.

$$\text{Percent of relative absorbance} = \left(\frac{\text{Absorbance of irradiated sample at time X}}{\text{Absorbance of dark sample (starting time)}} \right) \times 100$$

CHAPTER III

RESULTS AND DISCUSSION

3.1 Syntheses of monomers

Since many polymers and oligomers with cinnamate moieties based on esterification polymerization have already been experimented in our laboratory, in this work, cinnamate/benzalmalonate monomers bearing active terminal double bond for free radical polymerization, were pursued to obtain the polymers with cinnamate/benzalmalonate on the side chain (Figure 3.1).

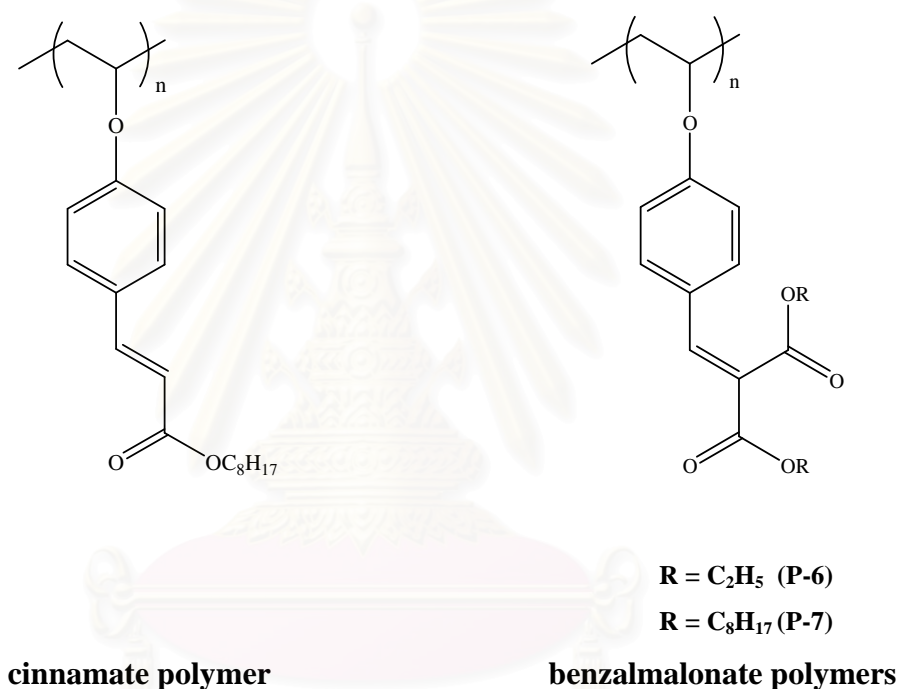
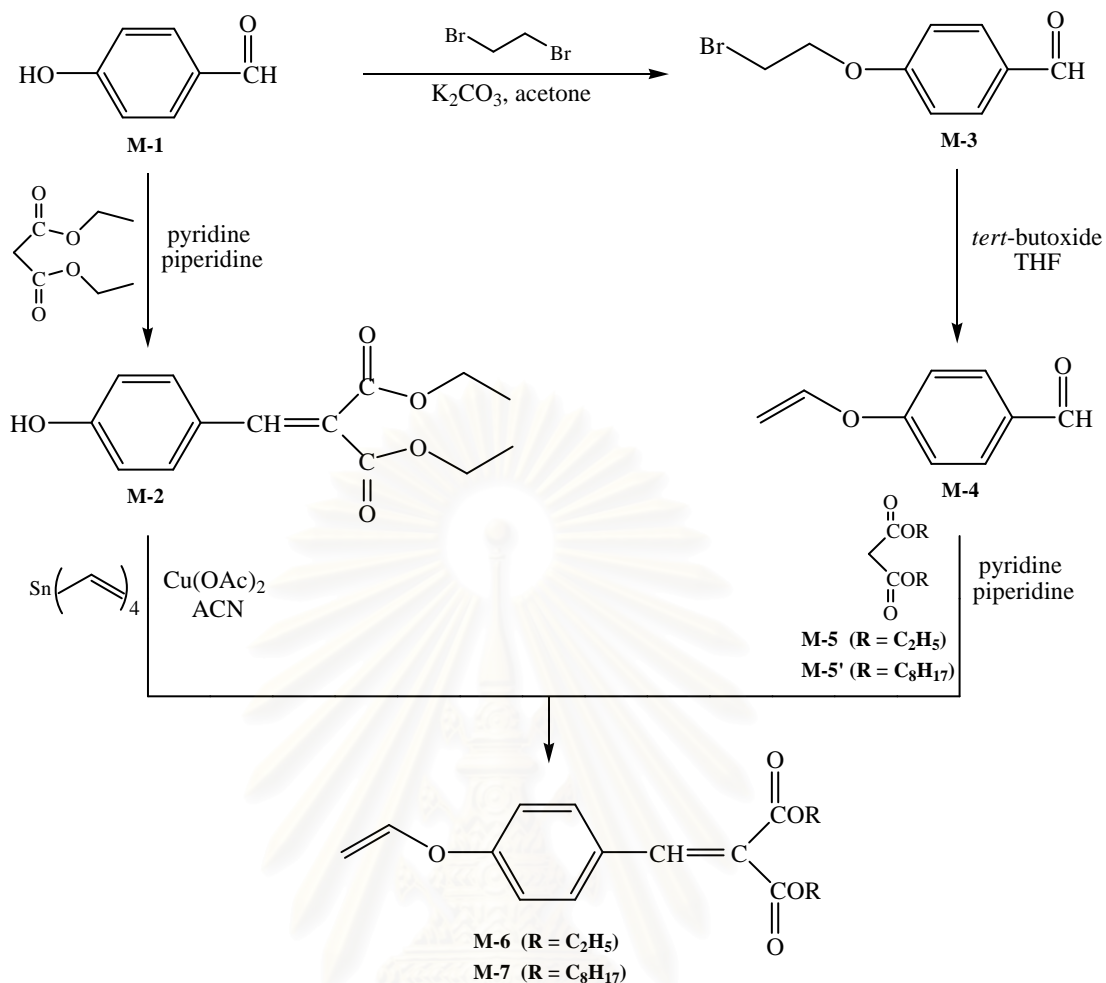


Figure 3.1 Expected oligomeric structures

As mentioned in the introduction that *cis-trans* photoisomerization of EHMC is accountable for the decrease in UV absorption efficiency (decrease ϵ value) when the compound is exposed to UV light. To solve this problem, the dialkylbenzalmalonate monomers were synthesized. The monomers also bear vinylic structural parts to undergo free radical polymerization. The overall synthetic reactions were depicted in Scheme 3.1.



Scheme 3.1 Syntheses of dialkylbenzalmalonate-4-vinyl ether

The syntheses of two monomers (M-6, M-7) were done through two pathways.

Pathway I

The first pathway (depicted on the left side of scheme 3.1) composed of 2 steps:

Step I : Knoevengel-Doebner condensation between one mole equivalent of 4-hydroxy benzaldehyde (M-1) and one mole equivalent of diethyl malonate in pyridine using piperidine as catalyst. The obtained diethyl-4-hydroxy benzalmalonate (M-2) was brown solid in 55% yield. The appearance of ¹H-NMR resonance at 7.65 ppm (ArCH=) in M-2 and the disappearance of the aldehydic proton peak at 9.90 ppm (ArCHO) confirm M-2 structure. The C=O stretching vibration of carbonyl at 1715 cm⁻¹ in M-2 also indicates M-2 structure.

Step II : Oxidation of one mole equivalent of M-2 using 1.40 mole equivalent of tetravinyltin as vinylating agent in acetonitrile. The obtained diethylbenzalmalonate-4-vinyl ether (M-6) was pale yellowish oil in 67% yield. The appearance of $^1\text{H-NMR}$ resonances at 4.54, 4.87 (CH_2CHO) and 6.64 ppm (CHOAr) in M-6 confirm M-6 structure. The C=C stretching vibration of terminal double bond at 1637 cm^{-1} in M-6 also indicates M-6 structure.

Pathway II

The second pathway (depicted on the right side of scheme 3.1) composed of 3 steps:

Step I : Alkylation of ten mole equivalent of dibromoethane to one mole equivalent of (M-1) using potassium carbonate as catalyst in acetone. The obtained 4-((2-bromo)ethoxy)benzaldehyde (M-3) was a white needle in 68% yield. The appearance of $^1\text{H-NMR}$ resonances at 3.67 (CH_2Br) and 4.38 ppm (CH_2OAr) in M-3 confirm M-3 structure. The C-H stretching vibration of methylene carbon at $2797, 2727\text{ cm}^{-1}$ and C-O stretching at 1248 cm^{-1} in M-3 also indicate M-3 structure.

Step II : Dehydrobromination of one mole equivalent of (M-3) using 1.2 mole equivalent of potassium *tert*-butoxide as a dehydrohalogenating agent in freshly distilled tetrahydrofuran. The reaction was experimented at various temperatures in order to get the maximum yield.

Table 3.1 Comparison of %yield in various temperatures

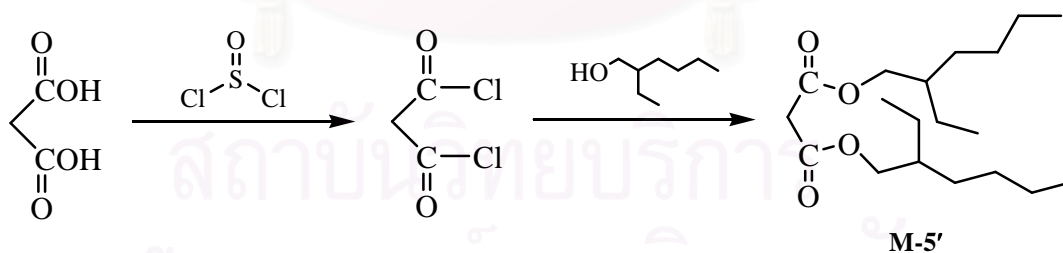
Temperature	%Yield of M-4
4°C	32%
10°C	42%
15°C	41%
room temperature	50%

Table 3.1 shows small differences of %yield of 4-vinyloxybenzaldehyde (M-4) obtained at various temperatures. The reaction was later carried out at room temperature.

The obtained 4-vinyloxybenzaldehyde (M-4) was pale yellowish oil in 50% yield. The appearance of $^1\text{H-NMR}$ resonances at 4.63, 4.95 (CH_2CHO) and 6.69 ppm (CHOAr) in M-4 and the disappearance of the resonances representing protons next to Br atom at 3.67 (CH_2Br) and 4.38 ppm (CH_2OAr) confirm M-4 structure. The $\text{C}=\text{C}$ stretching vibration of terminal double bond at 1637 cm^{-1} in M-4 also indicates M-4 structure.

Step III : Knoevengel-Doebner condensation between one mole equivalent of (M-4) and one mole equivalent of diethyl malonate (M-5) in pyridine using piperidine as catalyst. The obtained diethylbenzmalonate-4-vinyl ether (M-6) was the pale yellowish oil in 61% yield. The appearance of $^1\text{H-NMR}$ resonance at 7.67 ppm ($\text{ArCH}=\text{C}$) in M-6 and the disappearance of the aldehydic proton peak at 9.93 ppm (ArCHO) confirm M-6. The $\text{C}=\text{O}$ stretching vibration of carbonyl at 1723 cm^{-1} in M-6 also indicates M-6 structure.

In order to prepare M-7, di(2-ethylhexyl)malonate (M-5') was first synthesized from malonic acid and 2-ethyl-1-hexanol using acid chloride method.



The obtained di(2-ethylhexyl)malonate (M-5') was pale yellowish oil in 70% yield. The appearance of $^1\text{H-NMR}$ resonance at 4.02 ppm (OCH_2) in M-5' confirms M-5' structure. The disappearance of the broadening O-H stretching vibration of carboxylic in M-5' also indicates M-5' structure.

Di(2-ethylhexyl)benzmalonate-4-vinyl ether (M-7) was derived from Knoevengel-Doebner condensation between M-4 and M-5' in the same condition with condensation reaction of M-6. The obtained di(2-ethylhexyl)benzmalonate-4-vinyl

ether (M-7) was the pale yellowish oil in 66% yield. Similar changes of NMR and IR spectra of M-7 to those of M-6 was found, i.e., the appearance of $^1\text{H-NMR}$ resonance at 7.67 ppm (ArCH=) in M-7 and the disappearance of the aldehydic proton peak at 9.93 ppm (ArCHO) confirm M-7. The C=O stretching vibration of carbonyl at 1727 cm^{-1} in M-7 also indicates M-7 structure.

The obtained yield of M-6 from the first and the second pathways are comparable (Table 3.2).

Table 3.2 Comparison of yielding from each pathway

Compound	%Yield
pathway I ; M-6	67%
pathway II; M-6	61%

The formation of two monomers (diethylbenzalmalonate-4-vinyl ether; M-6) and (di(2-ethylhexyl)benzalmalonate-4-vinyl ether; M-7) could be monitored by TLC. Column chromatography allowed the isolation of dialkylbenzalmalonate-4-vinyl ether in a purity. Both M-6 and M-7 were yellowish oil soluble in both polar and non polar solvents including hexane, dichloromethane, ethyl acetate, chloroform, acetone, methanol and ethanol. The structure of the synthesized compounds was confirmed through various spectroscopic data including ^1H , $^{13}\text{C-NMR}$, IR and MS spectra (see section 3.6).

UV absorption profiles of the two monomers are shown in Figure 3.2. Both monomers show UVB absorption profiles similar to EHMC. This is because the chromophoric units are similar.

By plotting a graph between absorbances (at λ_{max}) and concentrations of each monomer sample, a linear relationship was obtained with its slope representing molar absorption coefficient value (ϵ) of the monomer. Both monomers gave similar λ_{max} and ϵ (Table 3.3).

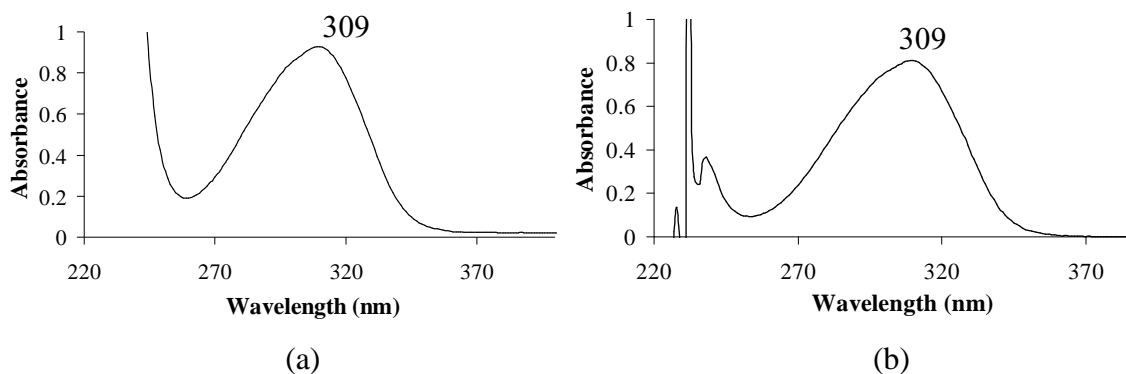


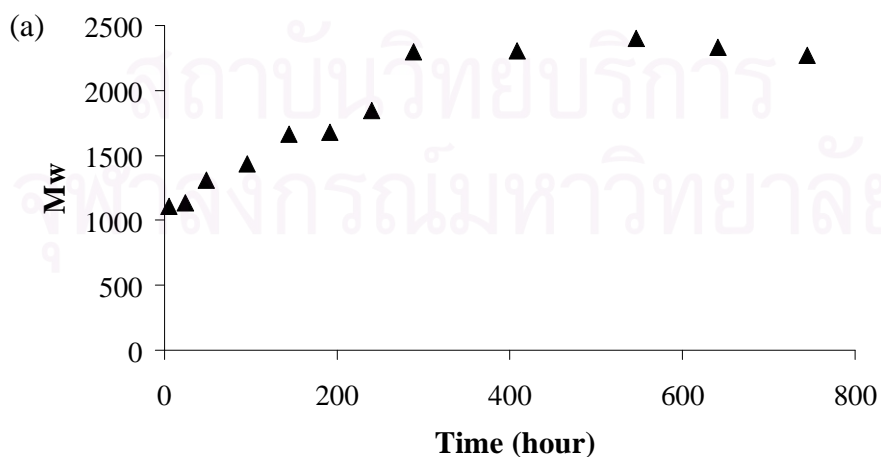
Figure 3.2 UV spectra of (a) M-6 and (b) M-7 in chloroform

Table 3.3 UV spectral data of monomers in chloroform

Monomer	λ_{\max}	ϵ ($M^{-1}cm^{-1}$)
M-6	309	26,000
M-7	309	22,000

3.2 Syntheses of polymers

After successful synthesis and characterization of dialkylbenzalmalonate-4-vinyl ether monomers which possess the functionality to permit free radical polymerization, free radical polymerization was induced by dibenzoyl peroxide (BPO) at 110°C in toluene. The progress of the polymerization reaction was followed by analyzing \bar{M}_w of the reaction mixture at various times using gel filtration analyses. The growth of the polymer is depicted in Figure 3.3.



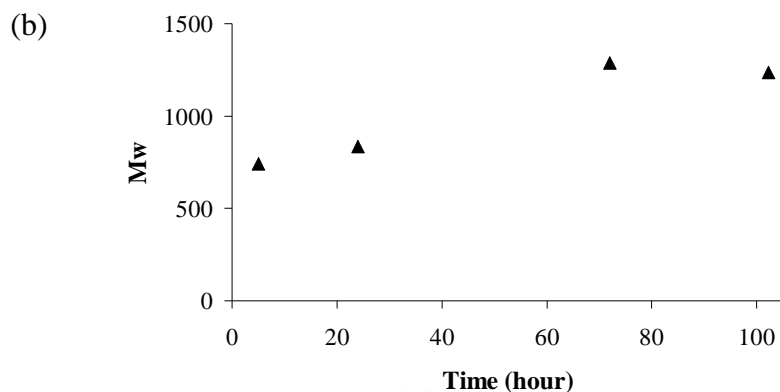
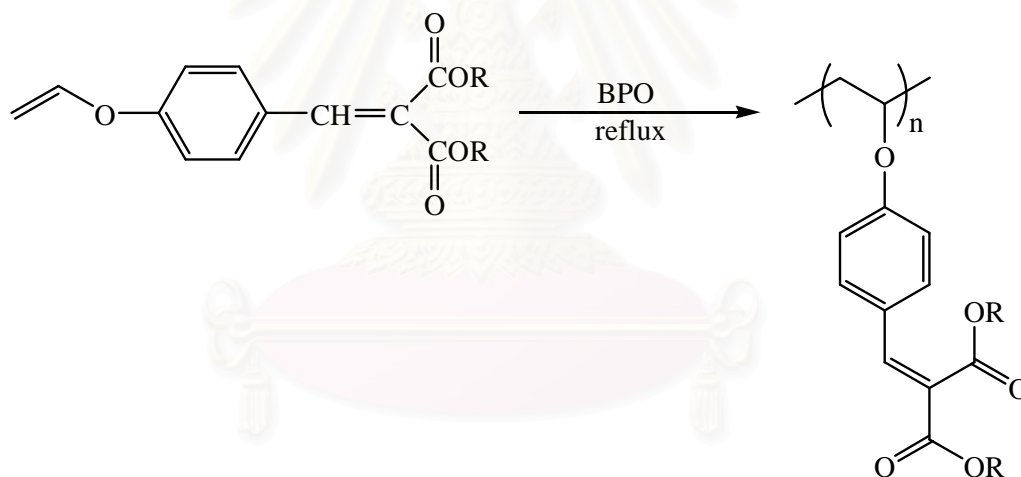


Figure 3.3 The conversion of polymerizations: (a) P-6 and (b) P-7

From the graph, polymer growth was built up rapidly at the beginning of the reaction, then propagated steadily and in the later times, the growth stopped.

It should be noted here that 2,2'-azo-bis-isobutyronitrile (AIBN) could not successfully induce the free radical polymerization of M-6.

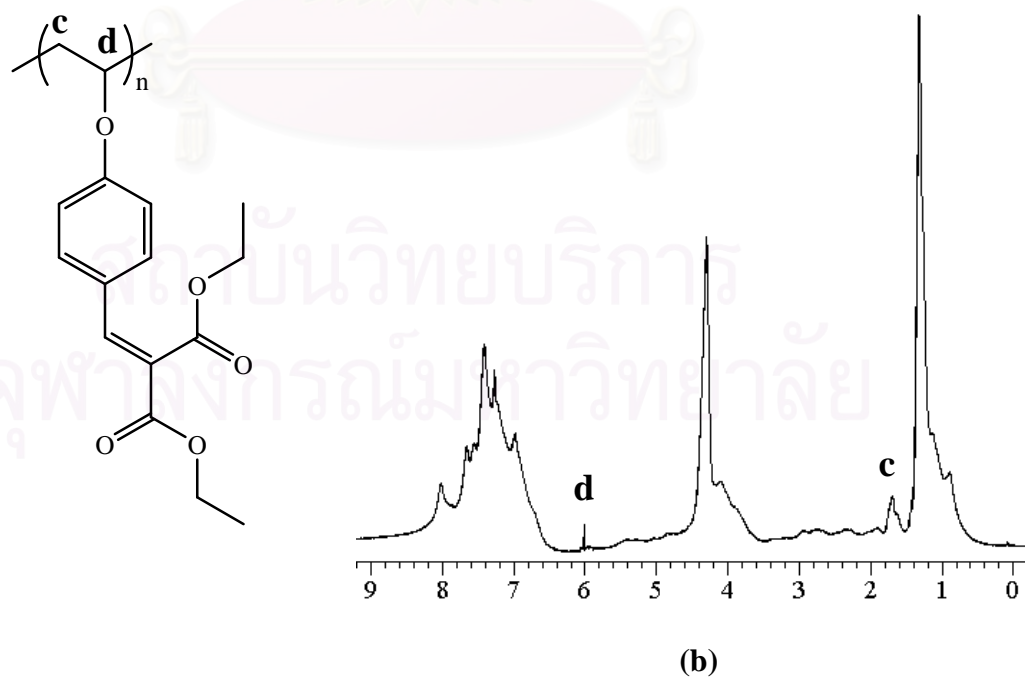
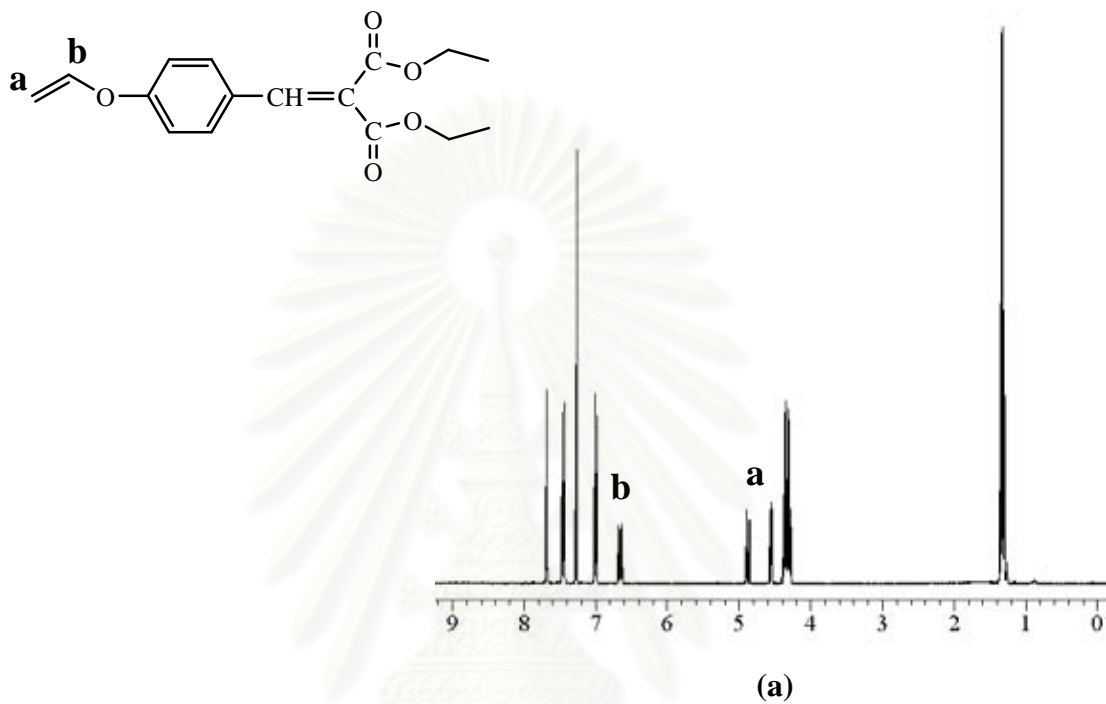


$R = C_2H_5$; P-6

$R = C_8H_{17}$; P-7

Sephadex column chromatography allowed the isolation of two polymers in a purity. The two polymers were subjected to 1H -NMR and IR spectroscopic analyses. 1H -NMR spectra of P-6 and P-7 show the disappearances of vinylic proton resonances at 6.64 ppm (m, 1H, $CHOAr$), 4.86 ppm (dd, 1H, CH_2CHO , $J = 12.8, 1.6$ Hz), 4.54 ppm (dd, 1H, CH_2CHO , $J = 7.6, 1.6$ Hz) together with the emergences of the backbone protons at 6.02 ppm (m, 1H, $CHOAr$) and 1.65 ppm (d, 2H, CH_2CHO , $J = 4.8$ Hz) and a broadening of all the resonances peaks, thus indicating successful

conversion of vinylic monomers into polymers (Figure 3.4). Furthermore, the decreases of C=C stretching vibrations at 1637 cm^{-1} in P-6 and at 1633 cm^{-1} in P-7 indicate the conversion of terminal double bond into single bond on carbon backbone of the polymers (Figure 3.5).



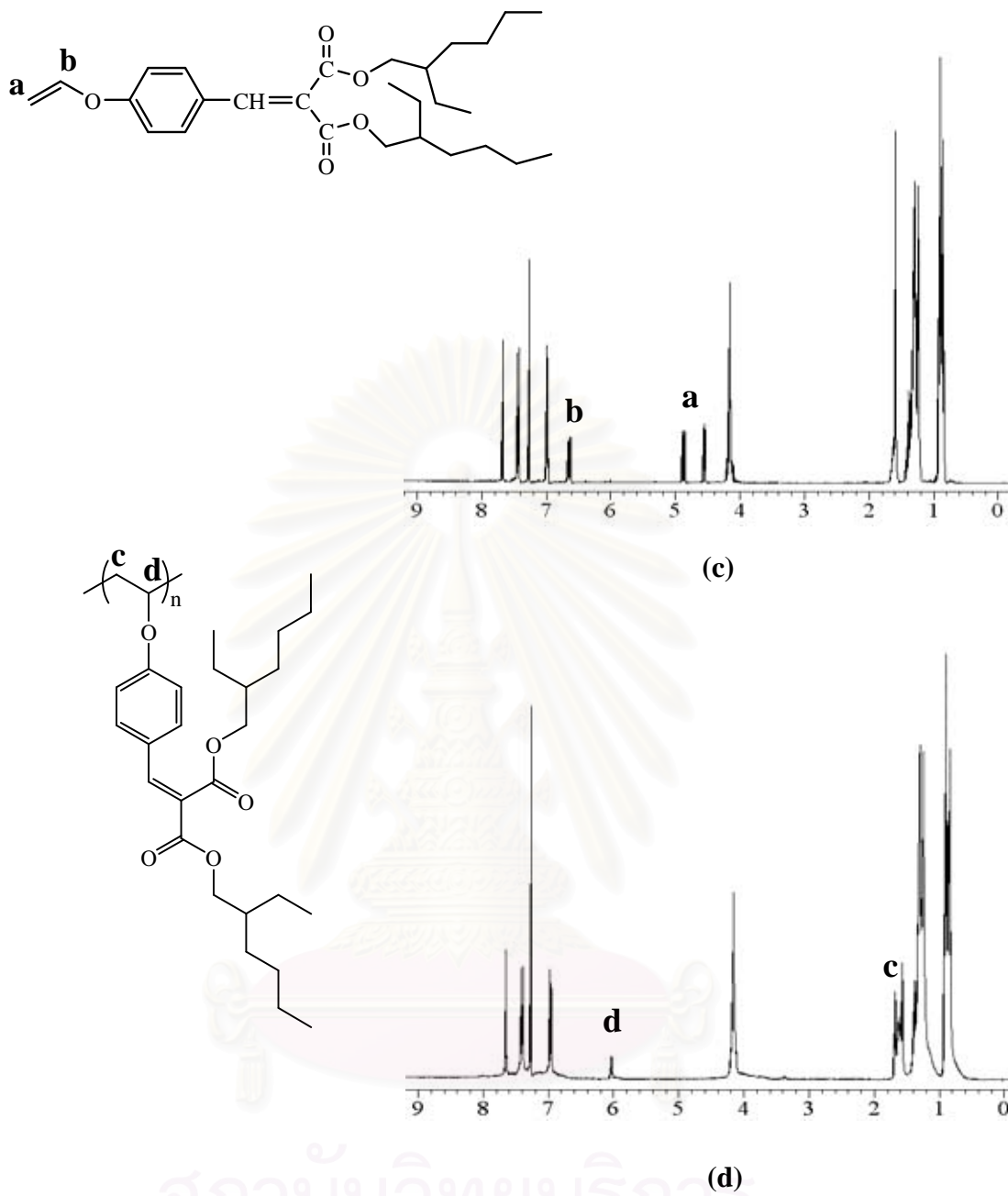


Figure 3.4 $^1\text{H-NMR}$ spectra of (a) M-6 (b) P-6 (c) M-7 and (d) P-7

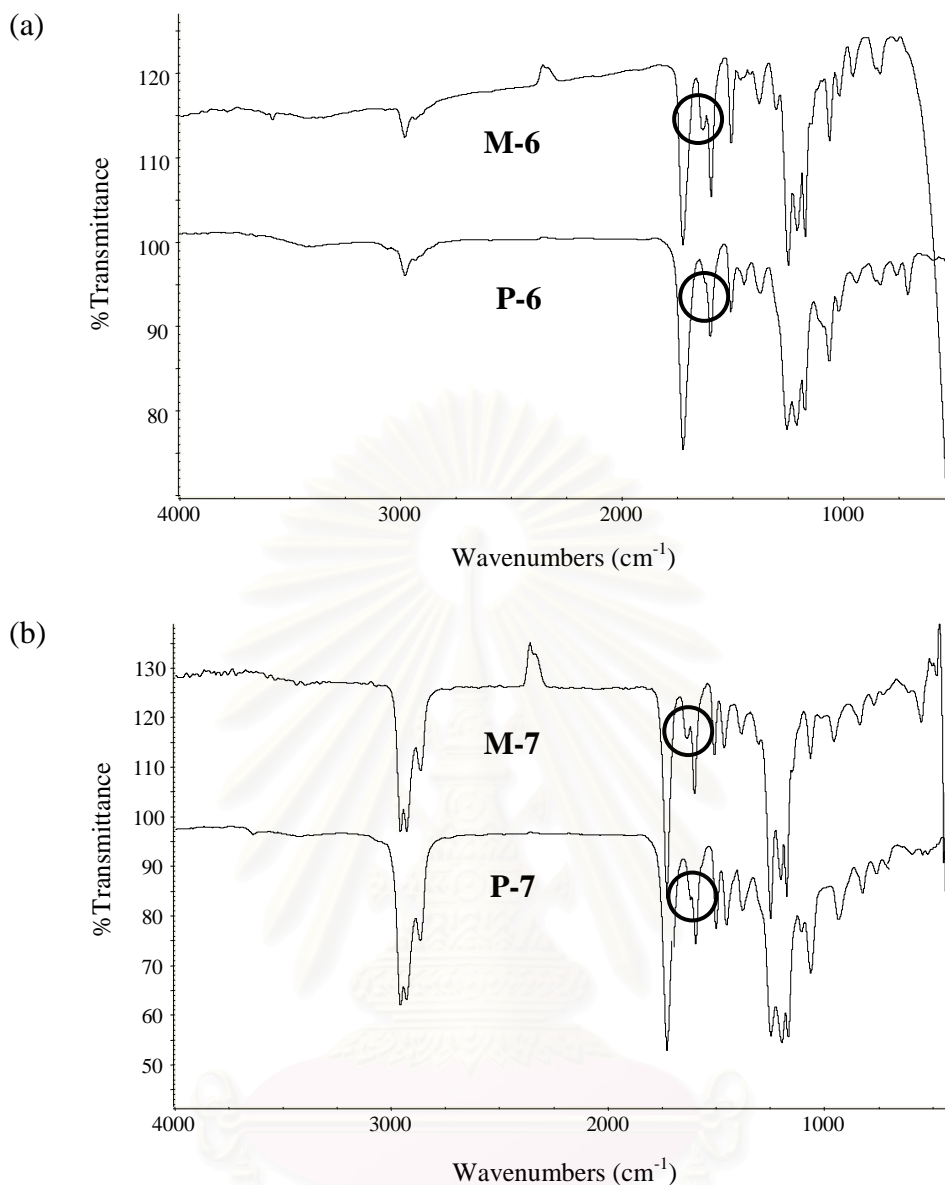


Figure 3.5 IR spectra of (a) M-6, P-6 and (b) M-7, P-7

The weight-average molecular weight (\overline{M}_w) of poly(diethylbenzmalonate-4-vinyl ether (P-6) and poly(di(2-ethylhexyl)benzmalonate-4-vinyl ether (P-7) obtained by gel permeation chromatography (GPC) technique were 3551 and 1889, with the polydispersity index (PDI) of 1.65 and 1.14 and the average degree of polymerization (\overline{DP}) were 12.24 and 4.12, respectively.

These obvious changes in NMR, IR together with molecular weight information from gel filtration confirmed that polymerization had been taking places.

Both oligomers show similar UVB absorption profiles which agree well with the fact that they contain similar chromophoric moiety. (Figure 3.6) Their absorption profiles are also similar to the absorption profile of M-6 and M-7. This indicated that

free radical polymerization reaction occurred at only the terminal double bond and all the conjugations within the chromophoric structure were not disturbed.

However, ϵ value of P-6 doubles that of P-7 (Table 3.4). In fact, the ϵ of P-7 is similar to that of its monomer. Although M-6's ϵ is $\sim 26,000 \text{ M}^{-1}\text{cm}^{-1}$, the ϵ of P-6, as calculated per monomeric unit, is $50,000 \text{ M}^{-1}\text{cm}^{-1}$. This increase may be a result of steric effect on the benzalmalonate moieties, which results in a more allowed electronic transition.

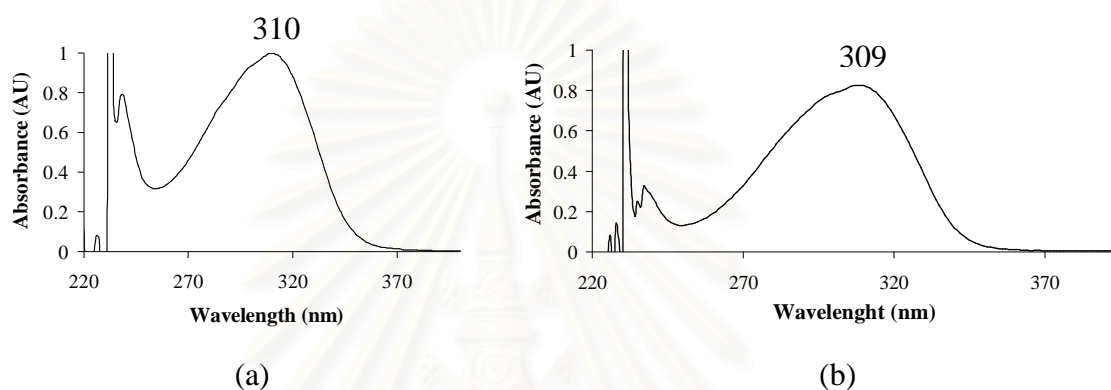


Figure 3.6 UV spectra of (a) P-6 and (b) P-7 in chloroform

Table 3.4 UV absorption properties of polymers (in chloroform)

Polymer	λ_{max}	$\epsilon (\text{M}^{-1}\text{cm}^{-1})^*$
P-6	310	50,000
P-7	309	24,000

*calculated per monomeric unit

3.3 Solubility test

Table 3.5 shows comparable solubility of monomers (M-6 and M-7) and polymers (P-6 and P-7). Although M-6 and M-7 differ by alkyl chain length, they have similar solubility in various organic solvents. Increased molecular weight in P-6 had made this oligomer slightly lost its solubility in methanol and ethanol when compared with M-6. This was also true when comparing the solubilities of P-7 and M-7. The outstanding characteristic of P-7 is that it is a reddish brown oily liquid miscible with silicone fluids used in cosmetic industry, thus applications of the material in cosmetic formation are very promising.

Table 3.5 Solubility of synthesized polymers and monomers

Solvent	M-6 (4 mg/mL)	P-6 (0.8 mg/mL)	M-7 (4 mg/mL)	P-7 (0.8 mg/mL)
water	--	--	--	--
acetonitrile	++	++	++	++
ethanol	++	+ ^a	++	++
methanol	++	+ ^a	++	+ ^a
acetone	++	++	++	++
ethyl acetate	++	++	++	++
tetrahydrofuran	++	++	++	++
chloroform	++	++	++	++
dichloromethane	++	++	++	++
diethyl ether	++	++	++	++
toluene	++	++	++	++
hexane	++	--	++	++
DC 200 ^b	ND	--	ND	--
DC 556 ^c	ND	--	ND	++

-- insoluble, +- partially soluble, ++ soluble

ND means not determined

a means heating of solvent

b means linear polydimethylsiloxane polymers

c means phenyl trimethicone

After successful preparation of P-6 and P-7 which are benzalmonate based oligomers, cinnamate based oligomer was pursued. Effort was made on the synthesis of cinnamate monomer with terminal double bond. The esterification with acid-catalyzed method failed because of the protonation of acid to terminal vinyl group. Therefore, the coupling agent (EDCI) method was experimented and it was found that the esterified product (cinnamate monomer) was obtained in low yield. As a result, only oligomers with benzalmonate structure were further studied.

3.4 Photostability test

Two synthesized oligomeric UV-filters, P-6 and P-7, were subjected to photostability test. The tests were carried out in chloroform at 8.30 mW/cm^2 UVA and 0.66 mW/cm^2 UVB irradiation. At various UV exposures, UV absorption property of the sample was checked. Both polymers showed comparable photostability. In addition, the two polymers were more photostable than EHMC (Figure 3.7). This can be explained through the lack of possible *cis-trans* photoisomerization in the polymer structures.

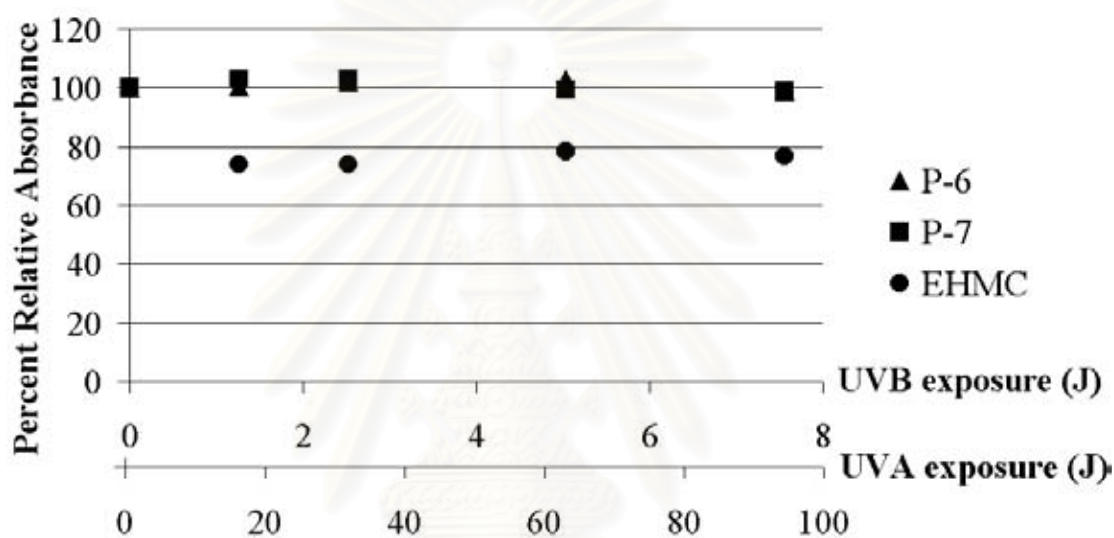


Figure 3.7 Photostability of P-6, P-7 and 2-ethylhexyl-*p*-methoxycinnamate (EHMC) in chloroform

Previous studies indicated that the decrease in UV absorption of EHMC is caused by *trans* to *cis* photoisomerization since the *cis*-configuration processes only half ϵ value comparing to that of *trans*-configuration [31]. Therefore by changing from cinnamate into benzalmalonate moiety, *trans/cis* photoisomerization can be avoided, resulting in more photostable materials.

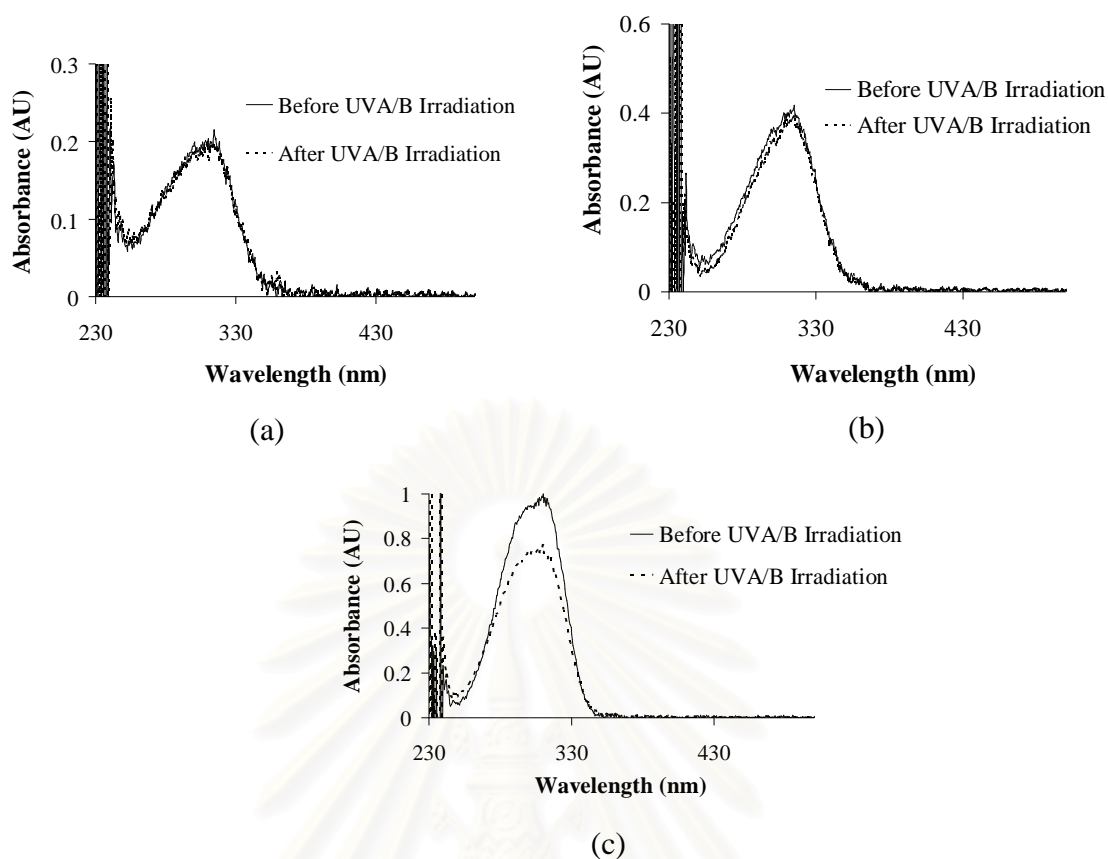


Figure 3.8 UV spectra of (a) P-6, (b) P-7 and (c) 2-ethylhexyl-*p*-methoxycinnamate (EHMC) in chloroform; the irradiation was done for 3 hours at 8.30 mW/cm² UVA and 0.66 mW/cm² UVB

3.5 Physical properties test

- Refractive indices

Refractive index values (n_D) of P-6 and P-7 were determined by casting film on the refractometer. At room temperature n_D of P-6 and P-7 were 1.5630 and 1.5191, respectively. Both numbers fall into the typical n_D values of general polymers (see Table 3.6).

Table 3.6 Refractive index of polymers [69]

Polymer	Refractive index
Poly(vinyl ethyl ether)	1.4540
Poly(vinyl <i>n</i> -butyl ether)	1.4563
Poly(vinyl <i>n</i> -hexyl ether)	1.4591
Poly(vinyl 2-ethylhexyl ether)	1.4626
Polyethylene, low density	1.5100
Polyethylene, high density	1.5400
Poly(<i>p</i> -isopropyl styrene)	1.5540
Poly(1-phenylallyl methacrylate)	1.5573
Polystyrene	1.5894
Poly(<i>p</i> -methoxy styrene)	1.5967

- *Thermal property*

Thermal properties of polymer can affect its mechanical properties at any particular temperature and determine the temperature range in which that polymer can be employed. Therefore, the glass-transition and crystallite melting temperatures were measured by differential scanning calorimeter (DSC) at a scan rate of 10°C/min under nitrogen from -80 to 200°C. P-6 and P-7 display the glass-transition temperatures (T_g) at 44.4°C and -45.9°C, respectively. No distinct melting endothermic peak can be observed in DSC traces (Figure B.23, B.28). This means that both polymers were non-crystalline.

High T_g observed in P-6 may be a result of a steric effect of the diethyl side chain on a polymer backbone. It is known that T_g of mono-substituted polymers increases with the bulkiness of the substituent (Table 3.7). This is because steric hindrance from neighboring branches will add further constraints to chain movements. However, in this case the side chain of P-7 (di(2-ethylhexyl)) is less bulky than that of P-6 (diethyl). It was speculated that a specific interaction from the diethyl side chain must be more rigid than that from the di(2-ethylhexyl) side chain. This was, in facts, reflected in an increased ϵ of P-6 when compared to that of P-7.

Besides the bulkiness of substituents, the T_g of polymers depend on a side chain or branch length and their molecular weight. [70] The experimentally observed

decrease of T_g of poly(α -olefin) with the length of the n -alkylic side chain has been attributed to an internal plasticizing effect [71] as can see in the right side of Table 3.7. As a results, it indicated that a longer side chain length of P-7 can lower the T_g value. This can explain that the increased volume, which resulted from the interforce of the molecular side chains, build up the free movement of polymeric molecules.

Table 3.7 Glass temperature of polymers bearing n -alkylic side chains [72]

Polymer	T_g (K)	Polymer	T_g (K)
Poly(methyl ethylene)	258-270	Poly(styrene)	373-377
Poly(n -butyl ethylene)	223	Poly(4-methyl styrene)	371-375
Poly(n -octyl ethylene)	232	Poly(4-ethyl styrene)	300
Poly(<i>iso</i> -butyl ethylene)	302	Poly(4-butyl styrene)	279
Poly(<i>tert</i> -butyl ethylene)	337	Poly(4-hexyl styrene)	246
Poly(methyl acrylate)	283	Poly(4-octyl styrene)	228
Poly(<i>iso</i> -butyl acrylate)	249	Poly(4-nonyl styrene)	220
Poly(<i>tert</i> -butyl acrylate)	316-346	Poly(4-decyl styrene)	208
Poly(methyl methacrylate)	378	Poly(4- <i>tert</i> -butyl styrene)	399
Poly(<i>iso</i> -butyl methacrylate)	326	P-6 (diethyl)	317
Poly(<i>tert</i> -butyl methacrylate)	391	P-7 (di(2-ethylhexyl))	227

3.6 Spectroscopic data of all synthesized compounds

The structures of all synthesized compounds were well characterized using various spectroscopic techniques including ^1H , ^{13}C -NMR, IR, MS and GPC (gel permeation chromatography). Spectroscopic spectra of all compounds are shown in Appendix B.

3.6.1 Infrared spectroscopy

Both monomers (M-6 and M-7) display the characteristic of common functional groups in IR spectra. The absorption band around 2980 cm^{-1} corresponds to C-H stretching of aliphatic hydrocarbons. The C=O stretching vibration is shown at 1723 cm^{-1} . The C=C stretching of terminal vinyl group at 1637 cm^{-1} , C=C (next to aromatic ring) stretching at 1505 cm^{-1} and C=C stretching of the aromatic ring at

1600-1400 cm^{-1} are also detected. The C-O stretching vibration is detected at 1252 cm^{-1} .

Similarly, the IR spectra of P-6 and P-7, display almost the same spectra as those of M-6 and M-7, i.e., the absorption band around 2976 cm^{-1} (C-H stretching), 1723 cm^{-1} (C=O stretching), 1505 cm^{-1} (C=C next to aromatic ring stretching), 1600-1400 cm^{-1} (C=C aromatic ring) and 1252 cm^{-1} (C-O stretching). In the case of P-6 and P-7, the IR spectra showed the disappearance of C=C stretching at $\sim 1630 \text{ cm}^{-1}$ which corresponds to terminal double bond.

3.6.2 NMR spectroscopy

^1H -NMR

For NMR spectroscopy, CDCl_3 was used as solvent for all compounds. The ^1H -NMR spectra of M-6 and M-7 show the singlet signal at 7.67 ppm which corresponds to ArCH= . Signals that were detected at 7.43, 6.98 ppm can be assigned for aromatic protons. Doublet of doublet signals of the vinylic protons at 4.86 (CH_2CHO) and 4.54 ppm (CH_2CHO) and the resonance peaks of aliphatic hydrocarbons at 4.37-0.83 ppm also confirm the structures of M-6 and M-7.

Similarly, the ^1H -NMR spectra of P-6 and P-7, display almost the same resonances as those of M-6 and M-7, i.e., the signals at 7.64 (ArCH=), 7.39 (ArH), 6.95 (ArH) and 4.19-0.82 ppm (alkyl). In the case of P-6 and P-7, signals at 6.02 (CHOAr) and 1.65 ppm (CH_2CHO) were assigned for polymer backbone.

^{13}C -NMR

The ^{13}C -NMR spectra of M-6 and M-7 display a signal belonging to carbonylic carbon around 167.0-164.0 ppm. The signals of olefinic carbon were detected at 141.2 (Ar-CH=) and 124.8 ppm ($=\text{C}(\text{COOR})_2$). The signals of aromatic carbons were detected at 131.4 and 116.8 ppm. The spectrum also shows signal of vinylic carbon atom at 146.8 ($=\text{CHOAr}$) and 97.0 ppm ($\text{CH}_2=\text{CH}$) and alkyl carbons around 68.0-11.0 ppm.

Similarly, the ^{13}C -NMR spectra of P-6 and P-7, display almost the same spectra as those of M-6 and M-7, i.e., the signals at 167.0-164.0 ppm ($2\times\text{-COOR}$), 141.2 (Ar-CH=), 125.0 ($=\text{C}(\text{COOR})_2$), 131.3 (aro.) and 117.0 ppm (aro.). In the case

of P-6 and P-7, signals at 97.4 and 19.9 ppm were assigned for carbon backbone of the polymer chain $\text{-(CH}_2\text{-CH-CH}_2\text{-CH)-}$.

3.6.3 Mass spectroscopy

The molecular weight of two monomers was confirmed by MS data (see Figure B.15, B.19). The molecular peak in MS spectra showed $m/z = 290$ in M-6 and $m/z = 458$ in M-7.

3.6.4 Gel permeation chromatography

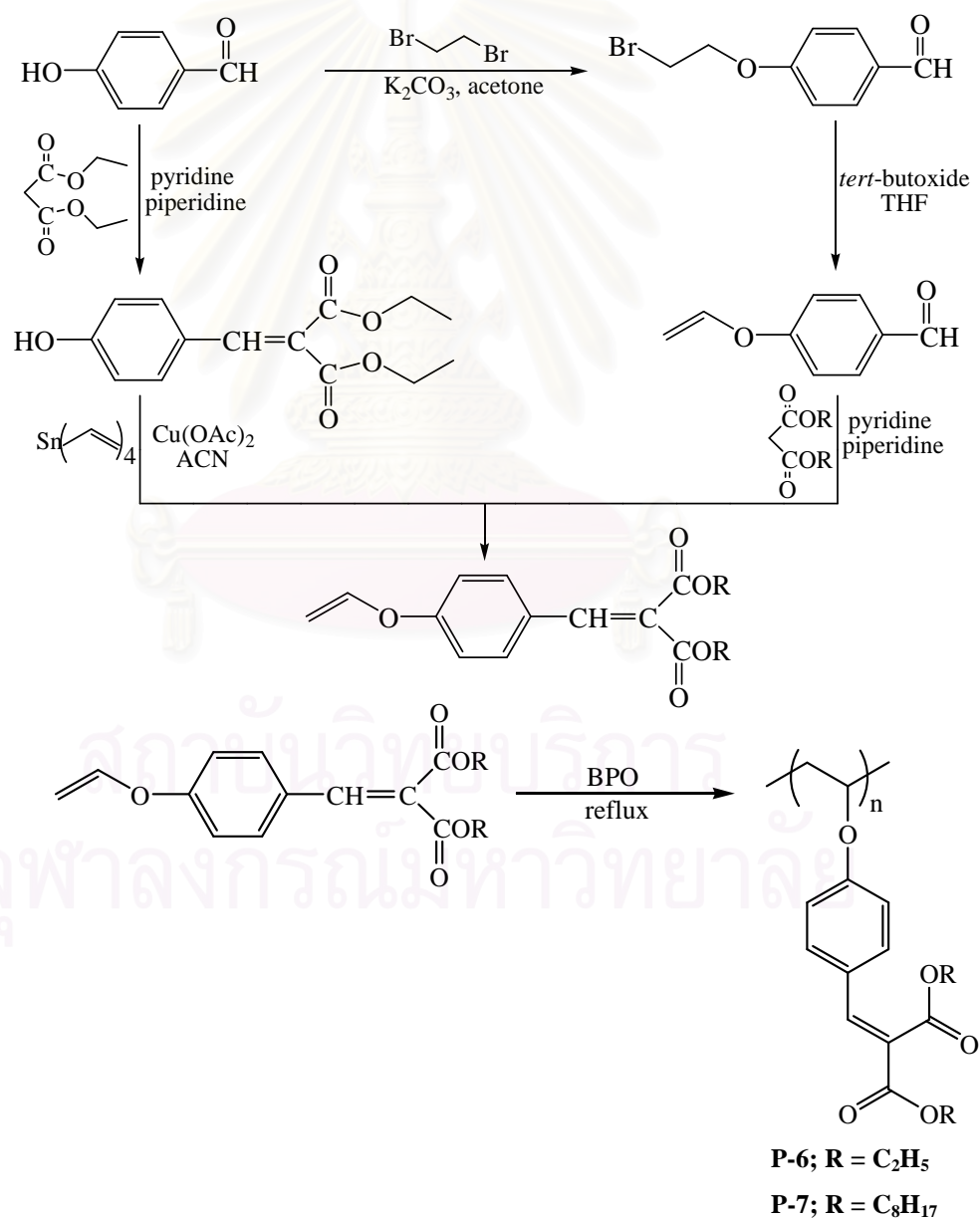
The weight-average (\bar{M}_w) and number-average molecular weight (\bar{M}_n) of both polymers were determined by gel permeation chromatography (GPC) (see Figure B.24, B.29). Table 3.8 summarized the results of the \bar{M}_w and \bar{M}_n of each polymer.

Table 3.8 Molecular weight of polymers from GPC technique

Compound	M_w	M_n	M_w/M_n
P-6	3551	2157	1.64
P-7	1889	1650	1.14

CHAPTER IV CONCLUSION

During the course of this research, the synthesis of poly(diethyl benzalmalonate-4-vinyl ether) and poly(di(2-ethylhexyl)benzalmalonate-4-vinyl ether) (Figure 4.1) were carried out with the aim to produce photostable UV-filtering oligomeric/polymeric materials with lower skin-permeation. Synthesis of two polymers were accomplished by free radical polymerization from diethylbenzalmalonate-4-vinyl ether and di(2-ethylhexyl)benzalmalonate-4-vinyl ether monomer which were synthesized through several reactions (Scheme 4.1).



Scheme 4.1 The overall syntheses of monomers and polymers

These oligomeric material showed similar UVB absorption band. The oligomeric materials were more photostable than EHMC and possess excellent solubility in most organic solvents, especial poly(di2-ethylhexyl)benzalmalonate-4-vinyl ether), a reddish brown oil, showed good solubility in cosmetic grade silicone fluid. Applications in cosmetic formulation would be very possible. Safety evaluation of the oligomers should be carried out and then further study on formulation, transdermal absorption and skin irritation of the compounds should be done.

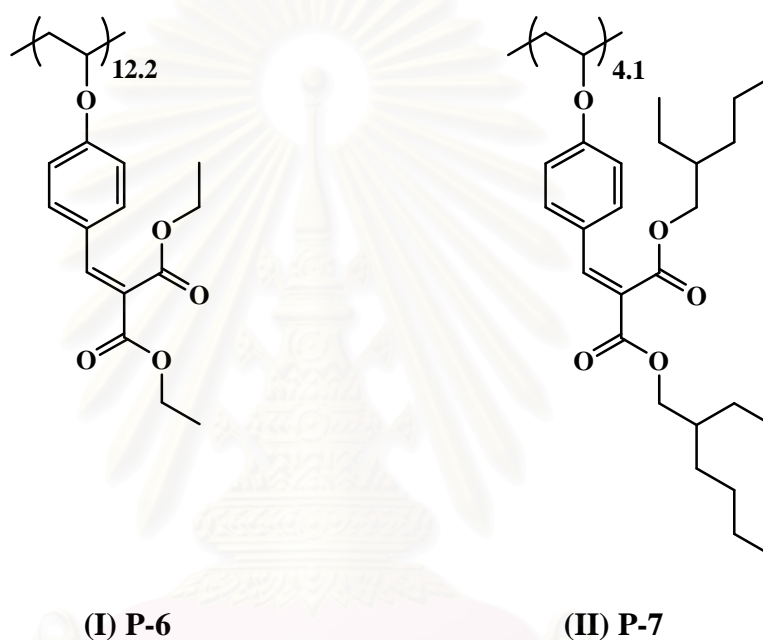


Figure 4.1 Structures of poly(diethylbenzalmalonate-4-vinyl ether) (I) P-6 and poly(di(2-ethylhexyl)benzalmalonate-4-vinyl ether) (II) P-7

สถาบันวิทยบริการ
จุฬาลงกรณ์มหาวิทยาลัย

REFERENCES

- [1] Debuys, H. V.; Levy, S. B.; and Murray, J. C. Dermatologic aspects of cosmetics. *Derm. Clin.* 18 (2000): 577-590.
- [2] Roberts, D. *Artificial lighting and the blue light hazard* [Online]. 2006. Available from: <http://www.mdsupport.org/library/hazard.html> [2006, November 21]
- [3] Umbach, W. *Cosmetic and toiletries development, production and use*. West Sussex: Elis Horwood, 1991, p. 96.
- [4] Stickland, K. K.; Krol, E. S.; and Liebler, D. C. UVB induced photooxidation of vitamin E in mouse skin. *Chem. Res. Toxicol.* 12 (1999): 187-191.
- [5] Gerlini, G.; Romagnoli, P.; and Pimpinelli, N. Skin cancer and immunosuppression. *Crit. Rev. Oncol. Hematol.* 56 (2005): 127–136.
- [6] Cadet, G.; Sage, E.; and Douki, T. Ultraviolet radiation-mediated damage to cellular. *DNA Mutation Research* 571 (2005): 3–17.
- [7] Courdavault, S.; Baudouin, C.; Charveron, M.; Canguilhem, B.; Favier, A.; Cadet, J.; and Douki, T. Repair of the three main types of bipyrimidine DNA photoproducts in human keratinocytes exposed to UVB and UVA radiations. *DNA Repair* 4 (2005): 836-844.
- [8] Hazane, F.; Sauvaigo, S.; Douki, T.; Favier, A.; and Beani, J. C. Age-dependent DNA repair and cell cycle distribution of human skin fibroblasts in response to UVA irradiation. *J. Photochem. Photobiol. B: Biol.* 82 (2006): 214-223.
- [9] Lim, H. W. American academy of dermatology consensus conference on UVA protection of sunscreens: summary and recommendations. *J. Am. Acad. Dermatol.* 44 (2001): 505-508.
- [10] Shue, C.; Kang, P.; Khan, S.; and Foote, C. S. Low-temperature photosensitized oxidation of guanosine derivative and formation of an Imidazole ring-opened products. *J. Am. Chem. Soc.* 124 (2002): 3905-3913.
- [11] Pouget, J. P.; Douki, T.; Richard, M. J.; and Cadet, J. DNA damage induced in cells by γ and UVA radiation as measured by HPLC/GC-MS and HPLC-EC and Comet assay. *Chem. Res. Toxicol.* 13 (2000): 541-549.

- [12] Ahmad, S. I.; Hargreaves, A.; Taiwo, F. A.; and Kirk, S. H. Near-ultraviolet photolysis of L-mandelate, formation of reactive oxygen species, inactivation of phage T7 and implications on human health. *J. Photochem. Photobiol. B: Biol.* 77 (2004): 55-62.
- [13] Gray, J. *Three types of ultraviolet radiation* [Online]. 2006. Available from: http://www.pg.com/science/skincare/Skin_tws_72.htm [2006, November 21]
- [14] Gamer, A. O.; Leibold, E.; and Ravenzwaay, B. The in vitro absorption of microfine zinc oxide and titanium dioxide through porcine skin. *Toxicol. Vitro* 20 (2006): 301-307.
- [15] Wolf, R.; Matz, H.; Orion, E.; and Lipozencic, J. Sun screens-the ultimate cosmetic. *Acta Dermatovenerol. Croat.* 11 (3) (2003): 158-162.
- [16] Gasparro, F. P. *Sunscreens photobiology: molecular, cellular and physiological aspects*. Berlin: Springer-Verlag, 1997.
- [17] Hoffmann, M. R.; Martin, S. T.; Choi, W.; and Bahnemann, D. Environmental applications of semiconductor photocatalysis. *Chem. Rev.* 95 (1995): 69-96.
- [18] U.S. Food and Drug Administration: Title 21, Volume 5, Part 352. *In: code of federal regulations*. Washington D.C.: Department of Health, Education and Welfare, Food and Drug Administration, 1999. (Mimeographed)
- [19] Gasparro, F. P.; Mitchnik, M.; and Nash, J. F. A review of sunscreen safety and efficacy. *Photochem. Photobiol.* 68 (1998): 243-256.
- [20] Maier, H.; Schauburger, G.; Brunnhofer, K.; and Honigsmann, H. Change of ultraviolet absorbance of sunscreens by exposure to solar-simulated radiation. *J. Invest. Dermatol.* 117 (2) (2001): 256-262.
- [21] Hagedorn-Leweke, U.; and Lippold, B. C. Absorption of sunscreens and other compounds through human skin in vivo: derivation of a method to predict maximum fluxes. *Pharmaceut. Res.* 12 (9) (1995): 1354-1360.
- [22] Hany, J.; and Nagel, R. Detection of sunscreen agents in human breast-milk. *Dtsch. Lebensm. Rundsch* 91 (1995): 341-345.
- [23] Hayden, C. G.; Roberts, M. S.; and Benson, H. A. Systematic absorption of sunscreen after topical application. *Lancet* 350 (1997): 863-864.

- [24] Gupta, V. K.; Zatz, J. L.; and Rerek, M. Percutaneous absorption of sunscreens through Micro-Yucatan pig skin *in vitro*. *Pharmacol. Res.* 16 (1999): 1602-1607.
- [25] Potard, G.; Laugel, C.; Schaefer, H.; and Marty, J. P. The stripping technique: *in vitro* absorption and penetration of five UV filters on excised fresh human skin. *Skin Pharmacol. Appl. Skin Physiol.* 13 (2000): 336-344.
- [26] Chatelain, E.; Gobard, B.; and Surber, C. Skin penetration and sun protection factor of five UV filters: effect of the vehicle. *Skin Pharmacol. Appl. Skin Physiol.* 16 (1) (2003): 28-35.
- [27] Sarveiya, V.; Risk, S.; and Benson, H. A. Liquid chromatographic assay for common sunscreen agents: application to *in vivo* assessment of skin penetration and systemic absorption in human volunteers. *J. Chromatogr. B* 803 (2004): 225-231.
- [28] Hanson, K. M.; Gratton, E.; and Bardeen, C. J. Sunscreen enhancement of UV-induced reactive oxygen species in the skin. *Free Radic. Biol. Med.* 41 (2006): 1205-1212.
- [29] Serpone, N.; Dondi, D.; and Albini, A. Inorganic and organic UV filters: their role and efficacy in sunscreens and sun care products. *Inorg. Chim. Acta* 360 (2007): 794-802.
- [30] Vanquerp, V.; Rodriguez, C.; Coiffard, C.; Coiffard, L. J. M.; and De Roeck-Holtzhauser, Y. High-performance liquid chromatographic method for the comparison of the photostability of five sunscreen agents. *J. Chromatogr. A* 832 (1999): 273-277.
- [31] Diffey, B. L.; Stokes, R. P.; Forestier, S.; Mazilier, C.; and Rougier, A. Sun care product photostability: a key parameter for a more realistic *in vitro* efficacy evolution. *Eur. J. Dermatol.* 7 (1997): 226-228.
- [32] Tarras-Wahlberg, N.; Stenhagen, G.; Larko, O.; Rosen, A.; Wennberg, A. M.; and Wennerstrom, O. Changes in ultraviolet absorption of sunscreens after ultraviolet radiation. *J. Invest. Dermatol.* 113 (1999): 547-553.
- [33] Pattanaargson, S.; and Limpong, P. Stability of octyl methoxycinnamate and identification of its photo-degradation product. *Int. J. Cosmet. Sci.* 23 (2001): 153-160.

- [34] Sayre, R. M.; Dowdy, J. C.; Gerwig, A. J.; Sheields, W. J.; and Lloyd, R. V. Unexpected photolysis of the sunscreen octinoxate in the presence of the sunscreen avobenzene. *Photochem. Photobiol.* 81 (2005): 452–456.
- [35] Serpone, N.; Salinaro, A.; Emeline, A. V.; Horikoshi, S.; Hidaka, H.; and Zhao, J. An in vitro systematic spectroscopic examination of the photostabilities of a random set of commercial sunscreen lotions and their chemical UVB/UVA active agents. *Photochem. Photobiol. Sci.* 1 (2002): 970-981.
- [36] Huong, S. P.; Andrieu, V.; Reynier, J. P.; Rocher, E.; and Fourneron, J. D. The photoisomerization of the sunscreen ethylhexyl *p*-methoxy cinnamate and its influence on the sun protection factor. *J. Photochem. Photobiol. Chem.* 186 (2007): 65-70.
- [37] Alvarez-Roman, R.; Barre, G.; Guy, R. H.; and Fessi, H. Biodegradable polymer nanocapsules containing a sunscreen agent: preparation and photoprotection. *Eur. J. Pharm. Biopharm.* 52 (2001): 191-195.
- [38] Perugini, P.; Simeoni, S.; Scalia, S.; Genta, I.; Modena, T.; Conti, B.; and Pavanetto, F. Effect of nanoparticle encapsulation on the photostability of the sunscreen agent, 2-ethylhexyl-*p*-methoxycinnamate. *Int. J. Pharma.* 246 (2002): 37-45.
- [39] Jimenez, M. M.; Pelletier, J.; Bobin, M. F.; and Martini, M. C. Influence of encapsulation on the in vitro percutaneous absorption of octyl methoxycinnamate. *Int. J. Pharm.* 272 (2004): 45-55.
- [40] Olvera-Martinez, B. I.; Cazares-Delgadillo, J.; Calderilla-Fajardo, S. B.; Villalobos-Garcia, R.; Ganem-Quintanar, A.; and Quintanar-Guerrero, D. Preparation of polymeric nanocapsules containing octyl methoxycinnamate by the emulsification-diffusion technique: penetration across the stratum corneum. *J. Pharma. Sci.* 94 (7) (2005): 1552-1559.
- [41] Godwin, D. A.; Kim, N. H.; and Felton, L. A. Influence of Transcutol[®]CG on the skin accumulation and transdermal permeation of ultraviolet absorbers. *Eur. J. Pharm. Biopharm.* 53 (2002): 23-27.
- [42] Scalia, S.; Casolari, A.; Iaconinoto, A.; and Simeoni, S. Comparative studies of the influence of cyclodextrins on the stability of the sunscreen agent, 2-ethylhexyl-*p*-methoxycinnamate. *J. Pharmaceut. Biomed. Anal.* 30 (2002): 1181-1189.

- [43] Yener, G.; Incegul, T.; and Yener, N. Importance of using solid lipid microspheres as carriers for UV filters on the example octyl methoxy cinnamate. *Int. J. Pharm.* 258 (2003): 203-207.
- [44] Gaspar, L. R.; and Campos, P. M. Evaluation of the photostability of different UV filter combinations in a sunscreen. *Int. J. Pharm.* 307 (2006): 123-128.
- [45] Hossel, P.; Wunsch, T.; and Dieing, R. cosmetic or dermatological sunscreen preparations. US Patent 2001/0021375 A1 (2001).
- [46] Aoyagi, T.; Terashima, O.; Suzuki, N.; Matsui, K.; and Nagase, Y. Polymerization of benzalkonium chloride-type monomer and applications to percutaneous drug absorption enhancement. *J. Contr. Release* 13 (1990): 63-71.
- [47] Akitomoto, T.; Aoyagi, T.; Minoshima, J.; and Nagase, Y. Polymeric percutaneous penetration enhancers synthesis and enhancing property of PEG/PDMS block copolymer with cationic end group. *J. Contr. Release* 49 (1997): 229-241.
- [48] Pattanaargson, S.; Hongchinnagorn, N.; Hirunsupachot, P.; and Sritana-anant, Y. UV absorption and photoisomerization of p-methoxycinnamate grafted silicone. *Photochem. Photobiol.* 80 (2004): 322-325.
- [49] Sovak, L. J. M.; Terry, R. C.; Douglass, J. G.; Bakir, F.; and Mar, D. Sunblocking polymers and their formulation. US Patent 5487885 (1996).
- [50] Richard, H.; and Leduc, M. Silicone-substituted cinnamamide/malonamide/malonate compounds and photoprotective compositions comprised thereof. US Patent 6080880 (2000).
- [51] O'Lenick, A. J.; and Dacula, G. A. Aromatic dimethicone copolyol polymers as sunscreen agents. US Patent 6346595 B1 (2002).
- [52] Koshti, N. M.; and Naik, S. D. Salt and heat sensitive, substantive UV-absorbing polymers. US Patent 7087692 B2 (2006).
- [53] Odian, G. *Principles of polymerization*. 4th ed. New York: John Wiley and Sons, 2004, pp 198-199.
- [54] Oriol, L.; Pinol, M.; Serrano, J. L.; and Tejedor, R. M. Synthesis, characterization and photoreactivity of liquid crystalline cinnamates. *J. Photochem. Photobiol. Chem.* 155 (2003): 37-45.

- [55] Gupta, P.; Trenor, S. R.; Long, T. E.; and Wilkes, G. L. In Situ Photo-Cross-Linking of Cinnamate Functionalized Poly(methyl methacrylate-co-2-hydroxyethyl acrylate) Fibers during Electrospinning. *Macromolecules* 37 (2004): 9211-9218.
- [56] Nakayama, Y.; and Matsuda, T. Surface fixation of poly(ethylene glycol) via photodimerization of cinnamate group. *J. Polym. Sci.: Polym. Chem.* 31 (1993): 299-305.
- [57] Tsutsumi, H.; Shibasaki, Y.; Onimura, K.; and Oishi, T. Preparation of photo-patterned polymer-hydroxyapatite composites. *Polymer* 44 (2003): 6297-6301.
- [58] Chae, B.; Lee, S. W.; Ree, M.; Jung, M. J.; and Kim, S. B. Photoreaction and molecular reorientation in a nanoscaled film of poly(methyl-4-(methacryloyloxy) cinnamate) studied by two-dimensional FTIR and UV correlation spectroscopy. *Langmuir* 19 (2003): 687-695.
- [59] Balaji, R.; Grande, D.; and Nanjundan, S. Photoresponsive polymers having pendant chlorocinnamoyl moieties: synthesis, reactivity ratios and photochemical properties. *Polymer* 45 (2004): 1089-1099.
- [60] Mahy, R.; Boufelja, B.; Oulmidi, A.; Challioui, A.; Derouet, D.; and Brosse, J. C. Photosensitive polymers with cinnamate units in the side position of chains: synthesis, monomer reactivity ratios and photoreactivity. *Eur. Polym. J.* 42 (10) (2006): 2389-2397.
- [61] Koo, J.; Fish, M. S.; Walker, G. N.; and Blake, J. 2,3-Dimethoxycinnamic acid. *Org. Syntheses, Coll.* 4 (1944): 327-328.
- [62] Blouin, M.; and Frenette, R. A new method for preparation of aryl vinyl ethers. *J. Org. Chem.* 66 (2001): 9043-9045.
- [63] Bong, P. H. Spectral and photophysical behaviors of curcumin and curcuminoids. *Bull. Kor. Chem. Soc.* 21 (2000): 81-86.
- [64] Tutar, A.; and Balci, M. Bromination of an N-carbethoxy-7-aza-2,3-benzonorbornadiene and synthesis of N-carbethoxy-7-aza-2,3-dibromo-5,6-benzonorbornadiene: high temperature bromination. Part 14. *Tetrahedron* 58 (2002): 8979-8984.
- [65] Harwood, L. M.; and Moody, C. J. *Experimental Organic Chemistry, Principle and Practice*. Oxford: Scientific, 1989, pp 443-444.

- [66] Lacaze-Dufaure, C.; and Mouloungui, Z. Catalysed or uncatalyzed esterification reaction of oleic acid with 2-ethyl hexanol. *Appl. Catal. Gen.* 204 (2000): 223-227.
- [67] Agrapidis-Paloympis, L. E.; and Nash, R. A. The effect of solvents on the ultraviolet absorbance of sunscreen. *J. Soc. Cosmet. Chem.* 38 (1987): 209-227.
- [68] Skoog, D. A.; West, D. M.; and Holler, F. J. *Fundamentals of analytical chemistry*. 7th ed. New York: Saunders College, 1997, pp 510-511.
- [69] Parker-Textloc. *Textloc refractive index of polymers* [Online]. 2007. Available from: http://www.textloc.com/closet/cl_refractiveindex.html [2007, March 5]
- [70] Schneider, H. A. Polymer class specificity of the glass temperature. *Polymer* 46 (2005): 2230-2237.
- [71] Vosloo, J. J.; Zyl, A. J. P.; Nicholson, T. M.; Sanderson, R. D.; and Gilbert, R. G. Thermal and viscoelastic structure-property relationships of model comb-like poly(*n*-butyl methacrylate). *Polymer* 48 (2007): 205-219.
- [72] Peiser, P. In: *Brandrup, J.; Immergut, E.H., editors Polymer handbook*. 3rd ed. New York: Wiley, 1989, pp VI/209-VI/227.



APPENDICES

สถาบันวิทยบริการ
จุฬาลงกรณ์มหาวิทยาลัย

APPENDIX A

A. Degree of polymerization of poly(dialkylbenzmalonate-4-vinyl ether); \overline{DP}

The weight average molecular weight (M_w) of poly(diethylbenzmalonate-4-vinyl ether; P-6) and poly(di(2-ethylhexyl)benzmalonate-4-vinyl ether; P-7) obtained by gel permeation chromatography technique (GPC) were 3551 and 1889, respectively.

The average degree of polymerization was calculated by the following equation:

$$\text{Average degree of polymerization} = \frac{M_w \text{ of polymer}}{\text{MW of monomeric unit}}$$

Since MW of monomeric units of P-6 and P-7 were 290 and 458, respectively,

$$\text{Therefore, the average degree of polymerization of P-6} = \frac{3551}{290}$$

$$= 12.24$$

$$\text{the average degree of polymerization of P-7} = \frac{1889}{458}$$

$$= 4.12$$

B. Calculation of molar absorptivity of polymer; ϵ

$$X \text{ ppm} = \frac{X \times 10^{-3}}{\text{Molecular weight}} \text{ moles of monomer/1000 mL}$$

$$= \frac{X \times 10^{-3}}{\text{Molecular weight (monomeric unit)}} \text{ moles of polymer/1000 mL}$$

Therefore, ϵ = slope of graph between absorbance (at λ_{max}) and concentrations of polymer

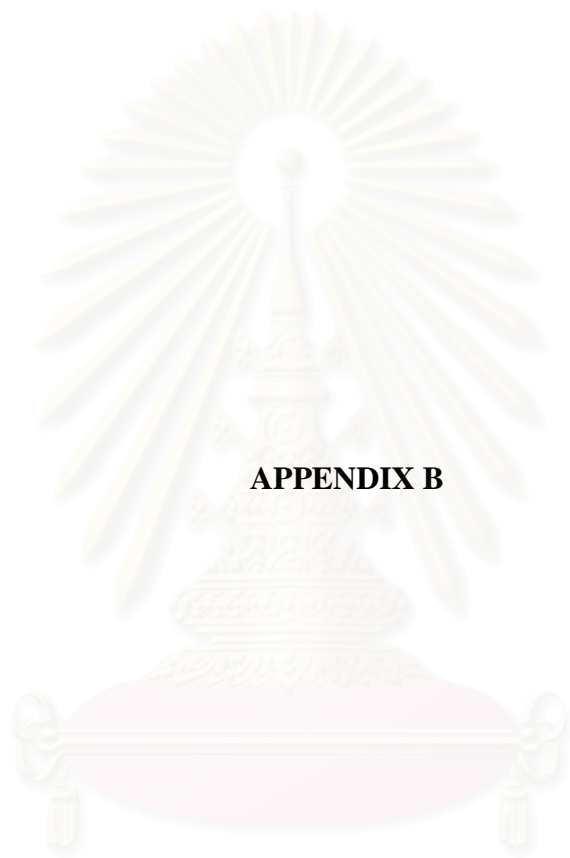
C. Photostability test

Table C.1 Percent relative absorbance of the synthesized oligomers in UVA and UVB region in chloroform

Time (h)	Percent relative absorbance		
	P-6	P-7	EHMC
0	100	100	100
0.30	93.93	98.13	75.50
1	92.99	97.43	71.90
2	91.12	93.22	77.30
3	91.12	92.99	73.30

Table C.2 Energy of UVA and UVB exposure (8.3 mW/cm^2 UVA and 0.66 mW/cm^2 UVB) at each irradiated time

Time (h)	Energy (J)	
	UVA irradiation	UVB irradiation
0	0	0
0.30	15.50	1.26
1	31.00	2.52
2	62.00	5.04
3	93.00	7.56



APPENDIX B

สถาบันวิทยบริการ
จุฬาลงกรณ์มหาวิทยาลัย

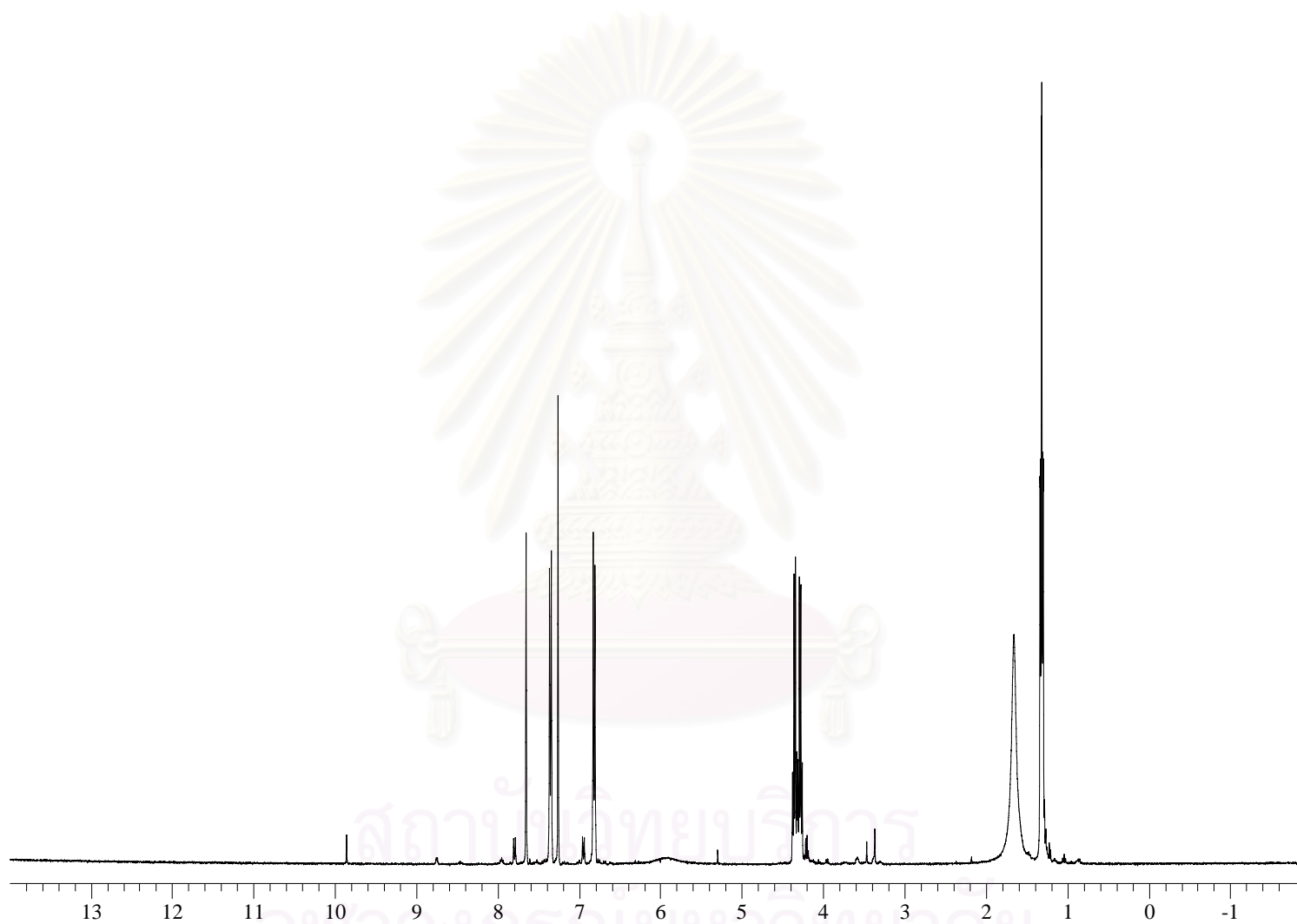


Figure B.1 $^1\text{H-NMR}$ (CDCl_3) spectrum of diethyl-4-hydroxy benzalmalonate (M-2)

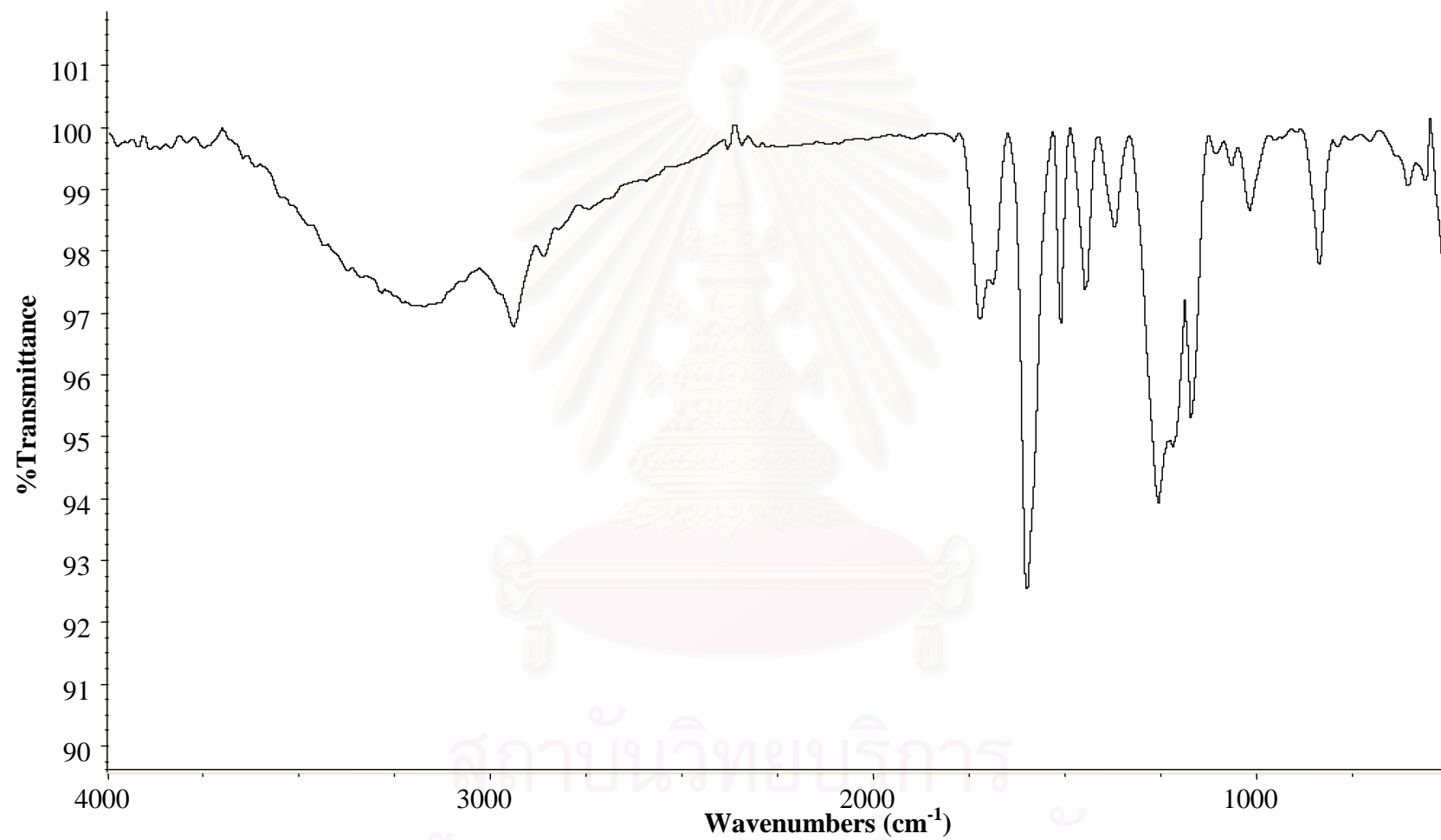


Figure B.2 IR spectrum of diethyl-4-hydroxy benzalmalonate (M-2)

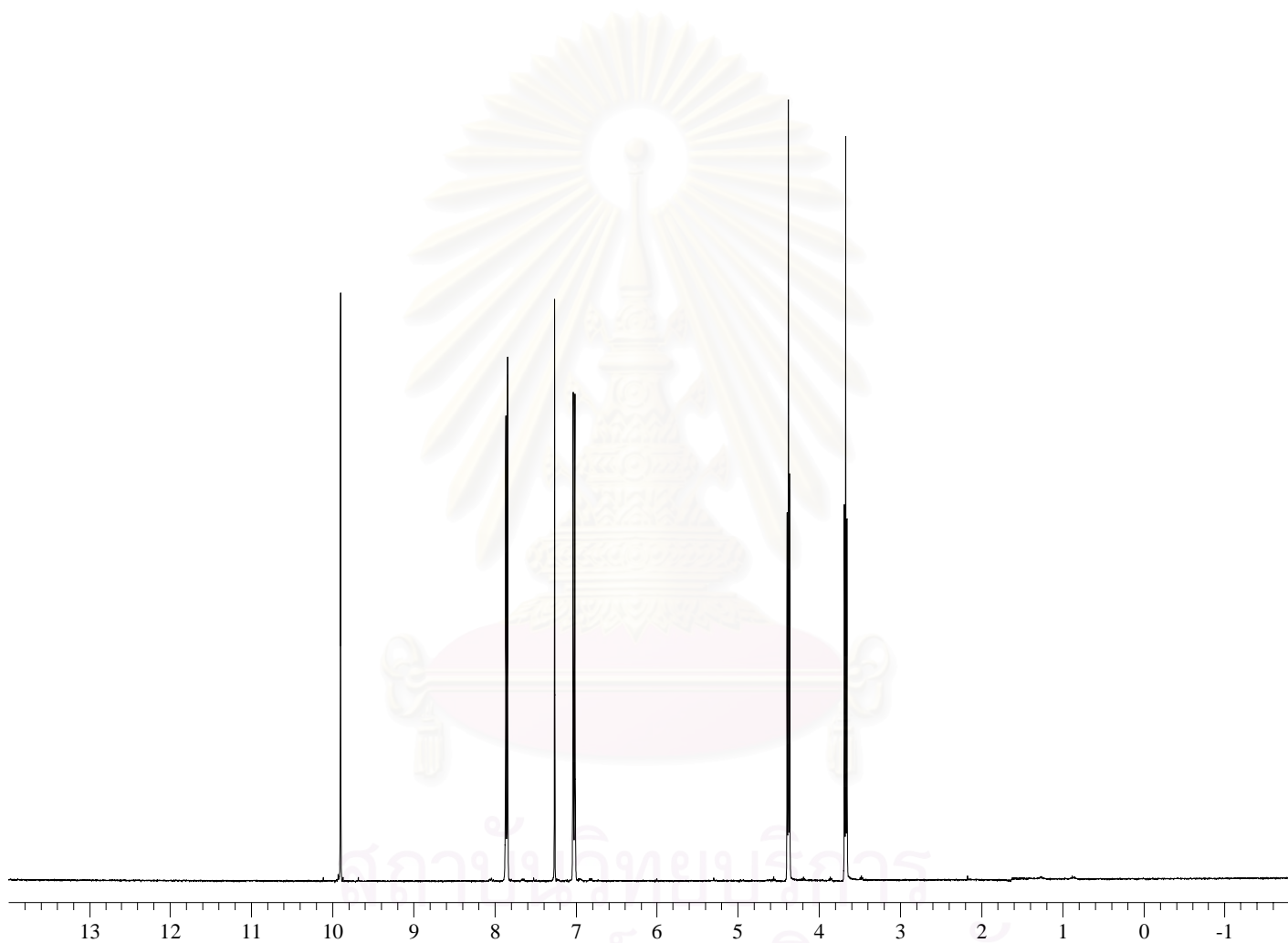


Figure B.3 $^1\text{H-NMR}$ (CDCl_3) spectrum of 4-((2-bromo)ethoxy)benzaldehyde (M-3)

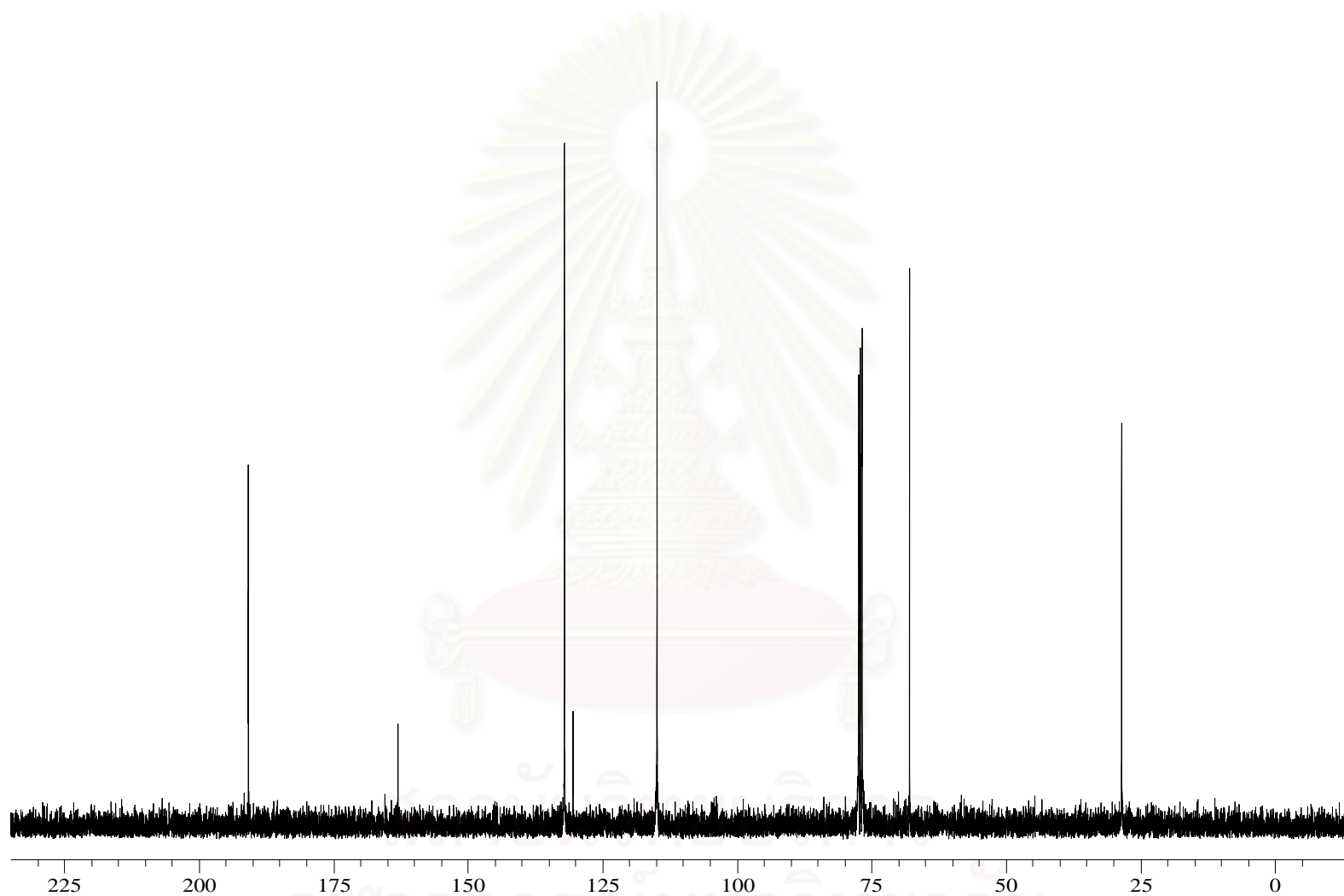


Figure B.4 ^{13}C -NMR (CDCl_3) spectrum of 4-((2-bromo)ethoxy)benzaldehyde (M-3)

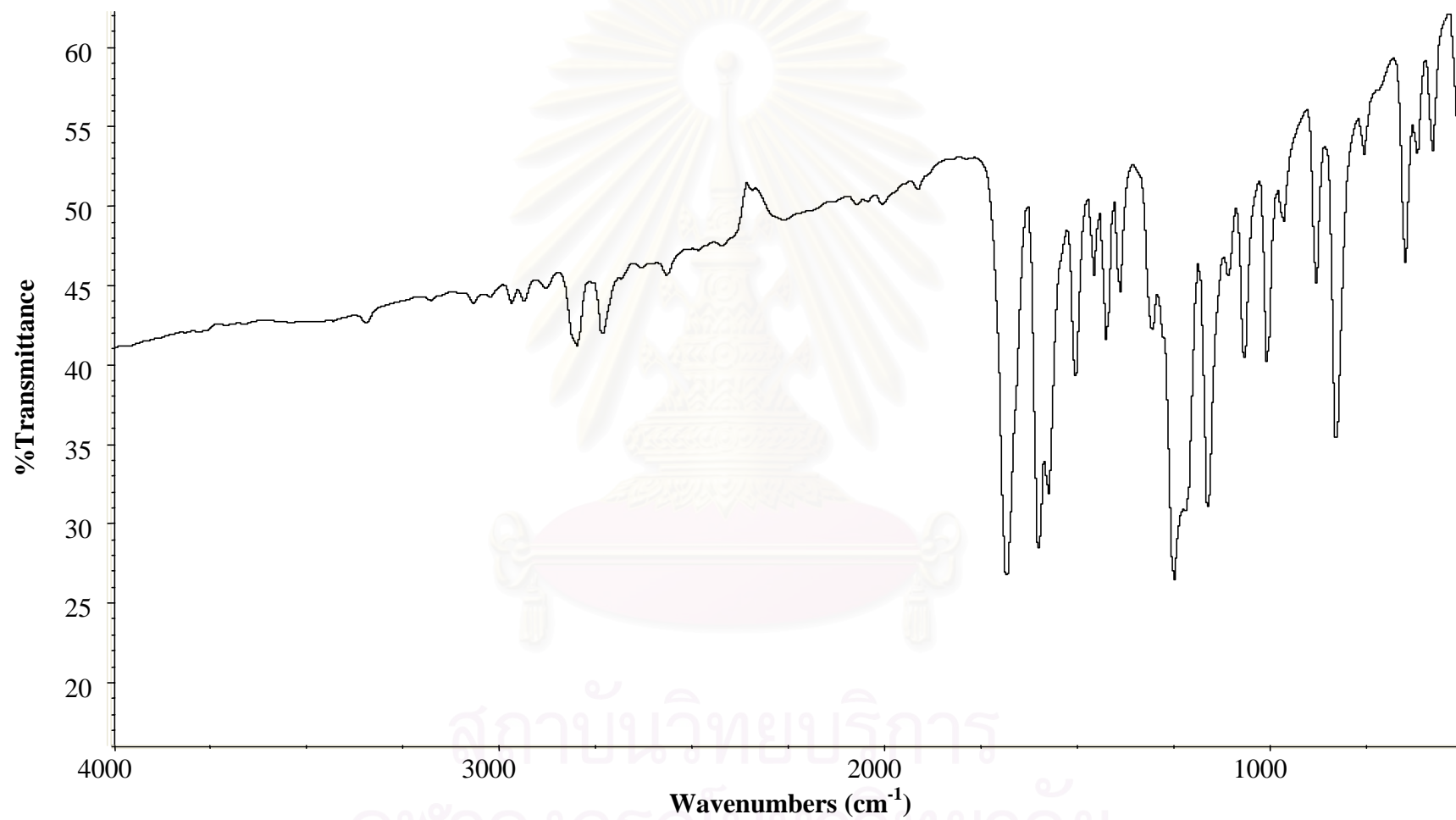


Figure B.5 IR spectrum of 4-((2-bromo)ethoxy)benzaldehyde (M-3)

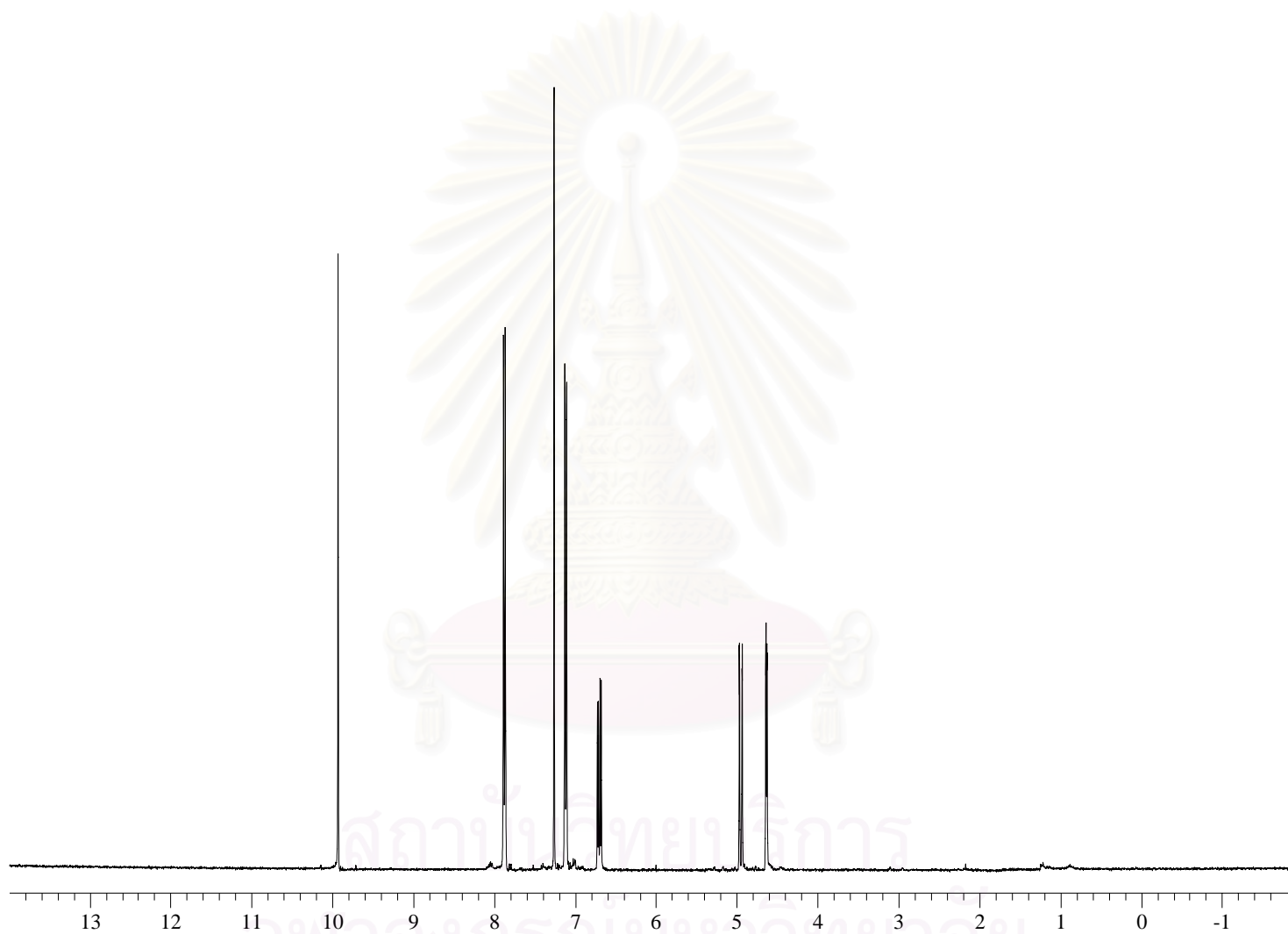


Figure B.6 $^1\text{H-NMR}$ (CDCl_3) spectrum of 4-vinyloxybenzaldehyde (M-4)

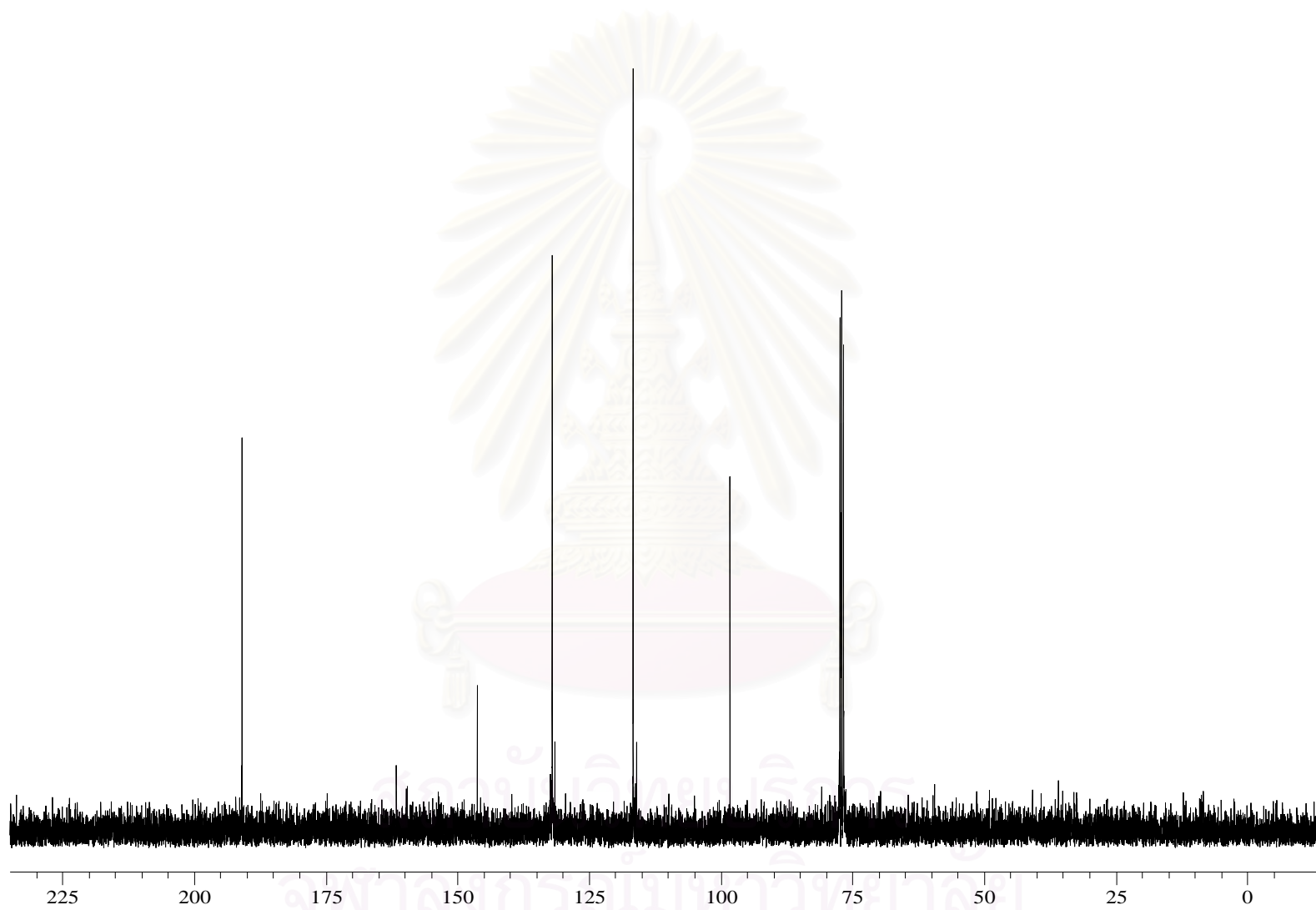


Figure B.7 ^{13}C -NMR (CDCl_3) spectrum of 4-vinylbenzaldehyde (M-4)

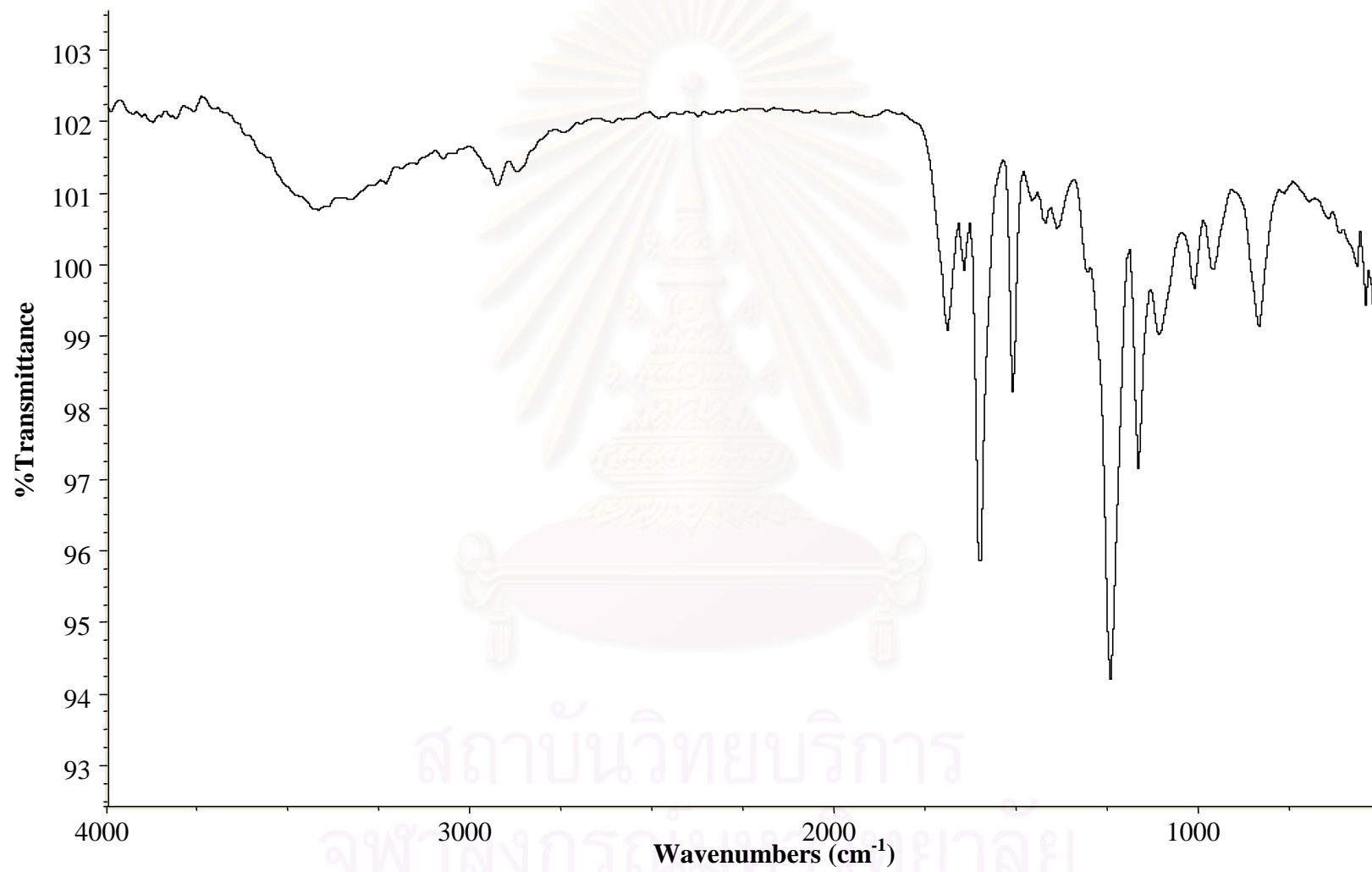


Figure B.8 IR spectrum of 4-vinylbenzaldehyde (M-4)

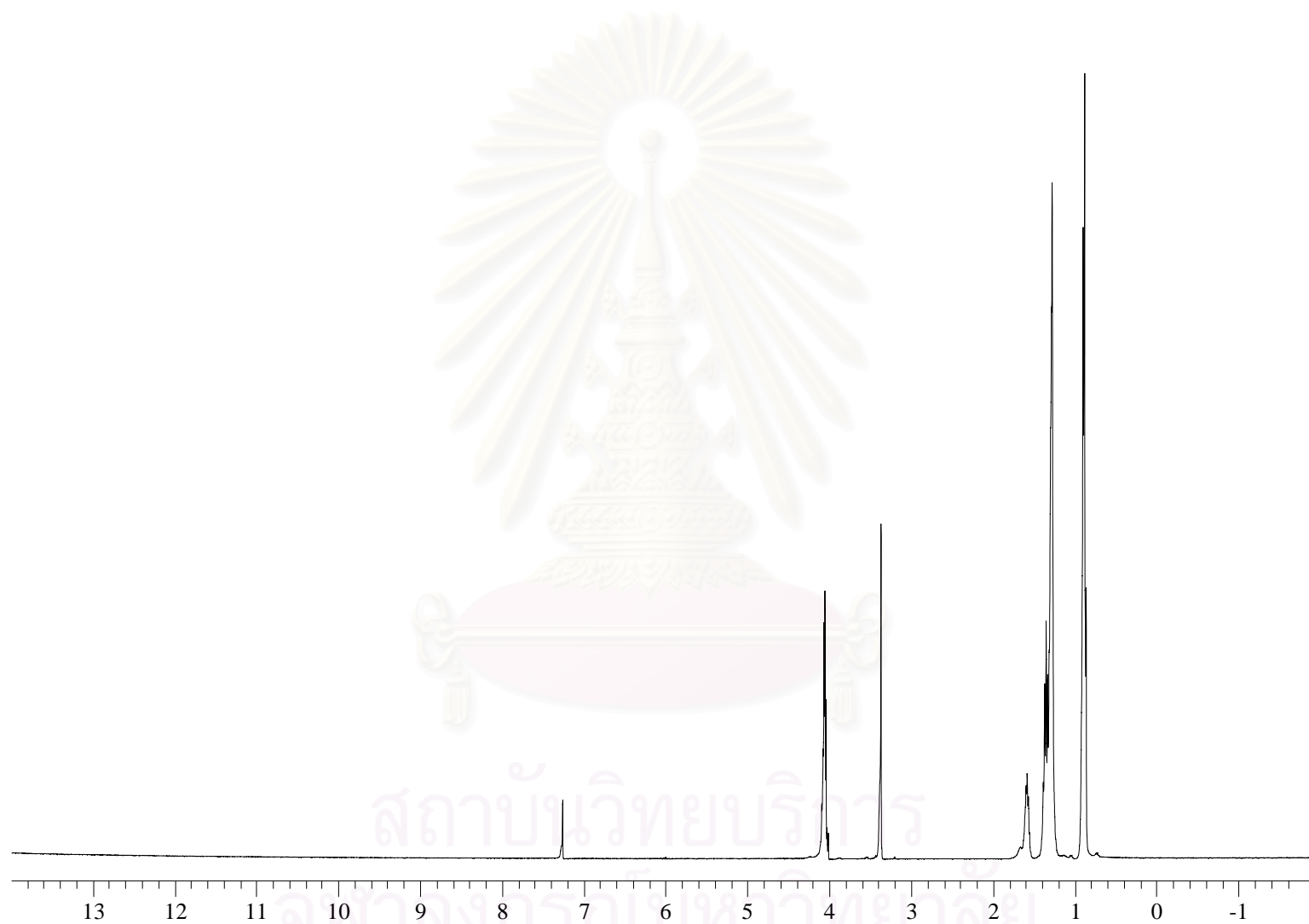


Figure B.9 $^1\text{H-NMR}$ (CDCl_3) spectrum of di(2-ethylhexyl)malonate (M-5')

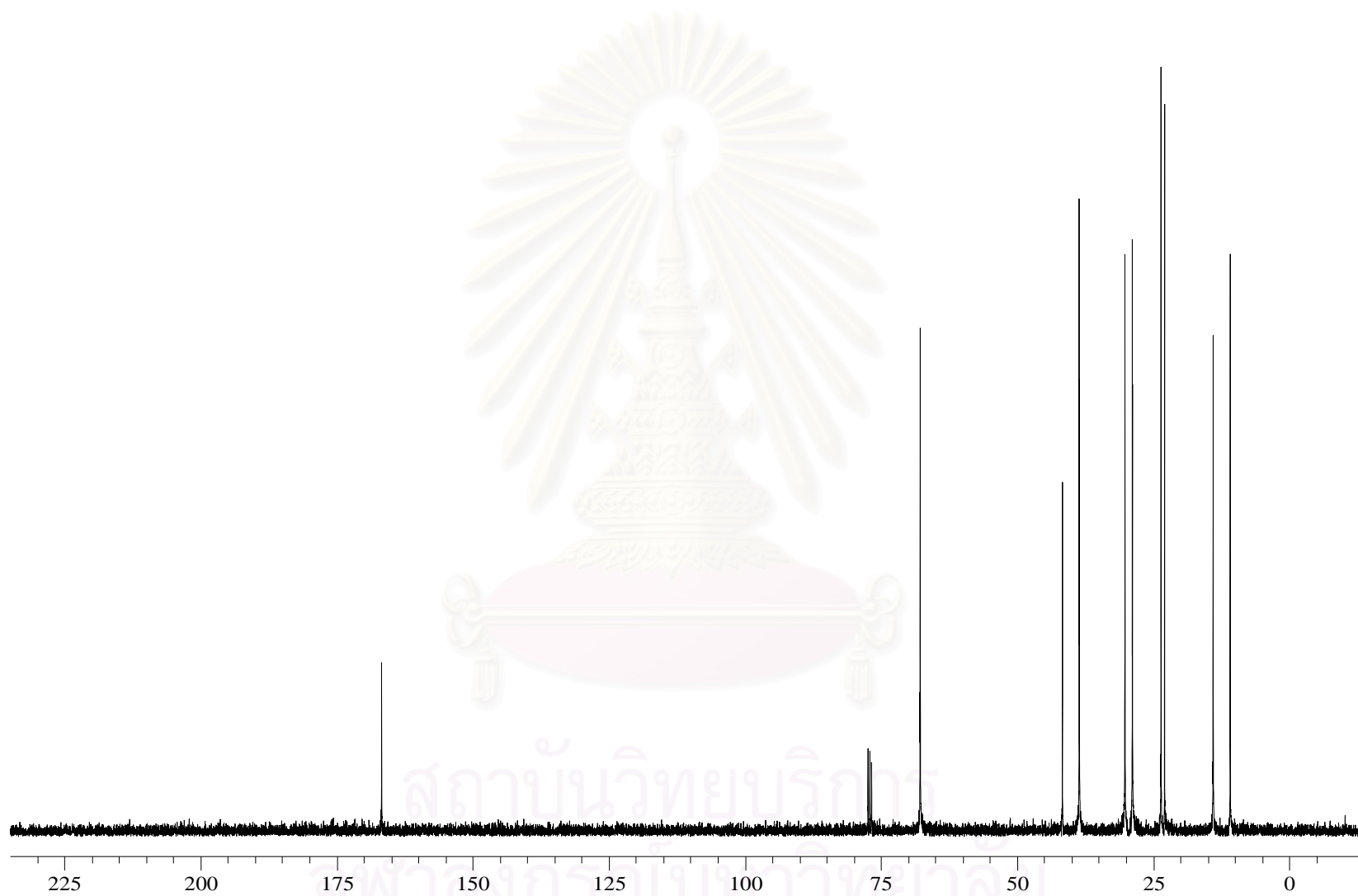


Figure B.10 ^{13}C -NMR (CDCl_3) spectrum of di(2-ethylhexyl)malonate (M-5')

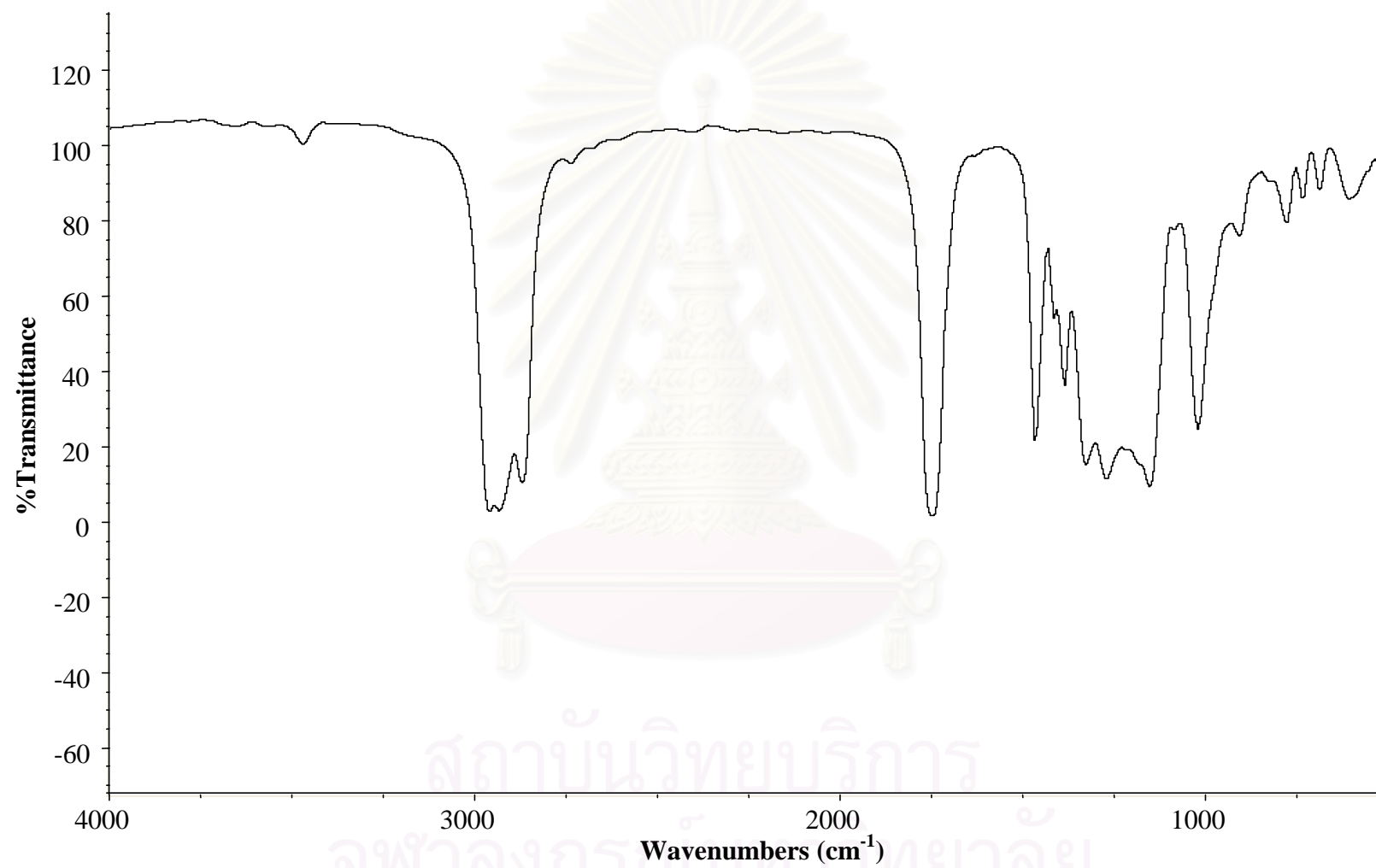


Figure B.11 IR spectrum of di(2-ethylhexyl)malonate (M-5')

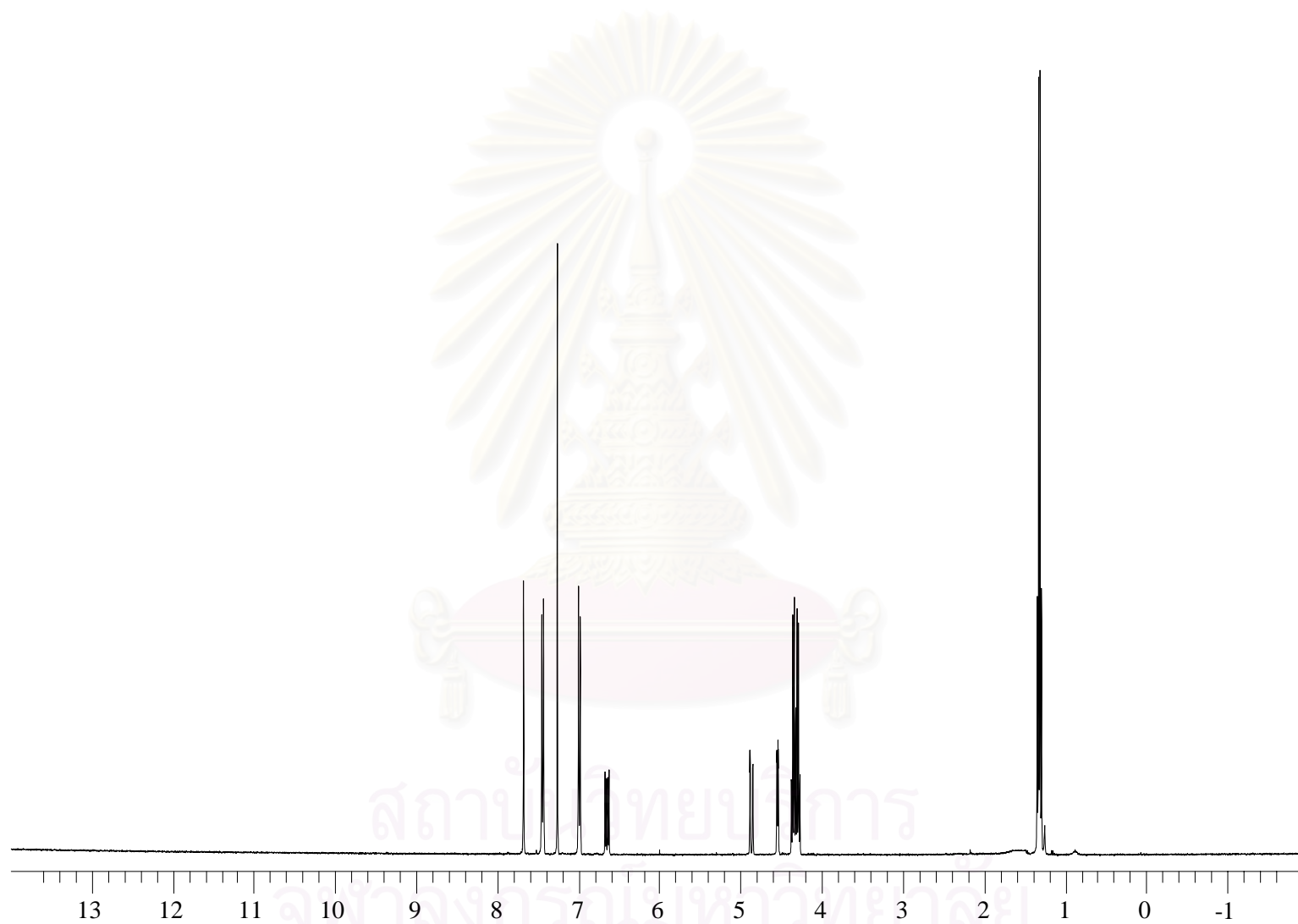


Figure B.12 $^1\text{H-NMR}$ (CDCl_3) spectrum of diethylbenzalmalonate-4-vinyl ether (M-6)

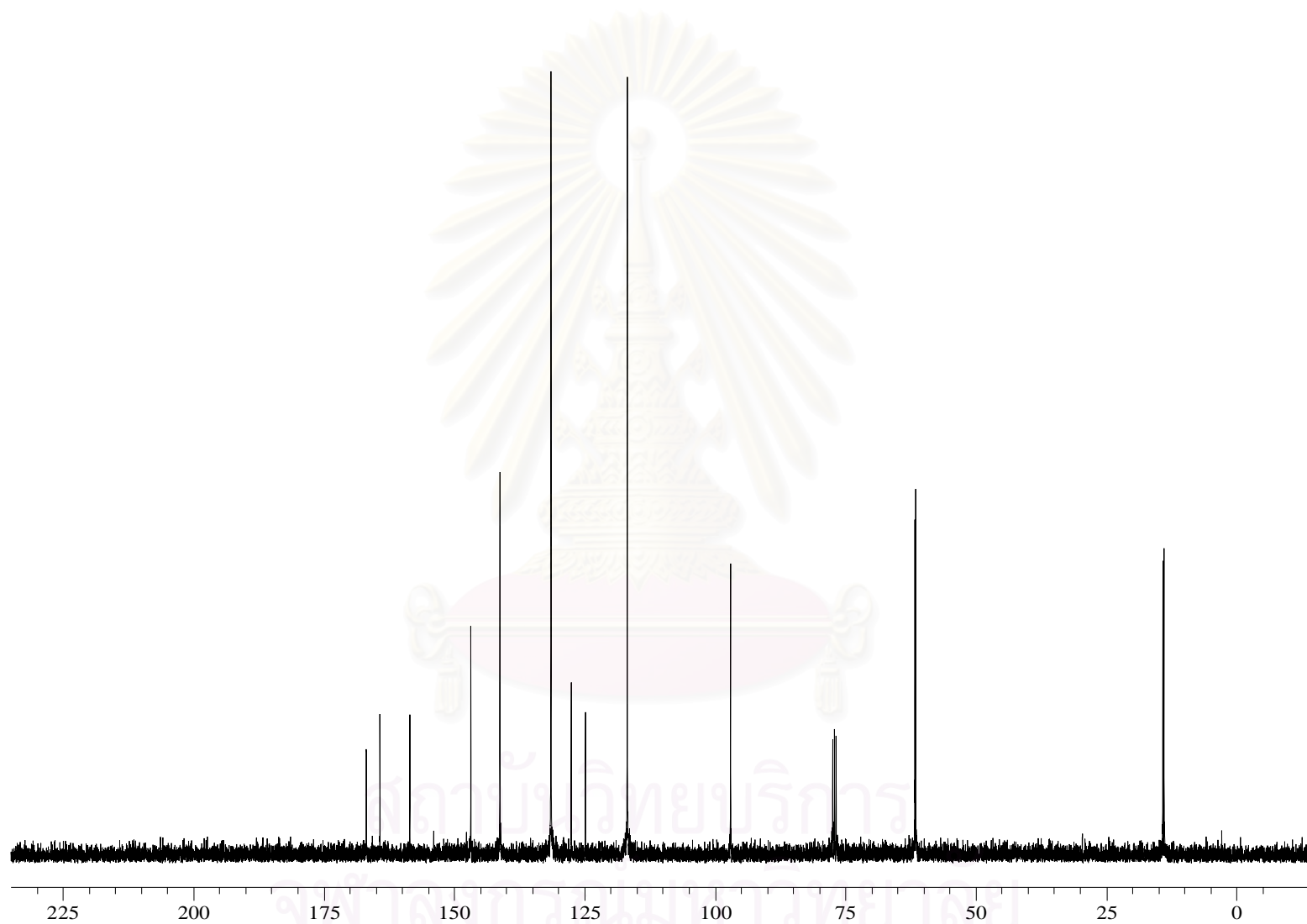


Figure B.13 ^{13}C -NMR (CDCl_3) spectrum of diethylbenzalmalonate-4-vinyl ether (M-6)

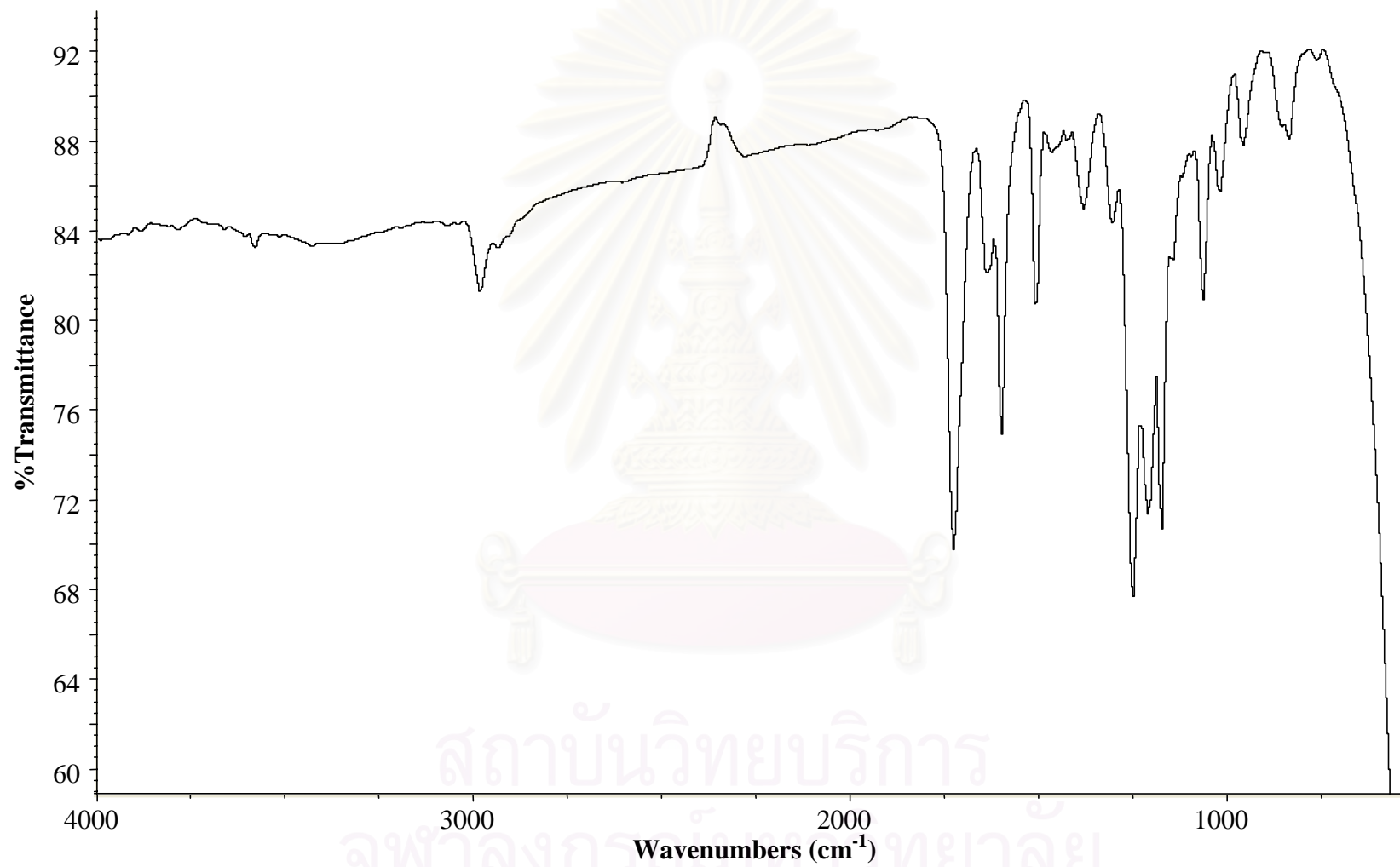


Figure B.14 IR spectrum of diethylbenzmalonate-4-vinyl ether (M-6)



Figure B.15 MS spectrum of diethylbenzalmalonate-4-vinyl ether (M-6)

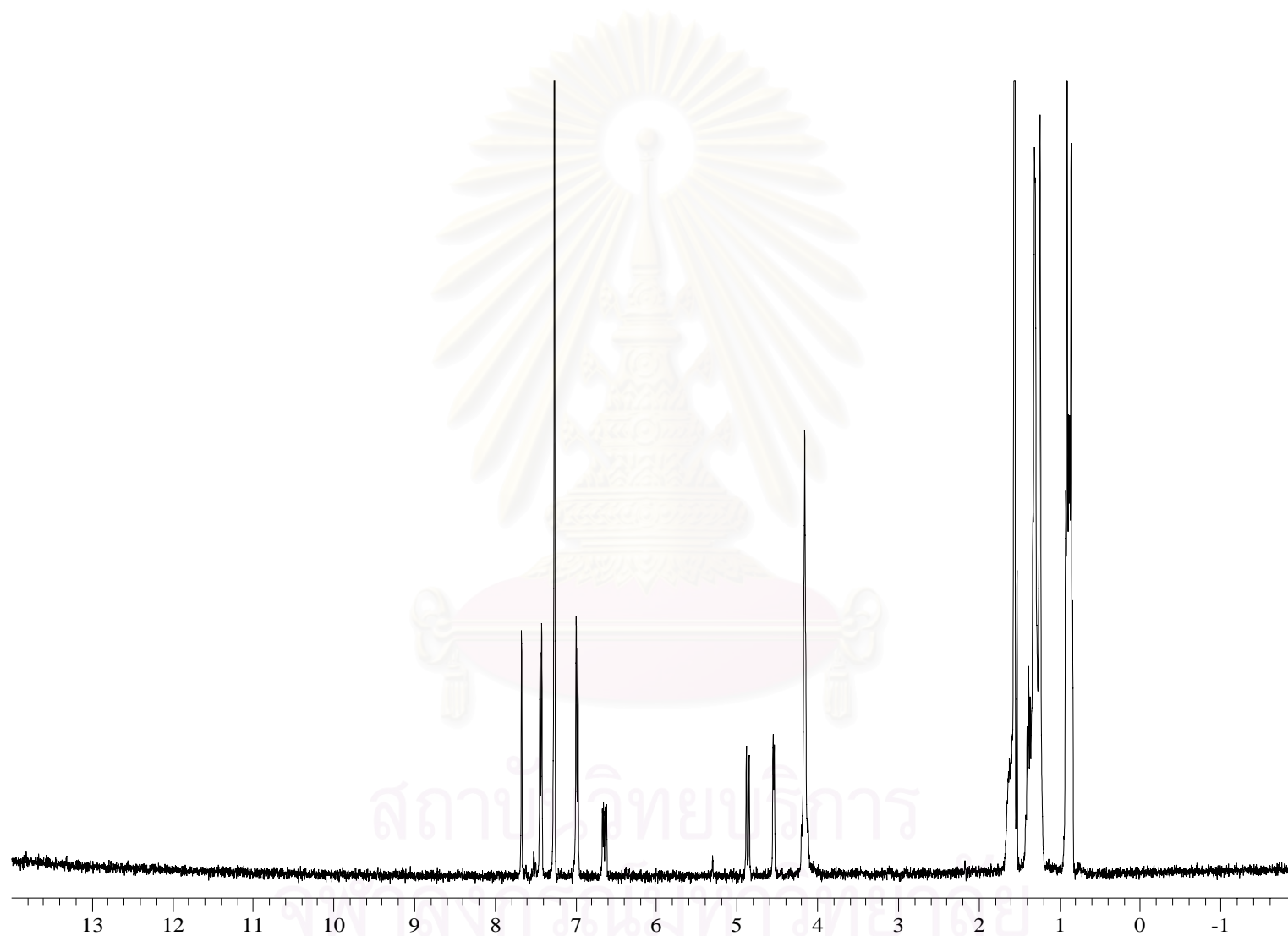


Figure B.16 $^1\text{H-NMR}$ (CDCl_3) spectrum of di(2-ethylhexyl)benzalmalonate-4-vinyl ether (M-7)

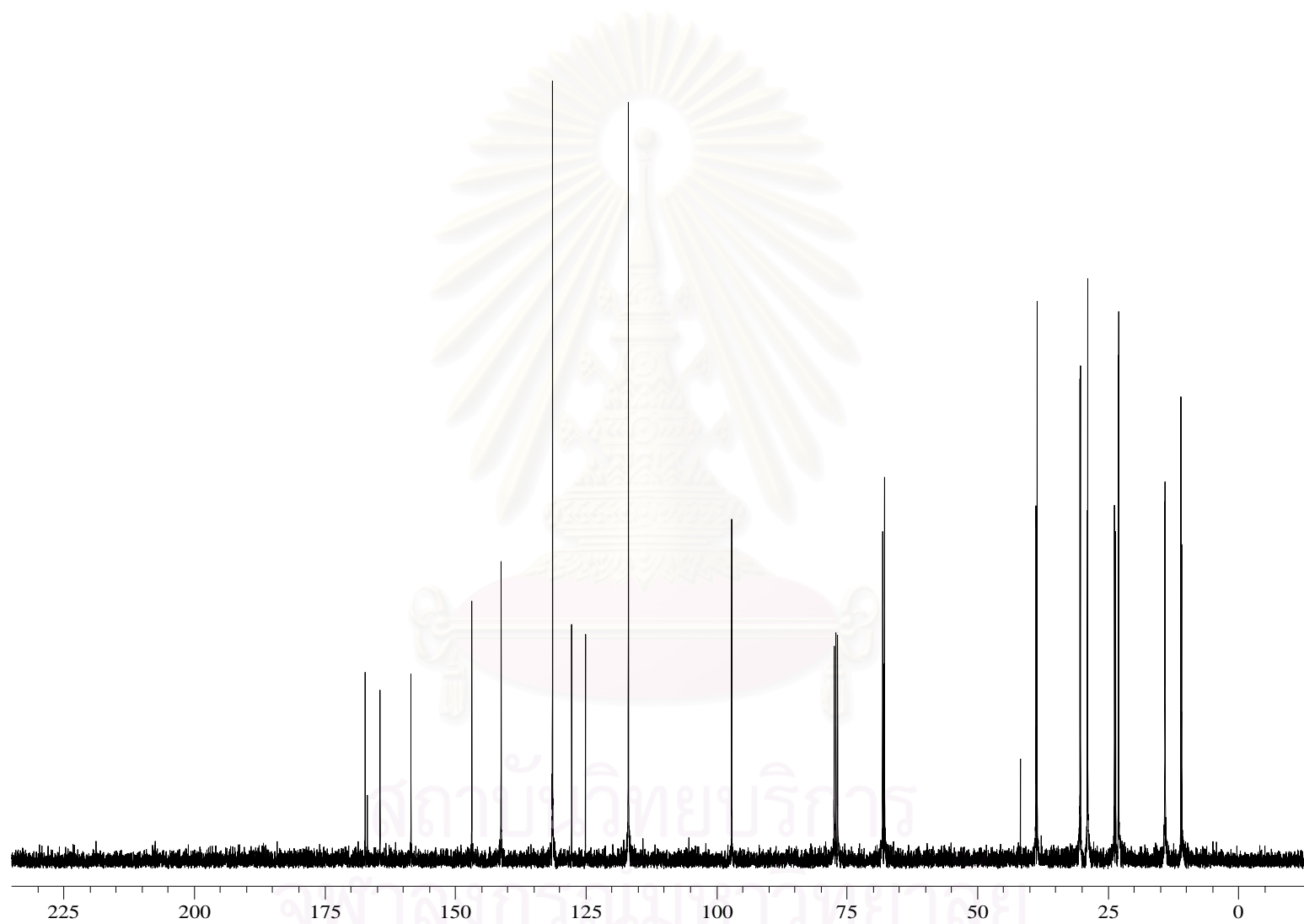


Figure B.17 ^{13}C -NMR (CDCl_3) spectrum of di(2-ethylhexyl)benzalmalonate-4-vinyl ether (M-7)

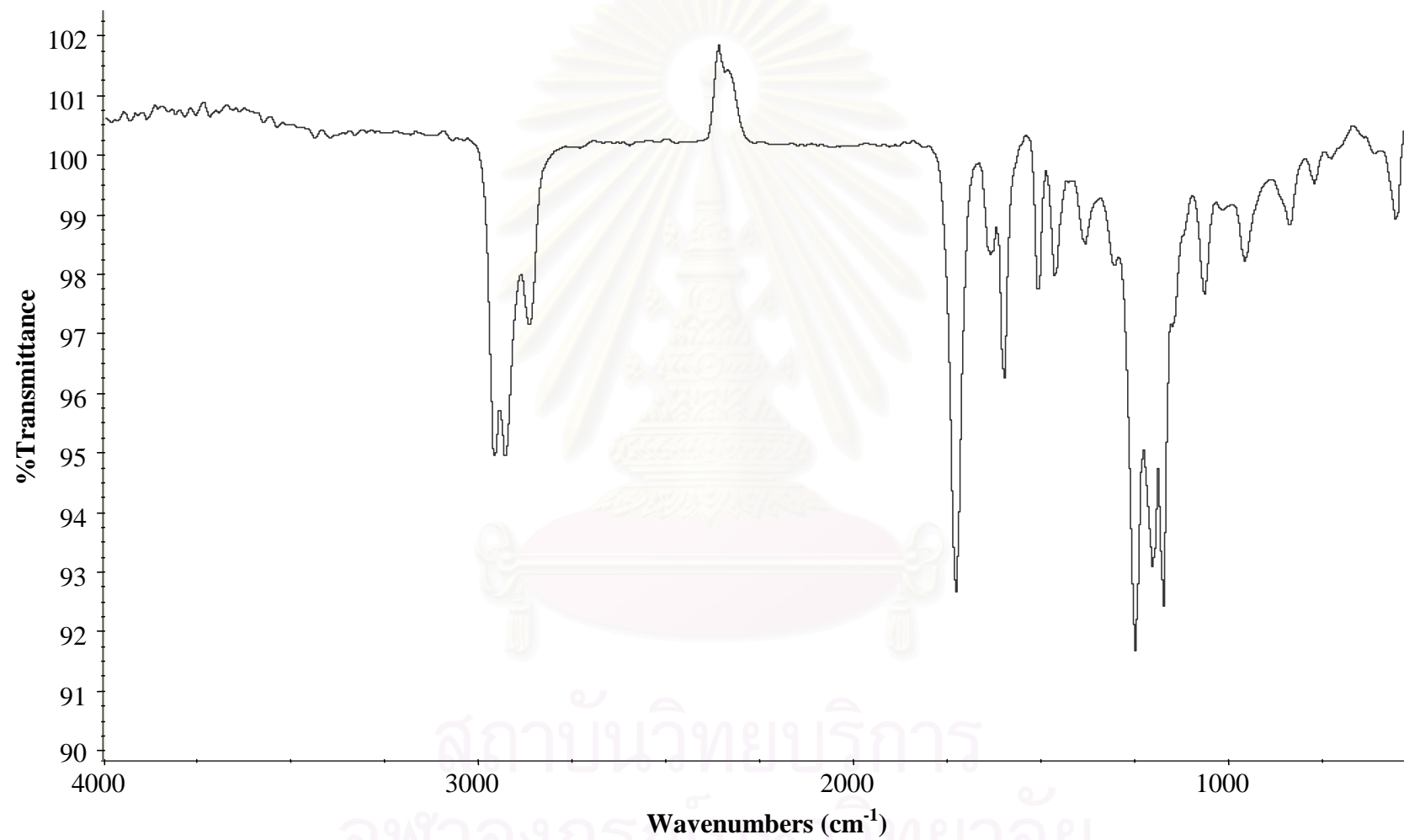


Figure B.18 IR spectrum of di(2-ethylhexyl)benzalmalonate-4-vinyl ether (M-7)

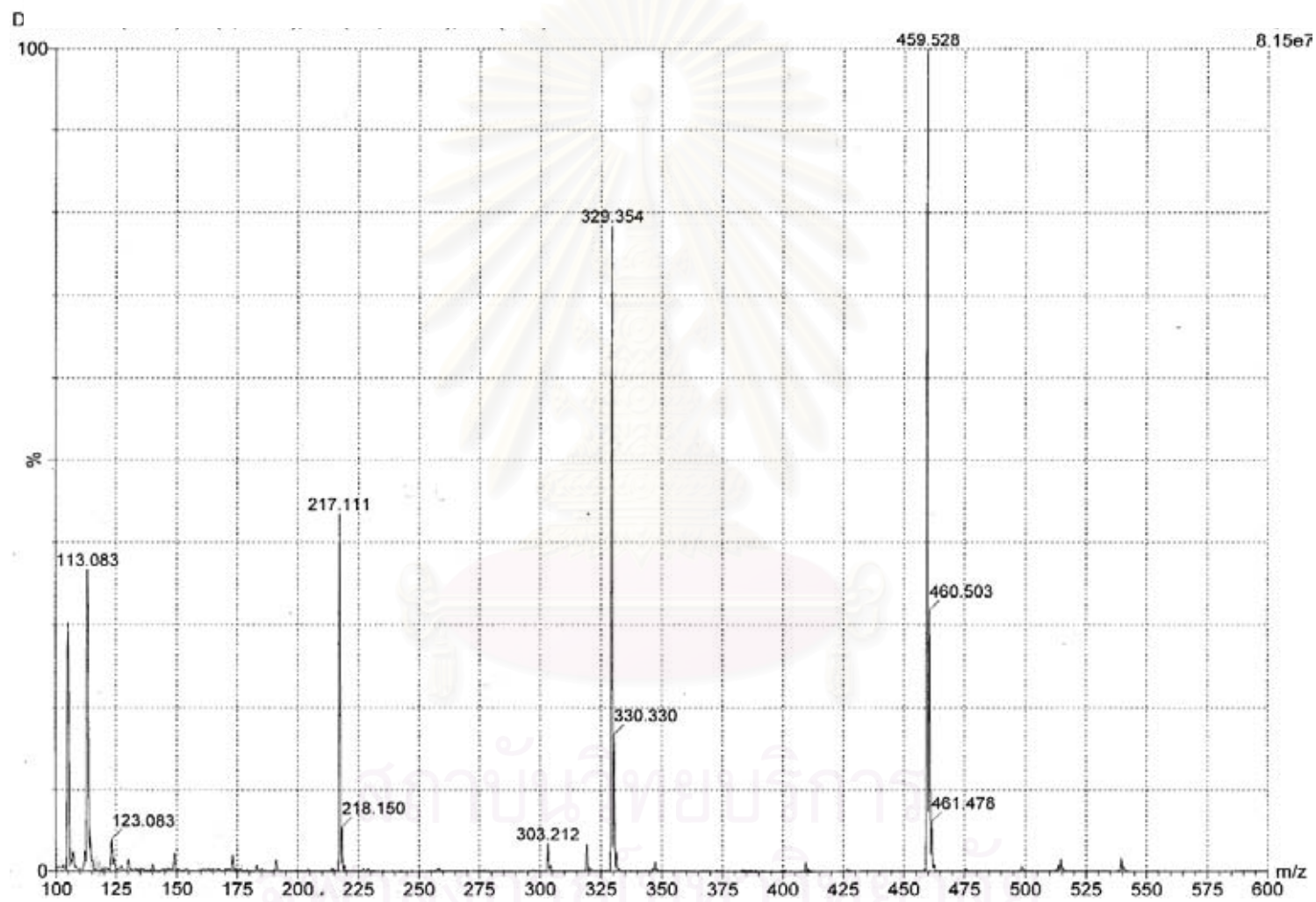


Figure B.19 MS spectrum of di(2-ethylhexyl)benzmalonate-4-vinyl ether (M-7)

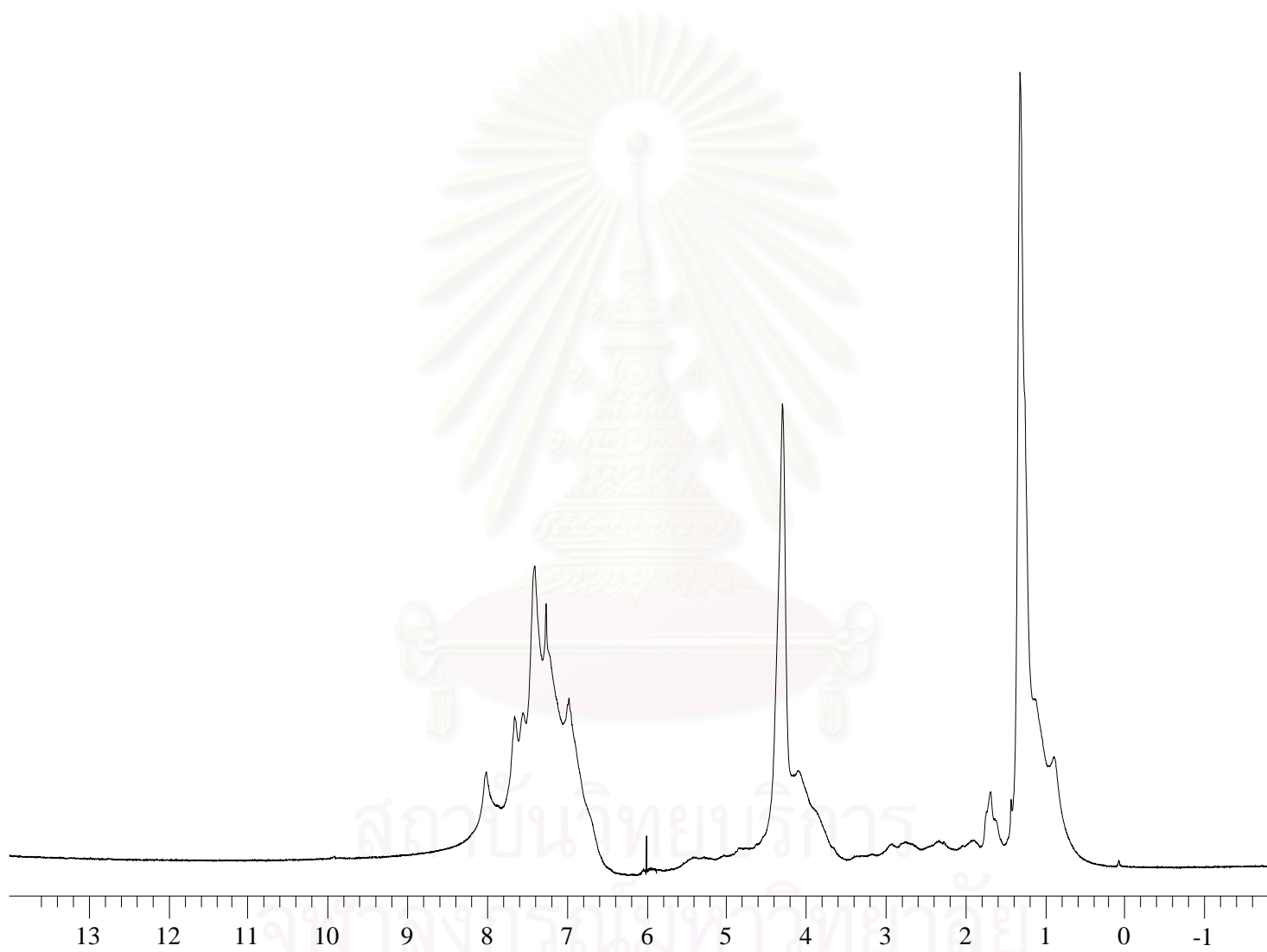


Figure B.20 $^1\text{H-NMR}$ (CDCl_3) spectrum of poly(diethylbenzalmalonate-4-vinyl ether) (P-6)

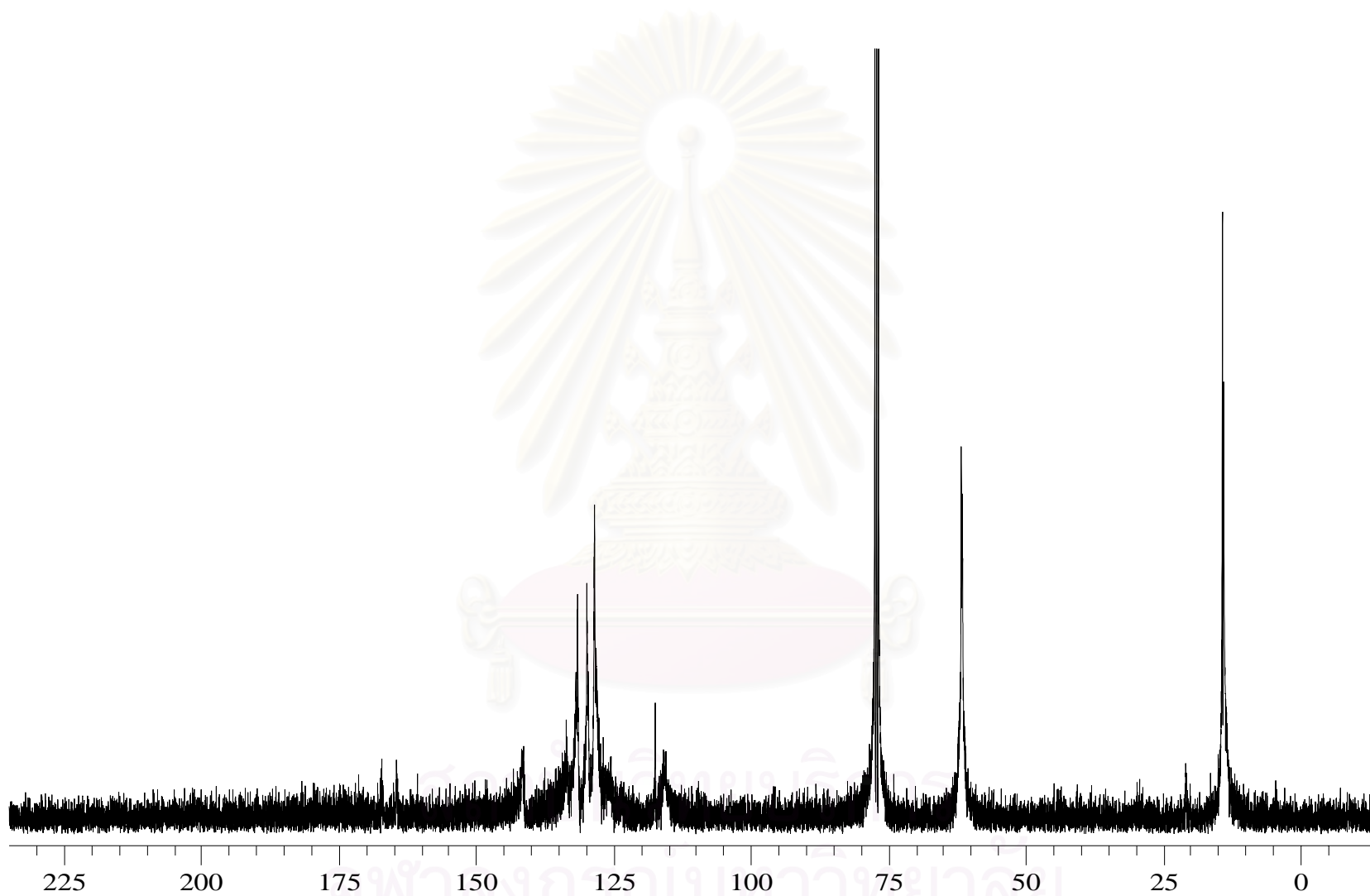


Figure B.21 ^{13}C -NMR (CDCl_3) spectrum of poly(diethylbenzmalonate-4-vinyl ether) (P-6)

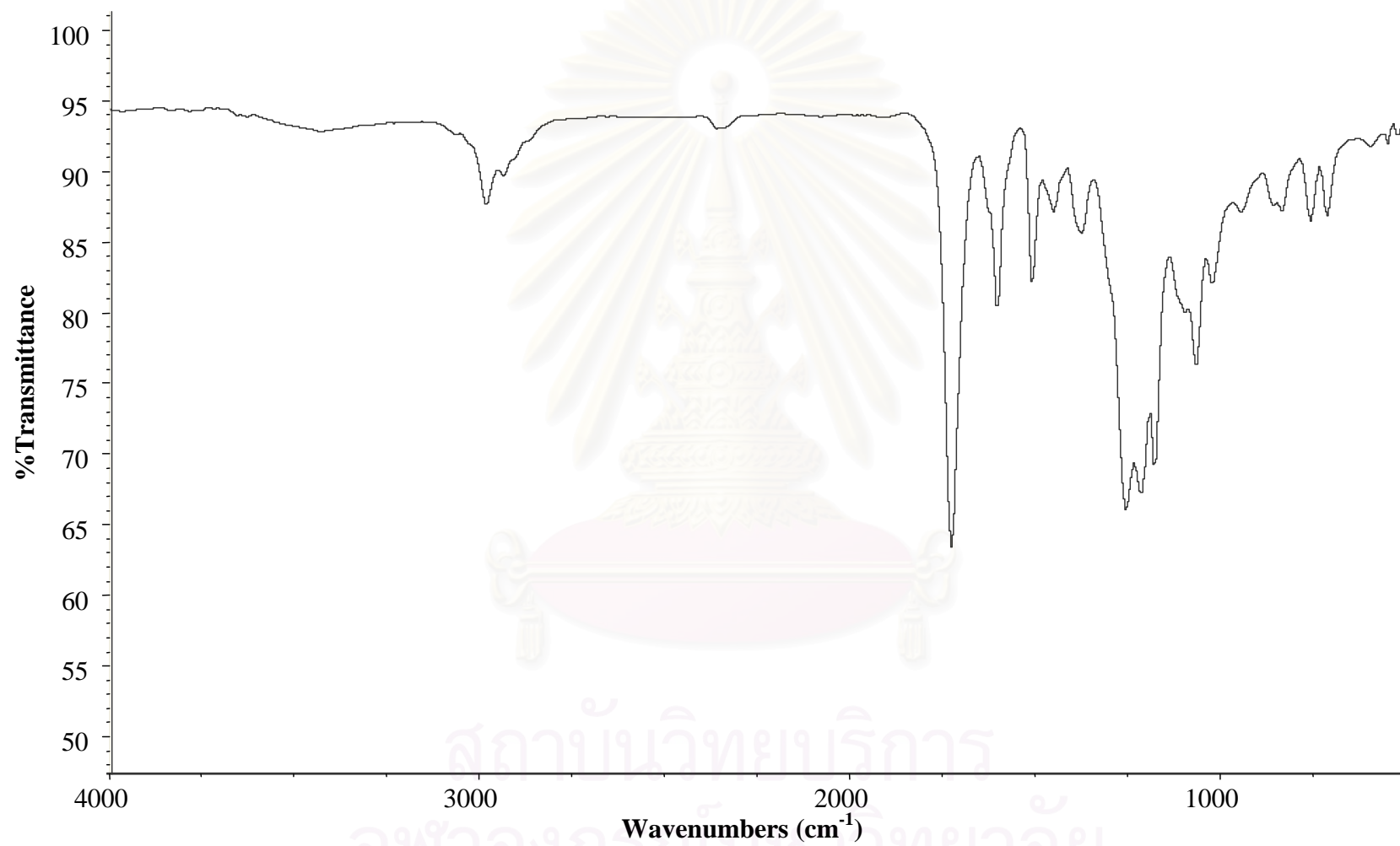


Figure B.22 IR spectrum of poly(diethylbenzalmalonate-4-vinyl ether) (P-6)

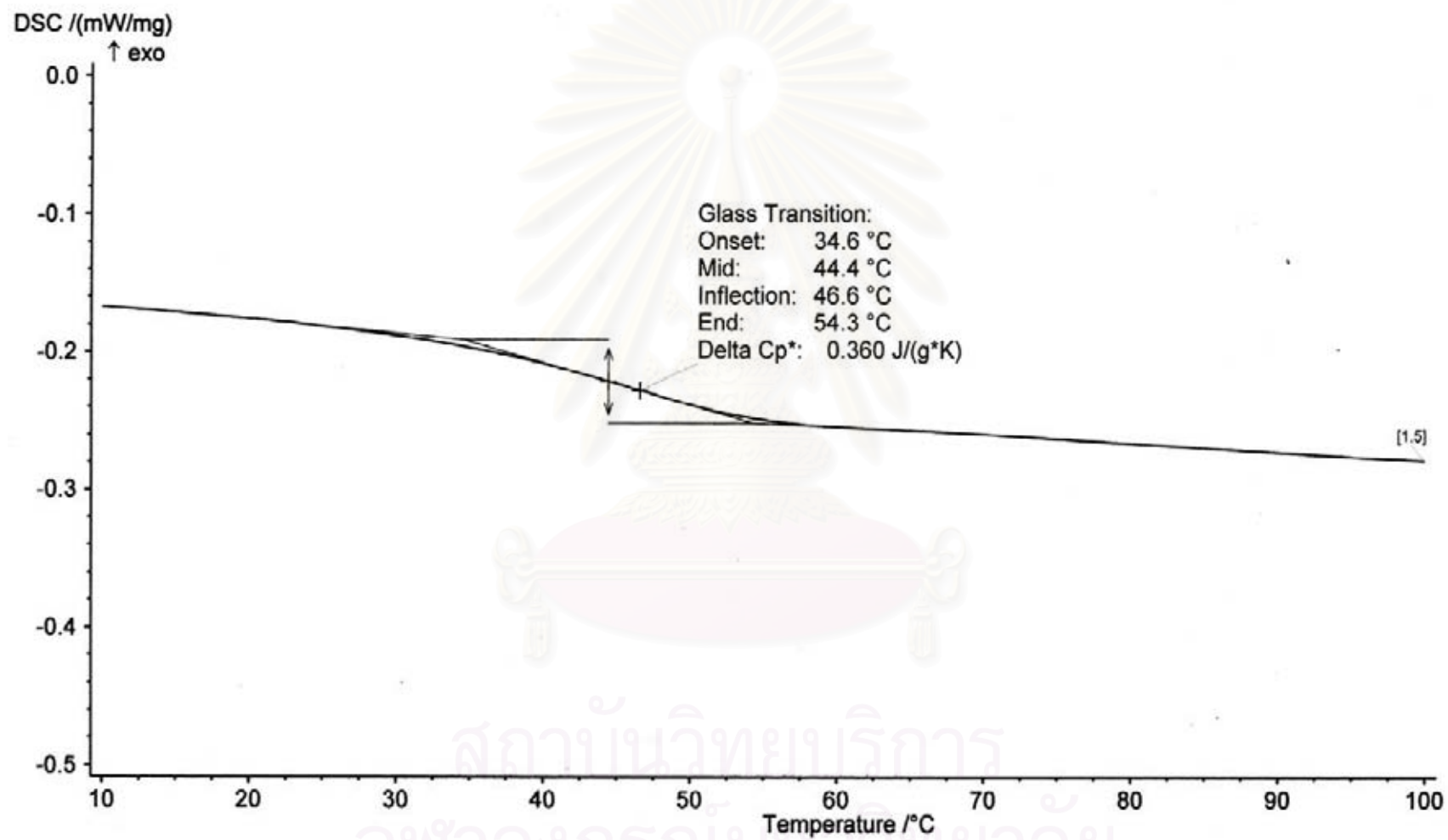


Figure B.23 DSC curve of poly(diethylbenzalmalonate-4-vinyl ether) (P-6)

Sample Information

Sample name Poly(diethylbenzmalonate-4-vinyl ether)
Injection Volume 50.00 μ l
Run Time 40.00 minutes

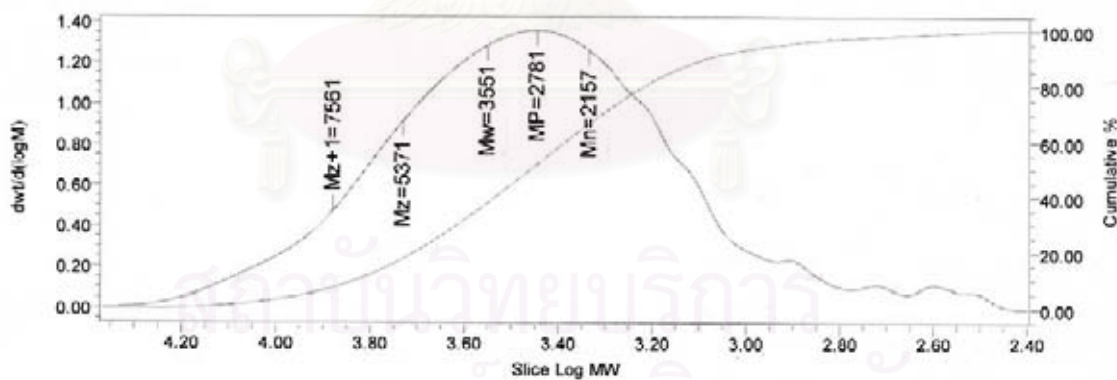
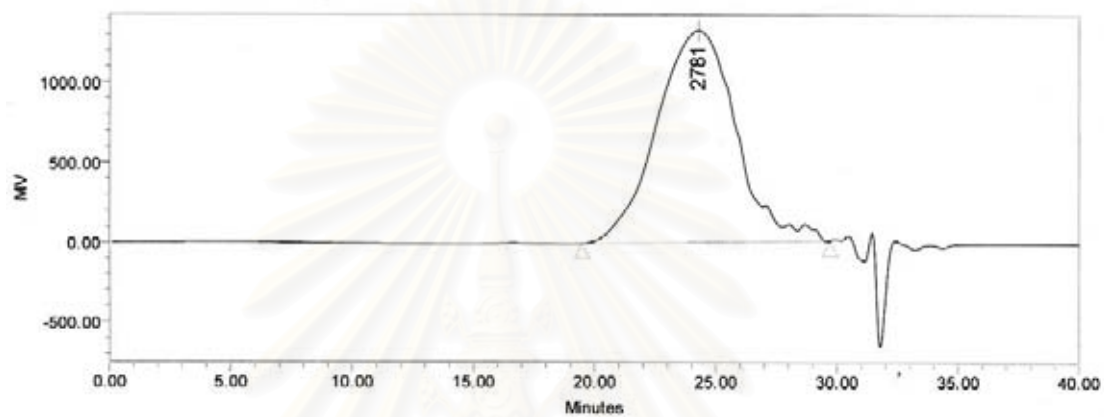


Figure B.24 GPC chromatogram of poly(diethylbenzmalonate-4-vinyl ether) (P-6)

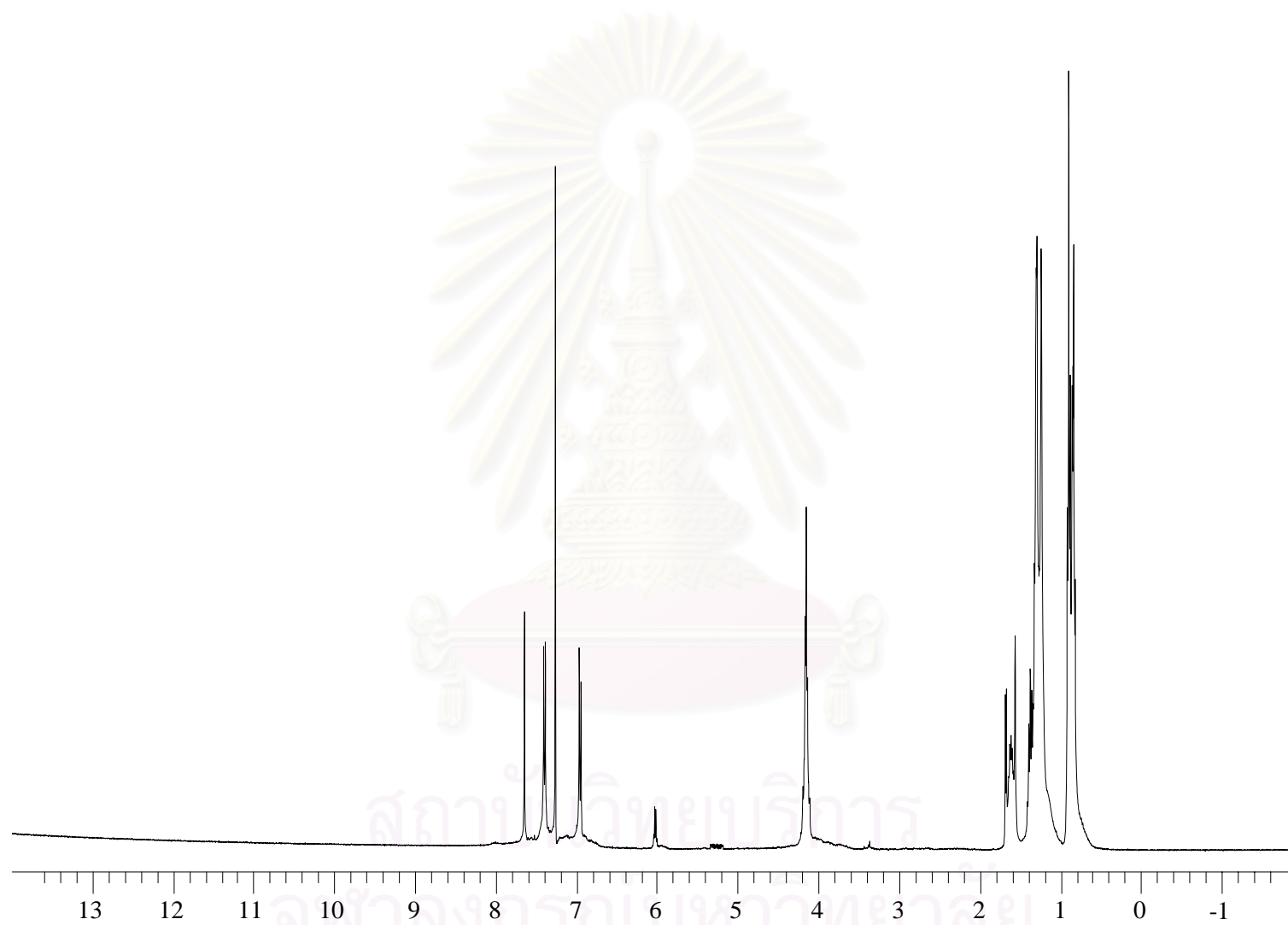


Figure B.25 $^1\text{H-NMR}$ (CDCl_3) spectrum of poly(di(2-ethylhexyl)benzalmalonate-4-vinyl ether) (P-7)

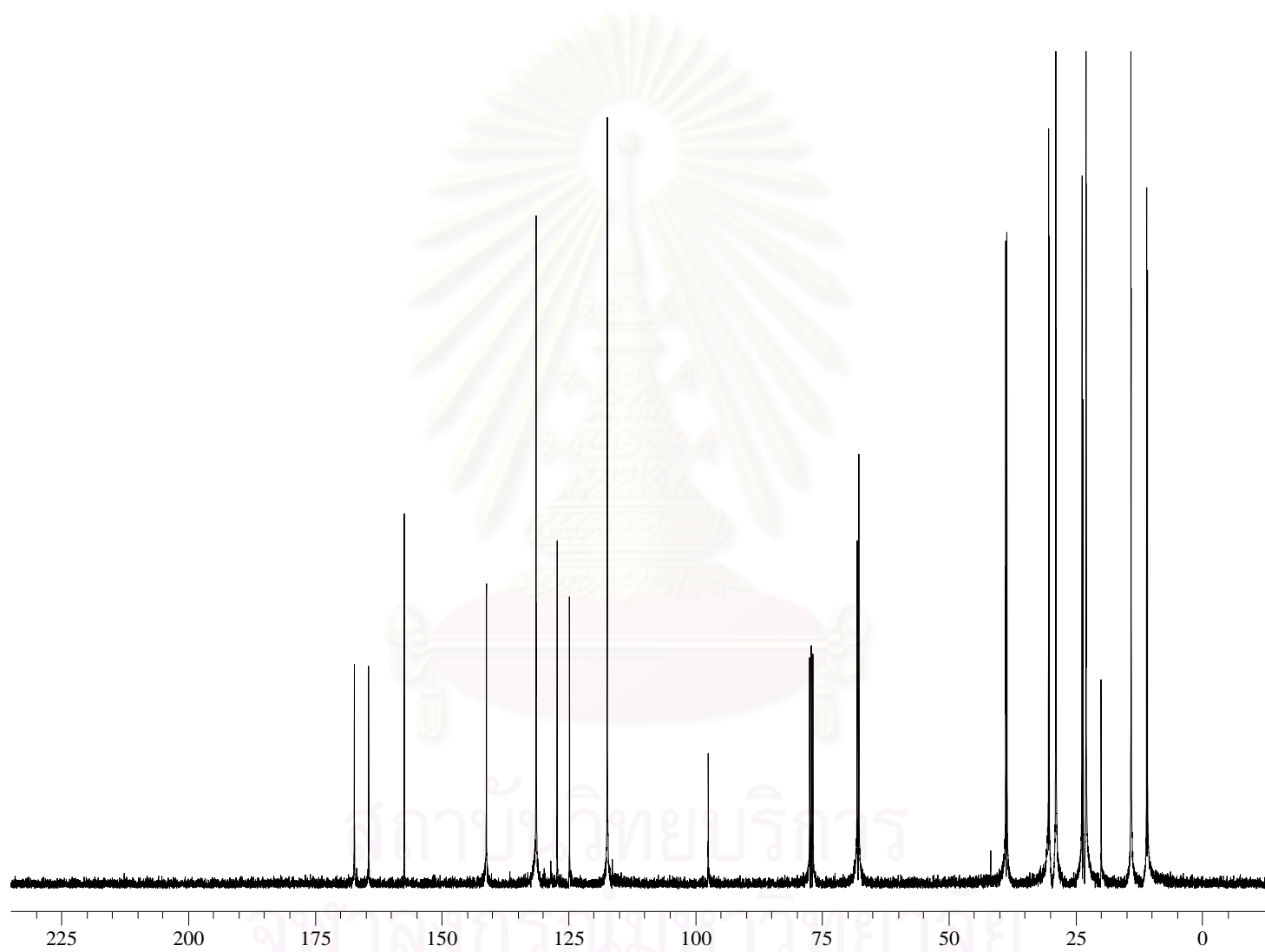


Figure B.26 ^{13}C -NMR (CDCl_3) spectrum of poly(di(2-ethylhexyl)benzalmalonate-4-vinyl ether) (P-7)

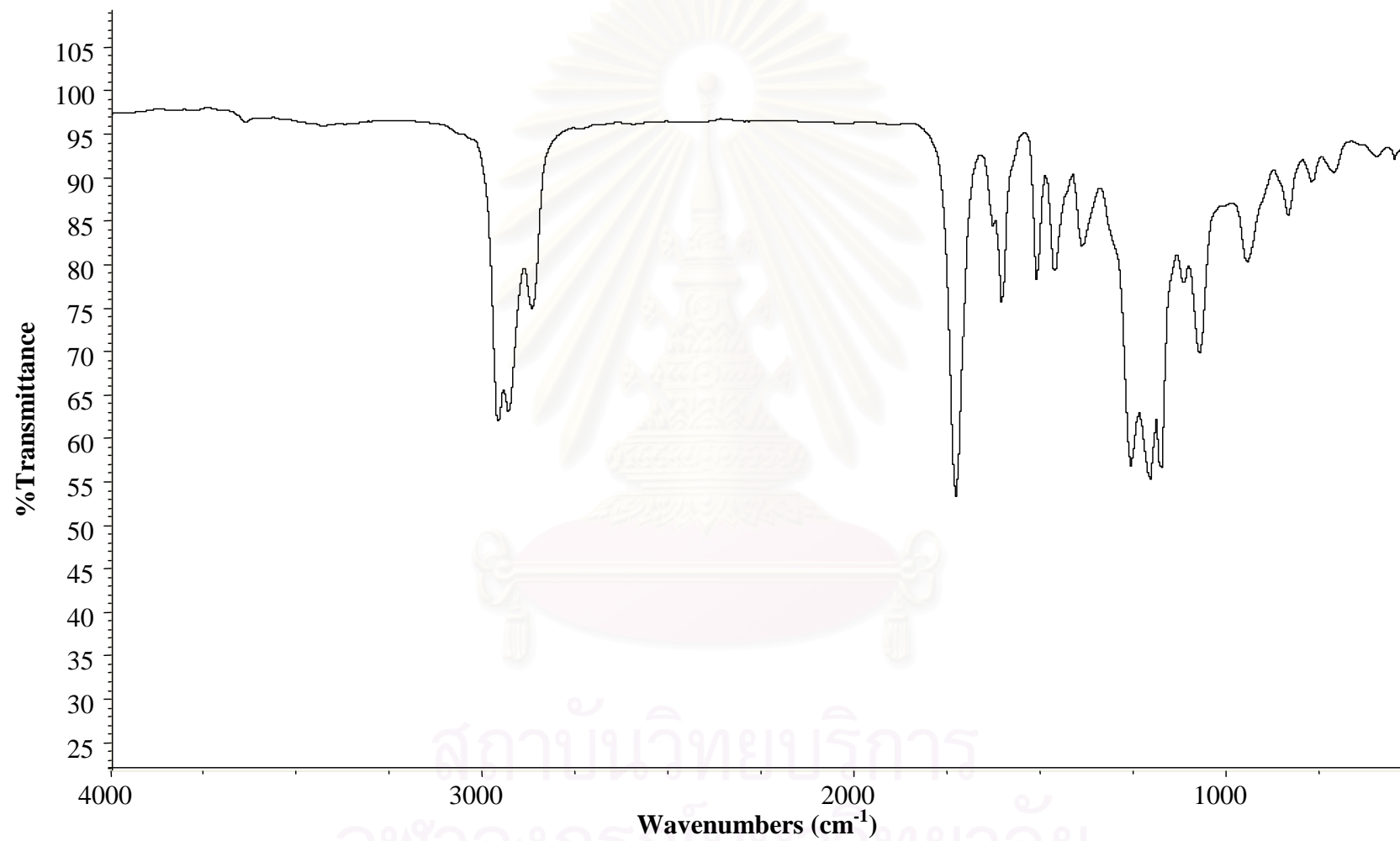


Figure B.27 IR spectrum of poly(di(2-ethylhexyl)benzalmalonate-4-vinyl ether) (P-7)

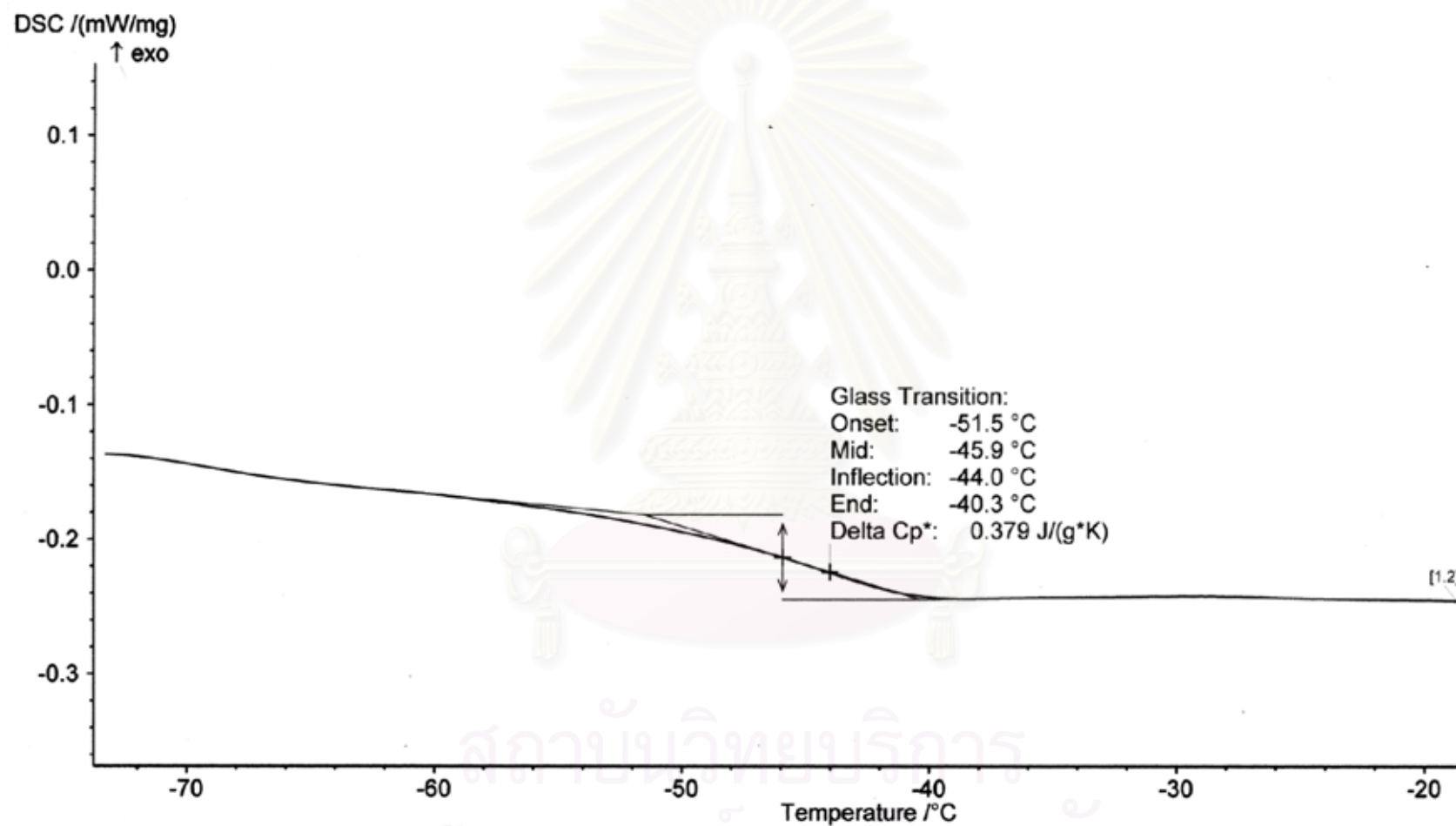


Figure B.28 DSC curve of poly(di(2-ethylhexyl)benzalmalonate-4-vinyl ether) (P-7)

Sample Information

Sample name Poly(di(2-ethylhexyl)benzalmalonate-4-vinyl ether)
Injection Volume 50.00 μ l
Run Time 40.00 minutes

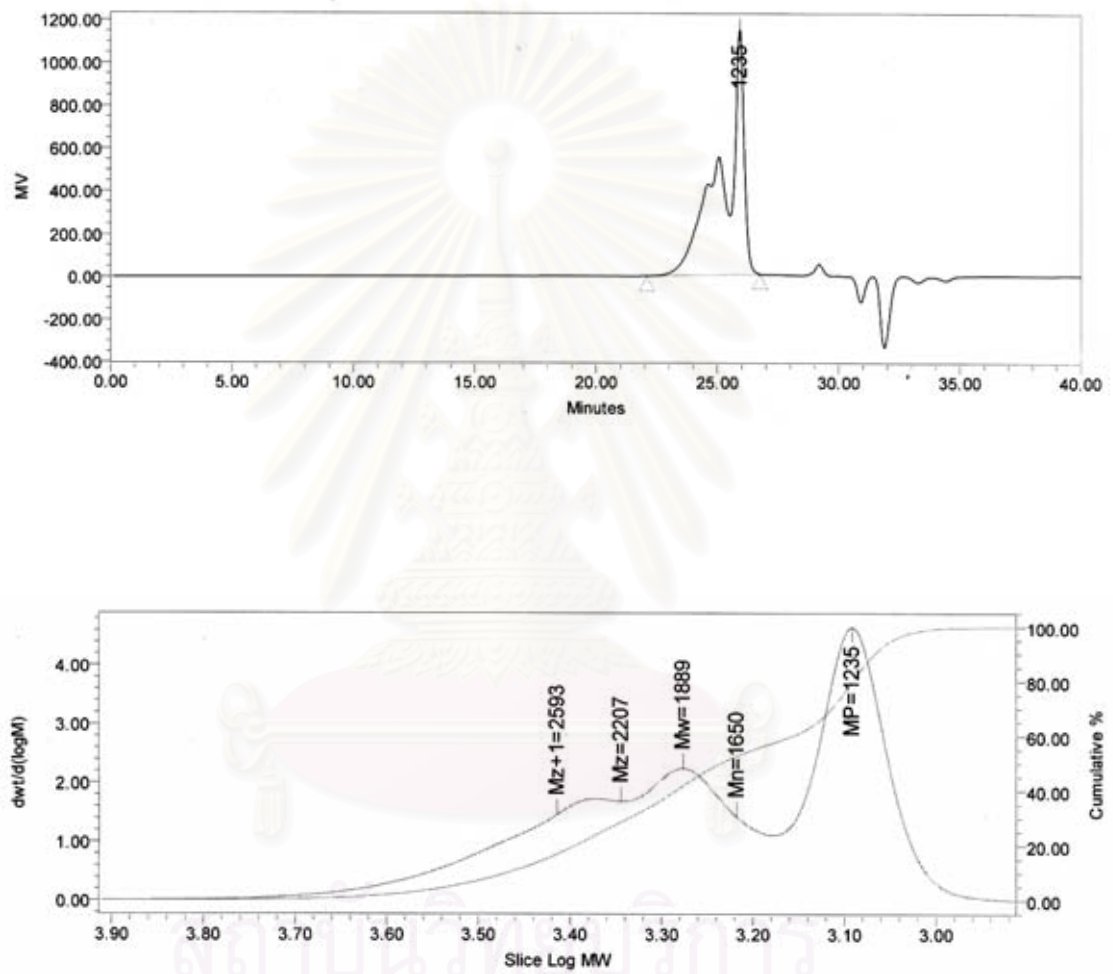


Figure B.29 GPC chromatogram of poly(di(2-ethylhexyl)benzalmalonate-4-vinyl ether) (P-7)

VITA

Ms. Rattanan Tuangudomsap was born on August 4, 1982 in Supranburi, Thailand. She got a Bachelor's Degree of Science in Chemistry from Srinakharinwirot University in 2004. After that, she started her graduate study a Master's Degree in the Program of Petrochemistry and Polymer Science, Faculty of Science, Chulalongkorn University and completed the program in 2007.

Her address is 334/7 M.1 Banrai, Uthaithani 61140, Tel. 086-417-5414, 056-539591.



สถาบันวิทยบริการ
จุฬาลงกรณ์มหาวิทยาลัย